Fractal Architecture of the Universe Based on Primary-Centric World-View - A Post Copernican Conjecture

Bijay Kumar Sharma*

B.TECH (IIT, KGP), MS(Stanford),PhD(Univ.of Maryland), Retired Professor, National Institute of Technology, India

***Corresponding Author**
Bijay Kumar Sharma, B.TECH (IIT, KGP), MS (Stanford),PhD(Univ.of Maryland), Retired Professor, National Institute of Technology, India.

Abstract
This paper investigates the fractal architecture of our Universe based on Primary-Centric Theoretical Formulation. Through theoretical analysis of Earth-Moon System, I arrived at the planetary satellite dynamics which was found to apply equally well to Solar and Exo-solar systems. This gave the theoretical foundation of the New Perspective of the birth and evolution of Exo-solar Systems. This was further extended to the theoretical analysis of star pairs and Neutron-Star pairs. This laid down the Primary-centric World View which I postulate as the physical process which has been shaping the evolution of the Universe and the hot-spots of the Cosmic Microwave Background Radiation right from 380,000 yrs after the Big Bang to date in top-down model resulting into Super-clusters, Clusters, Galaxies and Solar Systems. Primary-centric analysis corresponds to keplerian Analysis for negligibly small mass ratio less than 0.001. In the Copernican Framework, Kepler's Third Law places no restriction on the orbit of the secondary component in a celestial pair. In Primary Centric Framework there is a very definite constraint on the permitted stable orbit, introduced due to periodic tidal deformations . There are two Clarke's Orbits which are fully circularized and synchronized and hence nondissipative and equilibrium orbits called inner and outer Clarke's orbits equivalent to two geo-synchronous orbits in Earth-Moon scenario. Outer Clarke's Orbit is permissible as a stable orbit if the mass ratio of secondary to primary is greater than 0.2, Inner Clarke's Orbit is permissible if mass ratio is less than 10-4 . If the mass ratio is between 10-4 to 0.2 then secondary spirals-out from inner Clarke's Orbit to outer Clarke's Orbit if it tumbles into super-synchronous orbit and spirals-in if it tumbles into sub-synchronous orbit destined to be destroyed by the primary. My conjecture states that every cosmological sub-system has a Monarch (or dominant) Primary (M_primary) Component anchoring the given sub-system and this Primary decides the stable equilibrium orbits of the secondary/secondaries. Planet-Satellite has a Planet as the M_primary, Solar System and exo-Solar Systems have a planet hosting star (PHS) as the M_primary, Galaxy has a Super-Massive Black Hole(SMBH) as the M_primary, Cluster has a cD galaxy (central dominant Galaxy) which is also known as Brightest Cluster Galaxy(BCG) as the M_primary, Super-Cluster has a massive Cluster hosting a QUASER/Blazer as the M_primary. This goes ad-infinitum until a Cosmic Web is woven with Cosmic filaments. This conjecture gains a definite credence after the recent discoveries of the over-massive Black Holes in M_Galaxies namely Messier 87 in Virgo Cluster, NGC 3842 in Leo Cluster, NGC 4889 in Coma Cluster[68] and NGC 1277 in Perseus Cluster[66] which had been proposed as M_Galaxies on general considerations even before the confirmation of over-massive black holes. In 2011, a group of floating planets have been discovered. This is a transitory event and is an exception to this conjecture.

Keywords: Galaxies, Clusters, Superclusters, Hyperclusters, Fractal Design, Cosmic-Web

1. The Primary-Centric World View
In Copernican frame-work, Kepler's three laws give the geometrical configuration of the planets around Sun but donot take into consideration the tidal effects between secondary-primary of a binary pair. If the two components are not in a triple synchrony where triple synchrony is defined as:

$$P_{spin\_pri} = P_{spin\_sec} = P_{orb} \quad 1$$

then the two bodies are bound to squeeze and stretch periodically and this will lead to tidal heating and this means the dissipative configuration will not be in a stable condition. But in Celestial Pairs through the studies of Earth-Moon System it has been found that Moon is spiraling out as shown in Figure 1 [1a,2].

Theoretical analysis of Earth-Moon System shows that there are two orbits where triple synchrony is satisfied and where non-dissipative conditions are achieved. These two orbits are known as inner and outer Clarke's Orbits (a_{G1} and a_{G2}) equivalent to inner and outer Geo-synchronous Orbits in case of Earth-Moon System [1a,2].

2. The Post Copernican Conjecture
The Solar System has a Star 1000 times or more massive compared to the planets, asteroid, Kuiper Belt Objects and comets. The planets which are significant fraction of the Planet Hosting Star (PHS) have two Clarke's Orbits-inner and outer , a_{G1} and a_{G2}, which are the roots of Equation 2 [1-4].

$$\frac{\omega}{\Omega} = E \times a^{3/2} - F \times a^2 = 1\,2$$

$$\text{Where } E = \frac{J_T}{BC} \text{ and } F = \frac{M_{sec}}{1 + \frac{M_{sec}}{M_{pri}}} \times \frac{1}{C}$$

And

$$B = \sqrt{G(E + m)}, C = 0.4 M_{pri} R_{pri}^2 =$$

moment of inertia arpound the spin axis

$J_T = Spin\ angular\ momentum\ of\ the\ primary$

$+ Spin\ angular\ Momentum\ iof\ the\ secondary$

$+ Orbital\ angular\ Momentum$

$= Total\ angular\ momentum\ of\ the\ binary\ system$

The secondary of Star-Planet system starts at aG1 which is an unstable equilibrium [SOM_Appedix A]. Hence any perturbation, such as solar wind, cosmic particles or radiation pressure, nudges the secondary either short or long of a_{G1}. Short of a_{G1}, the planet is trapped into a sub-synchronous death spiral as Phobos is with respect to Mars [1b] In a death spiral through a gravitational runaway process planet spirals into a headlong collision with the primary body or partly engulfed and partly vaporized or completely vaporizes before the collision depending on the mass ratio of the secondary to the primary [3,5-7].

Long of a_{G1}, the planet experiences an impulsive torque through a phenomena known as Gravitational Sling Shot Effect [8-11]. When the impulsive torque terminates at a_2[Mean Motion Resonance Position 2:1] , the planet is launched on an expanding spiral path much in the same way as our Moon was launched after the Giant Impact [2]. Figure 1 describes the expanding spiral path of Moon from inner Clarke's Orbit (also known as inner Geo-synchronous Orbit in Earth-Moon System) to the Outer Clarke's Orbit (or outer Geo-synhronous Orbit).

The time scale of evolution depends on the mass ratio of secondary to primary. If the mass ratio is between 0.2 to 1, secondary falls into the outer Clarke's Orbit configuration on a time scale of months/years as is the case in pulsar pairs, star pairs or in Brown Dwarf pairs. The secondary and primary are formed by the hydrodynamic instability process [12].

If the ratio is from 0.2 to 10^{-4} the time scale varies from thousand to kilo to Mega to Giga years. The formation of the secondary is by core-accretion process [13].

If the mass ratio is less than 10^{-4} then time scale of evolution approaches infinity and outer Clarke's Orbit also approaches infinity and the secondary remains stay put at a_{G1}(inner clarke's Orbit). That is it has no evolutionary history as is the case with Star and SMBH pair in a Galaxy or as is the case with geo-synchronous satellites around Earth [16].
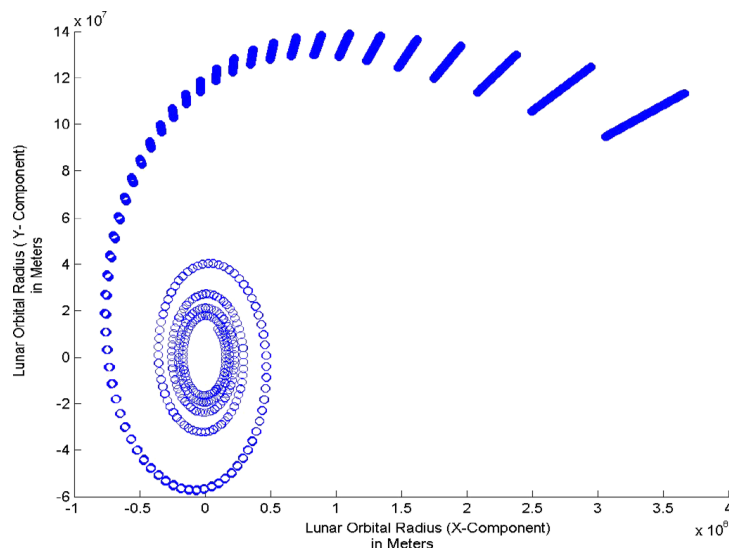

Figure 1: Lunar Orbital Radius expanding spiral trajectory obtained from the simulation for the age of Moon (i.e. from the time of Giant Impact to the present times covering a time span of 4.53Gyrs).

After the termination of the impulsive torque due to gravitational sling-shot at a_2 (mean-motion resonance point of 2:1), the planet coasts on its own until it reaches outer Clarke's Orbit a_{G2} in much the same way as Charon has done with respect to Pluto [6]. The inner Clarke's Orbit is an energy maxima whereas outer Clarke's Orbit is an energy minima [SOM_Appendix A]. *In super-synchronous orbit as secondary is traversing the non-keplerian spiral path, the binary system is moving from highest energy configuration to the lowest energy configuration as it should in order to achieve a stable equilibrium configuration.* This golden rule is being followed by the Universe in its small scale structure (e.g. at planetary level), medium scale structure (e.g. at galactic level) as well as in large scale structure (e.g. cluster and super cluster level).

The subsequent history of Earth-Moon system after reaching a_{G2} depends on the overall orbit configuration. The secondary may remain stay put in a_{G2} orbit or it may be launched again on a contracting spiral orbit due to the third body effect. In Moon-Earth system, Sun is the third body. In Pluto-Charon case Charon is remaining stay put at it's a_{G2} since Charon's Orbital Plane around Pluto is transverse to the radius vector from Sun to Pluto hence Sun's tidal effect on Charon is nullified [6]. In our Solar System the Super Massive Black Hole (SMBH) Saggittarius A* (SgrA*) at the galactic center of the Milky Way acts as the third body while analyzing Planet-Sun system [14].

In sub-synchronous orbit, ω/Ω = (orbital period)/(spin period of primary) is less than Unity and secondary's tidal torque is spinning up the primary hence secondary is transferring momentum and energy to the primary. There is tidal heating due to repeated stretching and squeezing of the primary. Since the secondary is in synchronous orbit it is tidally locked, its shaped permanently oblate and hence it experiences no tidal heating. But if it was not tidally locked it will experience tidal heating. This leads to a gravitational runaway collapsing orbit. Here the secondary is doomed to complete destruction either by impacting the primary or being pulverized as soon as it enters Roche's limit. Hence this is known as a death spiral.

This final merger in a death spiral takes place in every binary system only the scale of the impact varies.
• In satellite-planet merger the impact will be of the scale several orders of magnitude greater than what was seen in Shoemaker Levy 9's Comet impact on Jupiter.
[foot note\< SL9 got captured by Jupiter in 1960s and it was launched on death spiral. It was moving in a highly elliptical orbit and in July 1992 its collapsing elliptical orbit grazed passed the Roche's Limit at 11,000Km from the center of Jupiter. This led to the fragmentation of SL9. These fragments eventually collided with the Planet's surface between July 16 and July 22 1994>]
• In planet-planet hosting star merger, there are clear accretion signatures in form of IR excess and ^{7}Li enrichment [5,15]. There can be tidal heating and bloating of the planet size as seen in HD20458b [16]. WASP-18b is racing to a similar fate of doomsday [17]. HD82943 has already engulfed its planet [18].
• In Star – Super Massive Black Hole at the center of a Galaxy interaction we have only recently observed 'a possible Relativistic Jetted Outburst from a Massive Black Hole fed by a tidally disrupted Star' [Appendix F, 19,20]] .

2.1 The origin of Primary-centric World View- the basis of the post Copernican conjecture

Till 1920, we had a static vision of the Universe. Galileo's observations had supplanted the Geo-centric World-View with Helio-centric World-View with final definiteness [21-23]. The Copernican Vision had gained respectability in scientific community still Universe was treated as a static system. Tycho Brahe stood a witness to a remarkable Supernova Explosion [24]. But till the end of 19th century and start of 20th century, we looked at Universe as something non-evolving. Einstein had introduced a cosmological constant to balance the gravitational collapse and obtain a static Universe [21]. Only in 1920 with the discovery of the "Expanding Universe" by Edwin Hubble that this Static Universe mold was broken [22,25]. In 1930 the proposition of Neutron Star by Chandrashekher and in 1939 the proposition of Black holes by Robert Oppenheimer and Hartland Snyder were put forward [26,27].

It was clear to the World Scientific Community that there was no such thing as a permanent equilibrium. The criteria of equilibrium is changing and the nature of matter also changes as we go from White Dwarf to Neutron Star to Black Hole. So we live in a constantly evolving Universe but we were oblivious of the laws of evolution of the Physical World. We were better at understanding the laws of evolution of the Living World because of the elaborate work done by Charles Darwin in form of "On the Origin of Species by means of natural selection or the preservation of favoured races in the struggle of life" (1859) and "The descent of Man and selection in relation to sex" (1871).

1967-72 Apollo Program allowed the scientists to make mathematical analysis of the Moon's recession and thereby make a theoretical formulation of Earth-Moon System. On seismological considerations: on kinematics consideration: personal communication http://arXiv.org/abs/0805.0100, Sharma personal communication http://arXiv.org/abs/0805.1454, Sharma [2,4,6,28-37]. In 60s and 70s advancement in Electronics and Instrumentations heralded the astronomy of the entire spectrum –Radio Astronomy , Microwave Astronomy, IR Astronomy, Optical Astronomy, UV Astronomy, X-Ray astronomy and γ-Ray Astronomy. NASA and ESA heralded the Space Observation Program such as Hubble Space Program, Spitzer Space Telescope and Herschel Space Observatory. Among the ground observatories, higher diameter 8- to 10-meter Telescopes and Very Long Baseline Interferometer (VLBI) based Telescopes in Radio Wave Range were established which facilitated sensitive observations over the entire IR region of spectrum. This in quick succession led to the discovery of Neutron Stars, Black Holes and Dark Matter. 90s established that all galaxies grow around Super Massive Black Holes and are regulated by SMBH [38,39]. By 2000 the Search for Extra-terrestrial Intelligence (SETI) and its natural corollary the hunt for extra-solar Earths within the habitable zone of Planet Hosting Stars had begun in real earnest. 2002 saw the complete theoretical formulation of Earth-Moon System and discovery of the two geo-synchronous orbits, inner

being unstable and outer being stable [Appendix A, 4, 40]. In 2004 the new perspective on the birth and evolution of the Solar System was presented which claimed that the planets are born at the inner Clarke's Orbit and migrate to outer Clarke's Orbit or get trapped in the death spiral and are eventually engulfed/vaporized or part of both by the PHS [7,41]. 2005 saw the migration theory of Jupiter and Saturn to be firmly established [41-44]. In 2011 the new Architectural Design Rules were applied to 12 single planet exo-solar systems, 4 Brown Dwarf-star systems and 2 Brown Dwarf pairs This marked the beginning of Primary-centric World-view.

SLOAN programme, Sloan Digital Sky Survey(SDSS), catalogued the entire population of Galaxies in the visible sky [45]. The fully calibrated optical spectra for one million galaxies in the local Universe is available for Research purposes. In 2011, on 28th March, an unusual long Gamma Ray Burst was detected by SWIFT. This established that a normal Sun-like-star can get trapped in death spiral around the galactic centre and eventually get tidally shredded by SMBH located at the galactic center[SOM_Apendix F]. The simulation of dark matter by numerical techniques gave evidence for a remarkable self-similar pattern of clustering properties as seen in Figure 2 and Figure 3. [Large Numerical Simulation for Dark Energy Surveys @ Marenostrum Supercomputer]. Dark matter pattern establishes the fractal architecture of our Universe with definiteness.
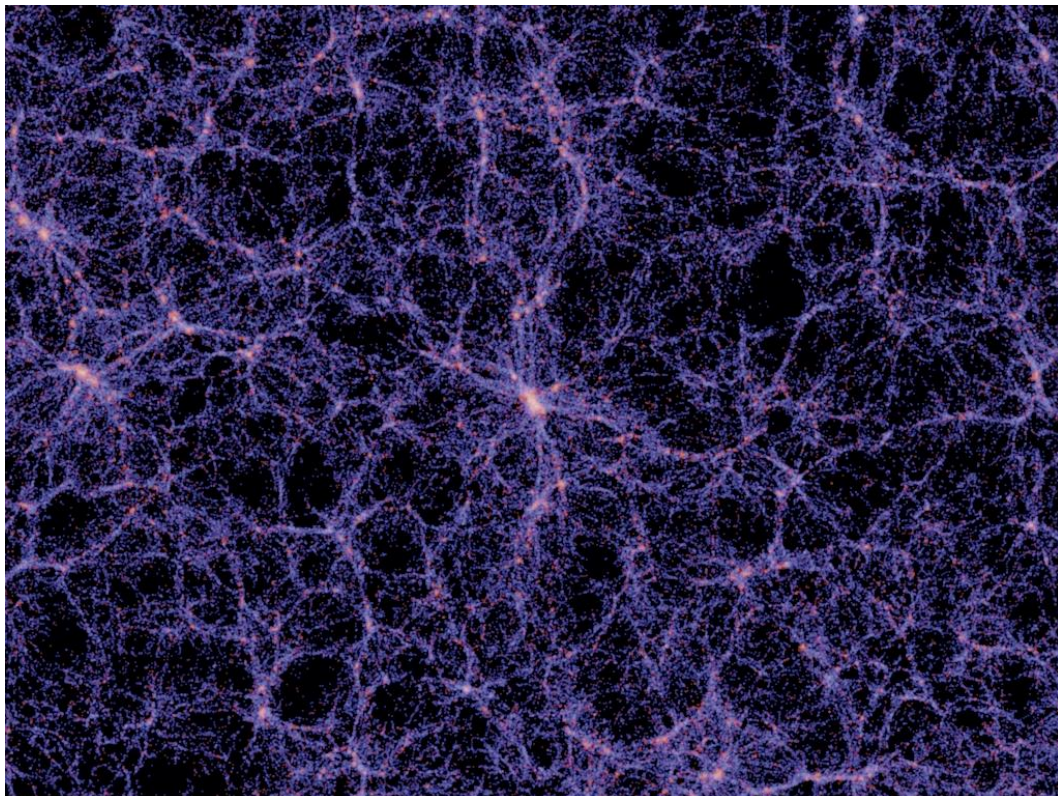

Figure 2: Large Scale Distribution of Baryonic Matter as evidenced by large scale light distribution.[Curtsey-Large Numerical Simulation for Dark Energy Surveys@Marenostrum Supercomputer]
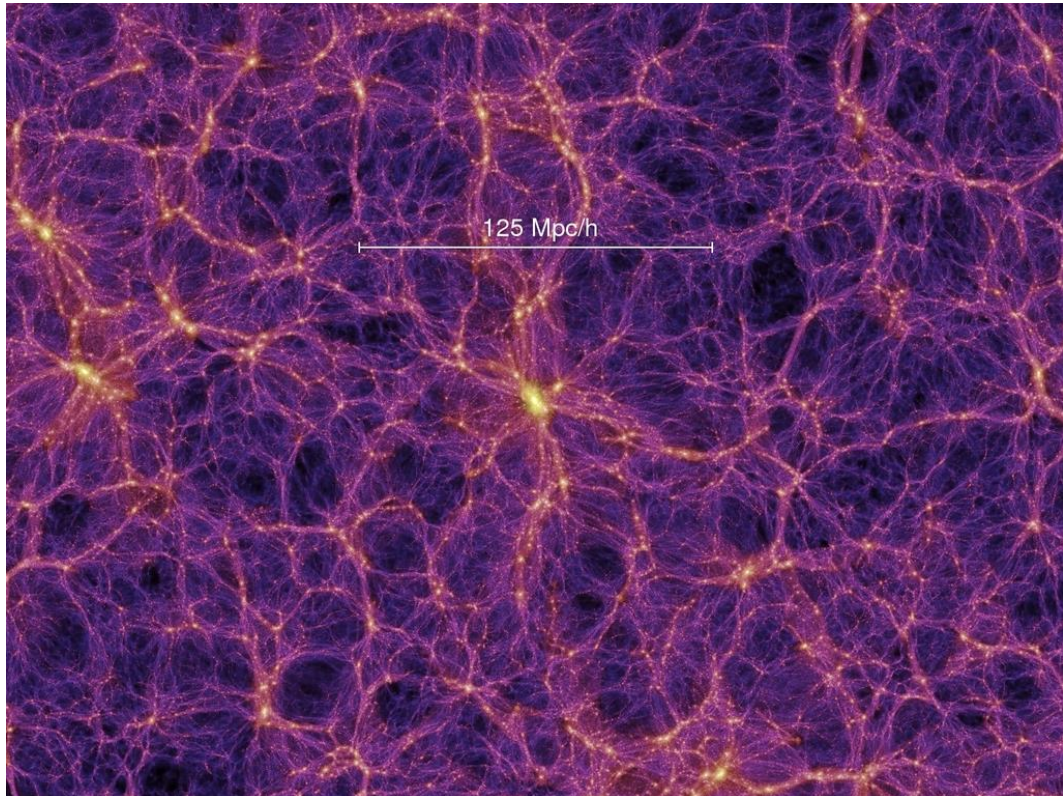
Figure 3: Large Scale Distribution of Dark Matter. [Curtsey-Large Numerical Simulation for Dark Energy Surveys@Marenostrum Supercomputer]

The Standard Model of particle physics and Big Bang theory of the birth of our Universe cannot account for large cosmological structures, so in the actual cosmology it is hypothesized that such structures as the Great Wall form along and follow web-like threads of dark matter. It is thought that this dark matter dictates the structure of the Universe on the grandest of scales. Dark matter gravitationally attracts baryonic matter, and it is this normal matter that astronomers see forming long, thin filaments and walls of super-galactic clusters. But then the big question arises as to how does dark matter distribute itself ?

Recent studies by WMAP(Wilkinson Microwave Anisotropy Probe) , SDSS (SLOAN Digital Sky Survey) and Supernova Cosmology Project have irrefutably established that the Age of our Universe is 13.7Gy, Hubble Constant (rate of expansion of our Universe) HO = 71 Km/(sec-Mpc), and we have an accelerating Universe which has Cold Dark Matter(CDM) dominating our ordinary baryonic matter in the ratio 5:1. After the Big Bang(BB) Universe cooled to 4000K in about 375,000y after the BB [46,47]. This is the instant when atoms neutralized and matter decoupled from radiation , it was Matter-dominated Universe and Universe plunged into dark ages. 400My after the BB, stars formation began, re-ionization resumed and Universe emerged from the dark ages. WMAP gives a resolution of ±200μK temperature in the early Universe map where the temperature fluctuation appears as colour variation. The curvature of the Universe is flat within 0.4% of the flat Universe. The ratio of dark matter/ordinary visible matter has been arrived at by deriving the percentage of ordinary matter : dark matter:dark energy which are 4% : 23%: 73% respectively.

The detailed method of arriving at mass ratio of ordinary matter to dark matter is given in SOM_Appendix G.

Primary-centric World-View inexorably leads to a Fractal Architecture of the Universe- a self-repetition of the evolving solar-system model from asteroid to planets to stars to galaxies to clusters, super clusters, hyper clusters to cosmic web. The World System at all levels locally or globally, tend to go from energy maxima to energy minima and energy minimization drives the re-configuration of celestial bodies right from the lowest mass binary configuration to the scaled up version at Super-Cluster level. An isolated celestial body is an exception, a transitory phenomena due to dynamical interactions[OGLE Collaboration(2011]. As a rule all celestial bodies are coupled in binary and higher order systems. These coupled systems are either moving towards Outer Clarke's Orbit configuration or already stabilized at the outer Clarke's Orbit configuration as Pulsar Pairs or Star Pairs are.

2.2 Solar System Repetition at Asteroid level, KBO Level and at Planet-Hosting-Star level

The Solar System configuration is there at asteroid level [48]. Asteroids with satellites are observed throughout the Solar System from sub-km near_Earth Asteroid pairs to systems of large and distant bodies in Kuiper Belt. 15% of near-Earth and main-belt asteroids with diameter under 10km have satellites. Main –belt asteroid Ida has its own moon Dactyl.

At Kuiper Belt Object (KBO) level, Pluto has four moons. One of them Charon is 1/5 Pluto's mass hence has an evolutionary

history. It has evolved from aG1 to aG2. Its present orbit is the outer Clarke's orbit. The other three are of insignificant mass fraction compared to Pluto hence they have inordinately long time constants of evolution . Therefore they are stay put in their respective first Clarke's Orbit. Another KBO, 'Haumea' has two moons [49]. There are nearly 100 known asteroid binaries, nearly half of which are in Kuiper Belt [50].

Solar System repeats itself at Earth, Mars, Jupiter, Saturn, Uranus and Neptune level. Earth has one Moon, Mars has two moons-Phobos and Deimos, Jupiter has 38 moons, Saturn has 33 moons, Uranus has four moons and Neptune has 13 moons.

Most of the stars are hosting planets giving rise to solar system and extra solar systems [51].

2.3 Solar System-like Galaxies

A Galaxy is also solar-system like. All the stars within a galaxy are orbiting around a Super Massive Black Hole (SMBH) which seems to be regulating the growth and the growth rate of the whole Galaxy [14,38,39,51]. The star stable orbits around SMBH are shown in Figure 4. In addition just as our solar system has an ecliptic plane and the planets are confined to ecliptic plane in a similar manner the stars in a Galaxy are confined to the galactic plane with a disk like structure as seen in Figure 3.
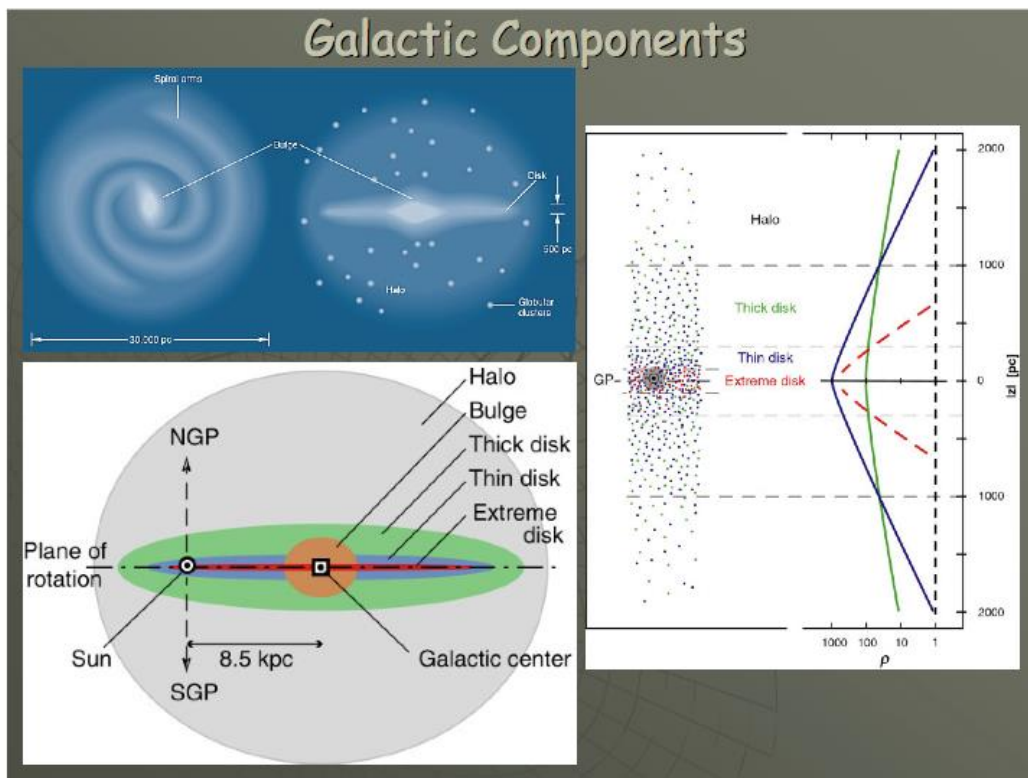

Figure 3: Edge-on view of Milky Way with disk, bulge and halo.

Our Galaxy Milky Way has a disk, bulge and halo as shown in Figure 3. Bulge is a spherical slowly rotating component that dominates the inner part of the Galaxy. Disk is the flat and more rapidly rotating component that dominates over the bulge at larger radii. Halo contains 'dark matter' and the major reservoir of gaseous feedstock for the birth of stars and for the growth of BH.

Disk contains Population I stars (3rd generation stars) whereas bulge and halo contains Population II and III stars(1st and 2nd generation stars). Among them are 200 Globular Clusters.

Globulars are concentrated towards the galactic nucleus These are made of most pristine materials and indicate the dynamical age of the Universe which is 14.2Gy±1.7Gy [53]. Disk has a diameter of 100,000 lightyears(ly). The thickness of disk is 2300ly to 2500ly. The thickness of the bulge is 16000ly and the radius of the halo is the radius of the disk i.e.50,000ly. There are 100 billion stars in our galaxy all orbiting around the center of the Galaxy as shown in Figure 3. These 100 billion stars in Milky Way are evolving gently and steadily, forming stars at a modest rate of 3 Solar Masses per year [Appendix B] [45].
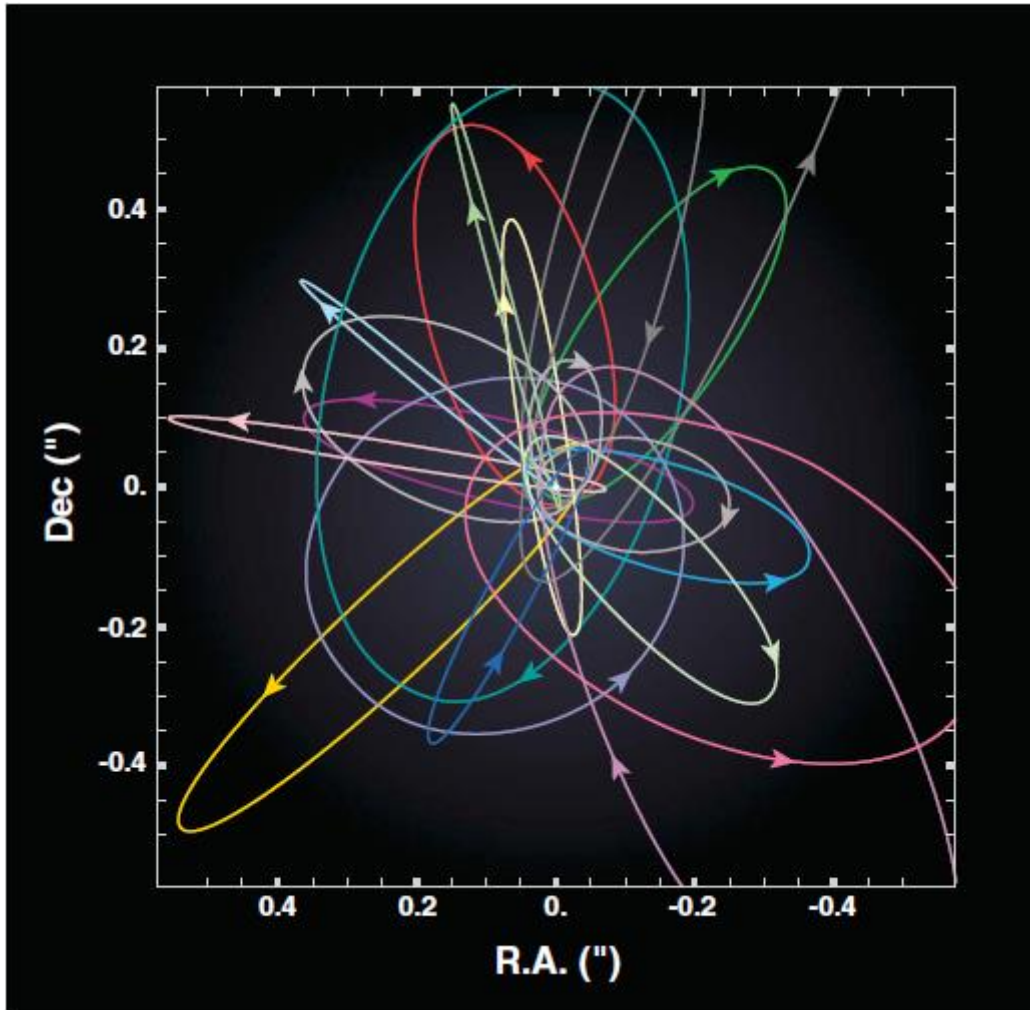
Figure 4: Plot of the orbits of stars around the supermassive black hole(SgrA*) in the nucleus of our own Milky Way. The supermassive black hole lies at the origin of the coordinate system, and the region shown is ~0.15 light years across. Applying Newton's law of gravity to these orbits yields a black hole mass 4 million times that of the Sun. Dec (declination) and R.A. (right ascension) are the sky coordinates relative to the supermassive black hole measured in seconds of arc ("). [Source: S. Gillesen et al., Max Planck Institute for Extraterrestrial Physics]

The Milky Way disk is spinning around its center Sgr A* with a period of 240million years per revolution.
From the equality of centripetal and centrifugal force we get:

$$\frac{GM_{Sun}M_{core}}{r^2} = \frac{M_{Sun}V_t^2}{r} \quad 3$$

Simplifying Eq 3 we get:

$$M_{core} = \frac{V_t^2 r}{G} \quad 4$$

Our Sun is situated at r = 8500pc and its observed tangential velocity is 220km/s and theoretically expected value based on the visible matter is 160km/s.
Based on visible matter, M_{CORE} = 9.787×10^{40}Kg = 4.92×10^{10}MO .
Based on the observed value of 220km/s, M^*_{CORE} =1.85×10^{41}Kg = 9.3×10^{10}MO .
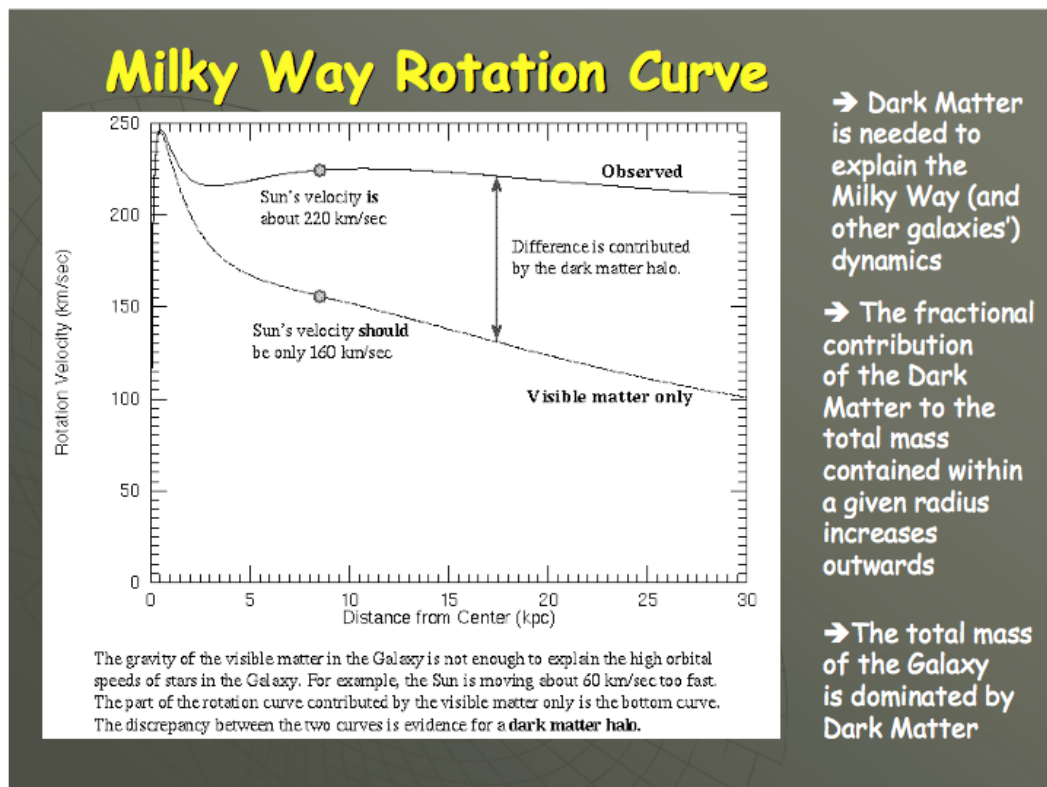Therefore the percentage of dark matter present in the core is 90%.

Figure 5: Observed tangential velocity profile of the stars in Milky Way at increasing distance from the center of Milky Way and theoretically expected value based on the visible matter only

We see, in Figure 5, that the observed value of the tangential velocity is almost constant with increasing distance from the center of Milky Way and this is solely due to 90% excess dark matter. This gives a ratio of 1:1.89 =Baryonic Matter: Dark Matter whereas at our Universe level it is 1:5. The contribution of Dark Matter goes on increasing as we go to the scaled up versions of the cosmological sub-systems[Appendix G]. SMBH (SgrA*) of Milky Way is a compact Radio Source, with an estimated mass of $3.7 \times 10^6 M_{Sun}$, and is presently very quiet and dim but in the past it was very active. The ultra dim nature of SMBH in non-Active Galactic Nucleii is explained by less gas, choked off Accretion and Radiatively inefficient mechanisms such as Advection Dominated Accretion Flow involved [54].

2.4 Primary-Centric Formulation as Applied to Galaxies
Figure 4 shows the stars orbiting the galactic center. It is hypothesized according to the New Perspective that stars are born at their respective first Clarke's Orbit ('aG1'). This orbit is highly unstable equilibrium. Hence they either fall short or fall long. If they fall long they are in expanding spiral orbit but since they are an insignificant fraction of the central SMBH their time constant of evolution is inordinately long so for all practical purposes they remain stay put at orbits only slightly larger than 'aG1'. The orbits have been determined in the paper by Schodal [14]. It remains to be shown that the orbits determined by Schodal are infact in the range of respective inner Clarke's Orbits [14].

If the incipient star falls short they will be launched on a death spiral. They will be on a contracting spiral orbit destined to be tidally shredded by the central SMBH once they enter the disruption radius of the SMBH. This kind of event was observed when GRB110328A was detected and analyzed. It was a Tidal Disruption Event (TDE).[Appendix F, 19,20].

It has also been confirmed that that Galaxies similarly tidally shred their satellite dwarf galaxies. In 1994, Ibata of Strasbourg Observatory in France observed a stream flowing into the Milky Way. It was identified as a flow of stars from the Sagittarius Dwarf Elliptical Galaxy. In 2001 Ibata again observed a dense line of stars piercing the Andromeda's Southern Halo and pointed to the center of Andromeda Galaxy. Possibly Andromeda Galaxy was tidally shredding the satellite dwarf galaxies M32 and M110 [55].

The discovery of the various tidal streams has convinced astronomers that chewing up of small galaxies by bigger ones-and more generally minor galaxy merger- are a frequent occurrence in the Universe [56]. Andromeda Galaxy has a much larger number of streams indicative of a more troubled past. Primary-centric formulation may explain the dynamics of minor merger with satellite dwarf galaxies. This has to be tested in future.

2.5 Architecture of the Universe as Proposed by Primary-Centric World View
Primary Centric World View proposes that in every sub-system of the Universe the most massive component is the Monarch of the given sub-system and acts as the pivot as well as the anchor of the given sub-system thereby stabilizing it and defining the

orbital configuration of its secondary components.
First level of hierarchy- BH is the Monarch of the Galaxy.
Second level of hierarchy- A Cluster is gravitationally bound Galaxies. The particular Galaxy in this family which hosts the heaviest BH attains the commanding position of the Monarch Galaxy of the given Cluster.
Third level of hierarchy- A Super-Cluster(SC) is gravitationally bound Clusters. The particular Cluster in this family of Clusters which hosts the Galaxy of the heaviest BH attains the commanding position of the Monarch Cluster.
This process of hierarchical gravitational bounding continues ad-infinitum. At every level of hierarchy the component hosting the heaviest BH attains the Monarchical Status.

2.6 Galaxies, their Types and Suitability as Anchors of Clusters and Super Clusters.[43,44,64 & Appendix C]]

Broadly speaking there are two types of Galaxies: Dorment and Active. Dorment Galaxies are the Galaxies where star formation has stopped due to non-availablity of cool gas and dust. Most of the massive elliptical Galaxies which are old have reached a limit of their growth. They will grow no further and the ratio of (mass of SMBH/mass of the bulge) = 1:1000. Dorment Galaxy is switched off in the sense that SMBH at its core has become passive. It has no accretion disc hence no radiation.

Active Galaxies are spiral galaxies hosting Active Galactic Nuclei(AGN). This implies that the SMBH at its core is rapidly accreting gas and dust and converting into IR, Optical Light, UV, X-ray and γ-ray by direct matter to energy transformation, by synchrotron radiation and by Inverse-Compton Upward Scattering. These Galaxies host SMBH which are less than 108MO and are known as Seyfert Galaxies.
When the mass of SMBH is greater than 108MO , then apart from being X-ray bright they have two powerful relativistic jets of atomic particles spiraling around the magnetic field created by rapidly spinning SMBH. In Figure F.15, Appendix F, an artist's conception shows a black hole surrounded by a disk of hot gas, and a large doughnut or torus of cooler gas and dust. The light blue ring on the back of the torus is due to the fluorescence of iron atoms excited by X-rays from the hot gas disk. Jets of high energy particles (white) are propelled away from the vicinity of the black hole by intense electric and magnetic fields.

Among the active Galaxies, 80% are Seyfert Galaxies and 20% are hosting SMBH which have polar conical relativistic jets. These are a sub-class of Blazers. In this sub-class, in a few cases the conical relativistic jets emerge out of the two poles of the galaxy and decelerate as they interact with the interstellar gas and dust and they turn on two radio-emitting lobes. This kind of Galaxy hosting Active Galactic Nucleus(AGN) with radio-emitting lobes is called QUASERS as shown in the Figure C.1, Appendix C_SOM.

Blazers and QUASERS Galaxies are the prospective candidates which will anchor the Cluster and super-cluster.
Among the Blazers and QUASERS we have cD Galaxy. This is also called centrally dominated galaxy or super-giant elliptical galaxy. These have a diameter of 1Mly as compared to 100,000ly diameter of Milky Way. This is a sub-set of more generalized Brightest Cluster Galaxy(BCG). Dynamical friction is believed to play an important role in the formation of cD galaxies at the center of a cluster.

Large galaxy in a cluster attracts smaller galaxies and dark matter in its wake. The over-density follows behind and slows down the large galaxy. Large galaxy spirals into the center of the cluster. Stars, gas, dust and dark matter follows and cD Galaxy is formed. These are massive elliptical galaxy or super-giant diffuse galaxy and generally BCG [58]. But cD Galaxy can be compact , lenticular galaxy also hosting exceptionally massive BHs as is the case of the recent finding of NGC 1277 (hosting BH of mass17billionMΘ where MΘ is the mass of Sun) in Perseus Cluster [59]. This is an example of nearby naked QUASER after being turned off: a monstrous BH in a tiny galaxy [60].Three giant elliptical galaxies have also been discovered hosting over-massive BHs namely Messier 87(hosting BH of mass 6.3billionMΘ) in Virgo Cluster, NGC 3842(hosting BH of mass 9.7billionMΘ) in Leo Cluster and NGC 4889(hosting BH of mass greater than 9.7billionMΘ) in Coma Cluster [61]. According to Primary-centric conjecture all the clusters should have cD Galaxies hosting over-massive BHs as their primary and as their anchor which imparts dynamical stability to the host Cluster.

Some of the prominent examples of cD Galaxies anchoring the clusters are [62,63].
NGC1277(lenticular compact galaxy) in Perseus Cluster hosted by Perseus-Pisces SC, NGC 6166 in Abell 2199 hosted by Hercules_a_SC, IC1101(supergiant lenticular galaxy) in Abell 2029 hosted by small SC Messier 87 in Virgo Cluster hosted by Local SC, NGC 1316(lenticular compact galaxy) in FORNAX Cluster hosted by Local SC, NGC 547 in Abell 194 hosted by ?SC, NGC 2832 in Abell 779 hosted by ?SC, NGC 4889 in Abell 1656 hosted by COMA SC, NGC 7768 in Abell 2666 hosted by a small SC [64,65]. My hypothesis tells me that these cD Galaxies (giant elliptical or compact lenticular) must also be hosting similarly over-massive BHs and are suitable targets for investigations as was done in case of NGC1277, M87, NGC3842 and NGC 4889.
Mcdonell over-massive BHs are found predominantly in BCGs. In early Universe (z = 2 to 4.5), QUASERS invariably host BHs with mass > 10billionMΘ . But in last 10Gy from today these extreme BHs have not been accreting enough but they have been powering their respective QUASERS radiation output as a result QUASERS have been scaled down to disk-dominant compact galaxies of radius 2kpc.

QUASERS and elliptical galaxy formation are predicted to rise from the mergers of elliptical galaxies triggered processes and there is growing evidence that present day massive elliptical galaxies once hosted the most luminous high-redshift QUASERS [66,67]. However definitive classification of these QUASER's host galaxies has remained elusive.
Measurement of over-massive BHs in giant elliptical NGC3842 and NGC4889 give circumstantial evidence that BCGs host the remnants of extremely luminous QUASERS.

The number density of BCG ($\sim 5 \times 10^{-6}$ Mpc^{-3}) is consistent with number density of BHs($\sim 3 \times 10^{-7}$ Mpc^{-3} to 10×10^{-6} Mpc^{-3}) with masses of $10^9 M_\Theta$ to $10 \times 10^9 M_\Theta$ predicted from mass of BH-Luminosity relation and from the luminous function of nearby galaxies. Dynamical measurement of BH mass now range over 4 orders of magnitude from $10^6 M_\Theta$ to $10^{10} M_\Theta$. We also find that the bulge (or the pseudo-bulge) luminosity is not a good predictor of the mass of BH.

This means BCGs are destined to be the Monarch Galaxies of their respective host Clusters.

2.7 Cluster of Galaxies

Galaxies are clumped in Clusters. It is not clumping. The galaxies are gravitationally bound into a Cluster. Milky Way belongs to the cluster named Local Group. Local Group is also a disk like structure with a diameter of 10 million ly. It comprises of 3 large galaxies and 46 dwarf galaxies and 700 billion stars in total. The three prominent galaxies present in the Local Group Cluster(LGC) are: Milky Way, Triangulum (M33) and Andromeda Galaxy. Their properties are given in Table 1. The center of mass(COM) of the two most massive galaxies , namely Milky Way and Andromeda Galaxy, constitute the center

of the cluster. This COM acts as the anchor of the whole system contributing to its stability. The disk of the Local Group is also rotating from Primary-centric point of view and from stability consideration though the scientists at present find no reason to speculate on possible rotation of the cluster around its center of mass [68].

Dark matter fills up the Local Group Halo. It interacts with the visible matter gravitationally and it is 10 times as abundant in Local Group. Quantum seeds caused matter to clump more densely in certain spots. Dark matter sits in these spots which grew into the structure that merged and became giant clouds called haloes. These haloes have trillion solar masses.

Milky Way has dwarf galaxies as satellite galaxies. These satellite galaxies are Large Magellan Cloud(LMC), Small Magellan Cloud(SMC), Sagittarius Dwarf Elliptical, Ursa Minor Dwarf, Draco Dwarf, Sextons Dwarf, Sculptar dwarf, Formax Dwarf, Leo I and Leo II.As we have already discussed in Section 1.4 that these dwarf satellite galaxies are responsible for the growth of our Milky Way through minor mergers.

	diameter	Absolute magnitude
Andromeda Galaxy	140,000ly	-21.1(Sb)
Milky Way	90,000ly	-20.6(SBbc)
Triangulum Galaxy(M33)	55,000ly	-18.9(Sc)

Table 1. The three prominent galaxies of the Local Group.

3. Super Cluster

Several clusters are gravitationally bound together to form Super-Cluster. Super-cluster is also disc like structure having a super-massive cluster as its primary to anchor the whole sub-system.

Our Local Group belongs to Local Super-Cluster(LSC) also known as Virgo Super Cluster. It has a diameter of 100 to 150 million light years. LSC has four Clusters(Virgo Cluster, Local Group , Fornax Cluster and Fridaurus Cluster) and 196 Groups of galaxies.

LSC contains 2500 large galaxies, 50,000 dwarf galaxies and 200 trillion stars. Amongst all these galaxies and dwarf galaxies, M87 in Virgo Cluster hosts the heaviest BH with mass 6.3billionMΘ [69]. Hence M87 is the Monarch Galaxy in Virgo Cluster and in turn lets Virgo Cluster attain the position of Monarch Cluster in LSC.

The most massive of the four clusters namely Virgo Cluster which hosts the Monarch Galaxy M87 is at the center of the Local Super Cluster giving stability to the LSC configuration. Hence Virgo Cluster attains the commanding position of Monarch Cluster. The Local Super-cluster consists of a flattened disk and spherical halo. Flattened disk is 5 million ly thick. It contains 60% of the galaxies and remaining 40% reside in the

halo.
This process repeats itself ad-infinitum as shown in Figure 3. Galaxies appear to be organized on the largest scale at first order in Clusters and at second order in Superclusters. Gregory and Thomson suggest three possible configurations of Superclusters [68]:
i. Single/halo supercluster- The prototype is the Local Super Cluster centered around VIRGO cluster and contains many outlying groups.
ii. Binary Supercluster- COMA(A1656)/LEO(A1367) in COMA SC are widely separated binary and A2197/2199 in Hercules SC are nearly in contact.
A. Extended linear Super cluster (Perseus-Pisces SC) such as the extended chain of clusters A426 through A347, A262 onto NGC507 & NGC383. Rich clusters can develop only in close association with super clusters. A426 hosts the most massive Galaxy1277 which in turn hosts the most massive BH discovered till now with BH mass = 17 billionMΘ [59]. Since this is an extended chain there must be a comparable Cluster hosting a comparable Galaxy with comparable BH mass on the far end of this extended chain as seen in Figure 2.

The first order, second order, third order clustering results in the development of thread like structure of the Cosmic Web as shown in Figure 2.
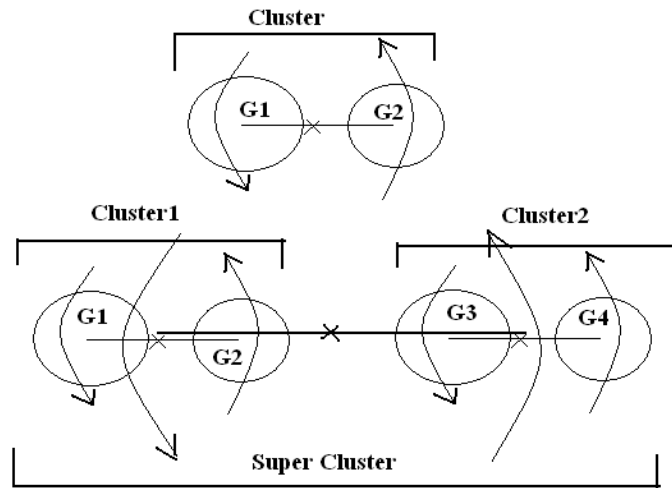
Edge on view of this extended linear Super Cluster will give rise to filament seen in the Cosmic Web.

Figure 6: Edge on view of the extended linear super cluster gives rise to the filament seen in the Cosmic Web.

Distribution of galaxies is anything but random. They are distributed on surfaces, almost bubble like, surrounding large empty regions or "Void". Galaxies tend to collect into vast sheets and super clusters of galaxies surrounding large voids giving the Universe a cellular appearance.[SOM_Appendix C]
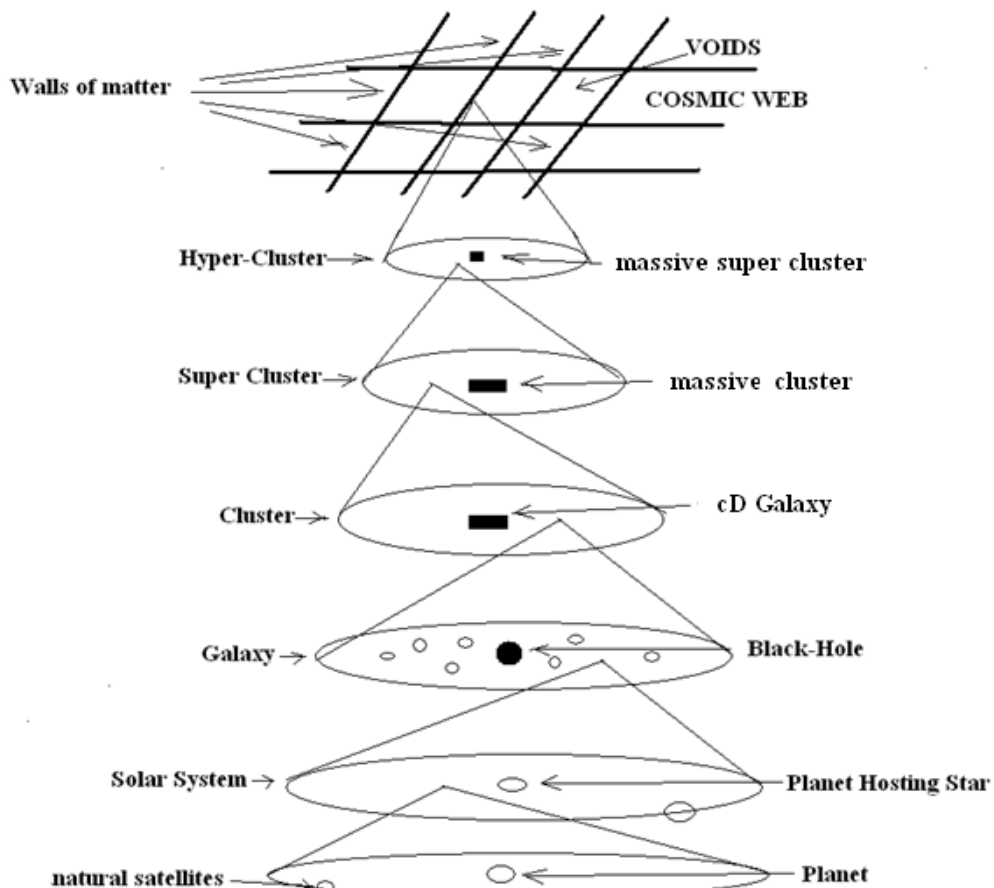

Figure 3: Fractal View of the Universe.
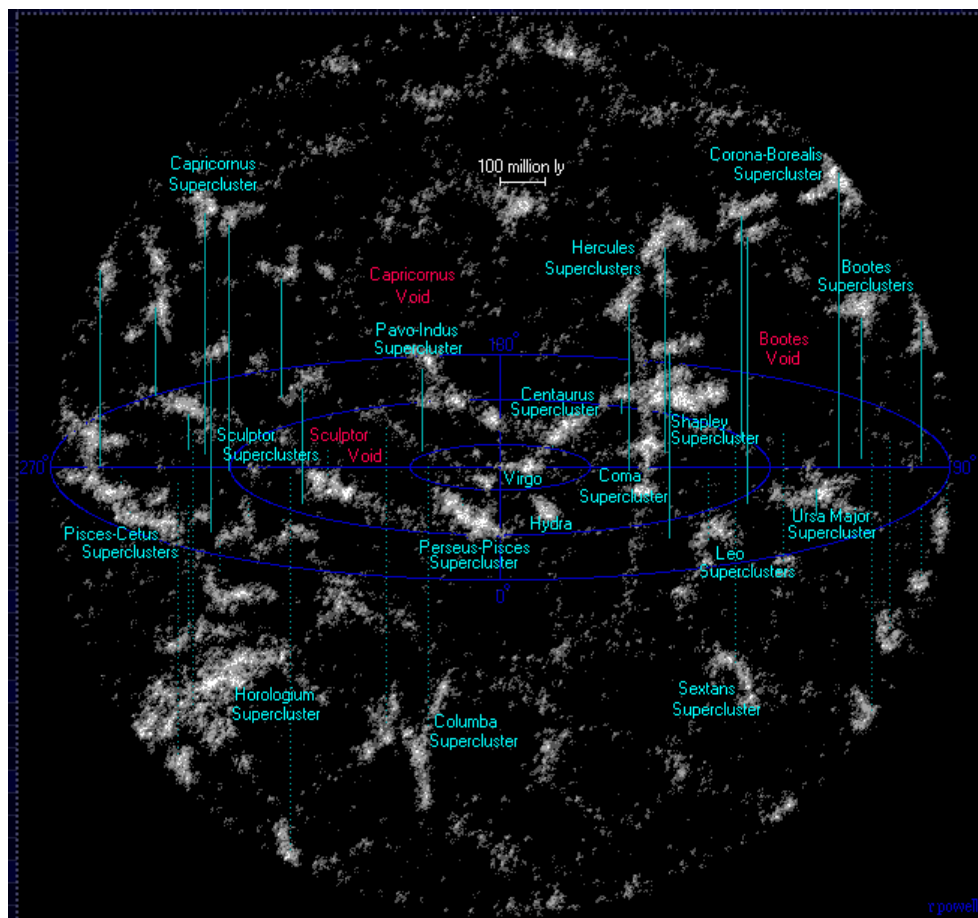
4. Large Scale Structure of the Universe

Figure 4: A map of the nearest Superclusters and Voids- the Universe within 1 billion light-years. [Credit: www.atlasoftheuniverse.com/superc.html]

A typical Supercluster flattened disk has a diameter of 100Mpc and its total mass is in the range of 1016MO. Galaxies and clusters of galaxies are not uniformly distributed in the Universe instead they collect into vast clusters and sheets and walls of galaxies interspersed with large voids in which very few galaxies seem to exist.

Ref	Supercluster	No.of clusters	No. of Galaxies	Total mass of the S.C	Dia.	Monarch Cluster	Monarch_Gal. BH mass ($\times 10^9 M_\odot$)
1,2	Corona Borealis (most distant-1bly)	10	1555	$10^{16} M_O$	26Mpc	A2065_nearest the centroid. Compact core of five clusters in a stage of rapid gravitational collapse.	C.O.M of PGC54888 & PGC54883
13, 14,15	Hercules 500Mly distant (binary super cluster)	Northern S.C. (3C) 400Mly; Southern S.C. (9C) 500Mly	(A2197, A2199, A2162) in Northern S.C. (A2148,A2151,A2152,A2147,A2063,A2052,A2107) in Southern S.C. The northern and southern S.C are interconnected By a wall of galaxies.			Center of mass of the A2199 & A2151	N6166_Large Type EGalaxy cD_BCG hosted by A2199 (North SC) N6056_ Lenticular Galaxy Hosted by A2151 (South SC)

8	COMA (binary super cluster)††	2 clusters(richness class 2) & 16 major groups				Center of mass of COMA (A1656) and LEO (A1367)	NGC4889 (>9.7) NGC3842 (9.7)resp.
5	Shapley*	25 significant clusters‡				A3558(nearest the centroid of SC,richness4)	ESO444-46 (enormous Elliptical G Dia=340kly)
7	Pavo-Indus	A3742& A3656 of richness 0 andA3698of richness 1; 8 prominent groups;				?	?
3,4	Centaurus**	Nearest large Super-cluster	Rich 0_A3526, A3574,A3581 Rich 1_A3565, A3627,A1060		30Mpc	A3565	A3565-BCG (largest Elliptical G) (1.3) [Benta et.al. (2007)]
9, 10, 11	Virgo or Local Group Supercluster† (irregular SC)	2 major clusters (Virgo and Local Group)	100 clusters & galaxy groups		33Mpc	Virgo Cluster	M87 (6.3)
3,4	Hydra	A1060, Antila Group, 12 Galaxy Groups	NGC3311,NGC3309,NGC3312,NGC3054, NGC3087,NGC3250/3318, NGC3256/3261,Antila, NGC3263/3366,NGC3347, NGC3393/3463,NGC3557		30Mpc	Hydra Cluster or A1060,richness class 1	NGC3311_ Giant elliptical Galaxy ,BCG (lies at center of local Pot.Well) [Fitchett et.al. (1988)]
12	Sculptor††† Two SC coupled as extended linear SC forming Sculptor Wall	6C Phoenix &5C Sculptor	PhoenixSC (A2896,A2836,A2731,A2877,A2870,A2806) SculptorSC (A2717,A4008, A4012,A4013, A4059)			?	?
16	Leo		A1228 and A1185 are rich clusters			A1185	NGC3550 (BCG)
6	Perseus-Pisces		A426 has 1000 galaxies, high ratio of spiral galaxies: elliptical galaxies;			A426	NGC1277 (17)
20	Horologium S.C.	40 clusters,	30,000 large galaxies, 1×10^{15}stars	$10^{17}M_O$	550Mly	Vertical Axis	?
16	Bootes	N.Bootes +S.Bootes	North(A1898, A1873,A1861, A1800,A1775) South(A1781, A1831,A1795, A1827,A1825, A1828)			?	?
21	Catalog No.154	A2023, A2028, A2066, A2029				A20291 [Walker et.al. (2012),Lewis et.al. (2002)]	IC1101[2] [Uson et.al. (1990)]
21	Catalog No.215	A2666, A2634				A2666 (small cluster)	NGC7768 (elliptical)

Table 2: List of Super-clusters and their core.

‡Shapley S.C. packs as much as 20 major clusters in a space $(60\times100\times200)$Mpc^{-3} occupied by Virgo S.C. which has only 1 major cluster. This is 50 times the average density of Abell Clusters at same declination~30°.

*Abell Catalogue contains only 5 clusters with richness 2 within 1 bly from the Earth. Three of the 5 rich clusters lie in Shapley S.C. These three are A3558, A3559 and A3560.

† Mass of LSC ($\sim7.5\times10^{14}$MO/h) is located in a filament roughly centered on the Virgo Cluster and extending over 40Mpc/h. Here h=HO/100km.sec-1Mpc^{-1} and HO =Hubble Constant=75 kmsec-1 Mpc^{-1}. Local Group is located in an adjacent smaller filament which is not a part of the main body of the LSC and has a peculiar velocity of 250km/s towards the Vigo Cluster. Milky Way, a thin rotating disk of 100 billion stars lies on the outskirts of a concentration of many thousand galaxies, This concentration is known as "The Great Attractor". Closest part of the Great Attractor is called LSC. This flattened concentration of galaxies lies along the supergalactic plane.

††The COMA Supercluster lies at the center of the Great Wall, a vast filament of galaxies that stretches over100Mly, one end terminating at Hercules Super cluster. This was one of the first Walls to be recognized.

††† Two Super Cluster in the Sculptor and Pheonix regions of the sky mark the position of a very long wall of thousands of Galaxy Groups stretching over nearly 1 Gly. This is probably the longest of the nearby wall of galaxies.

**Centaurus Super Cluster lies near the Great Attractor and its dominant cluster A3526 is held responsible for this great attraction.

1 A2029 is a dark matter dominated Cluster with a total mass of 100 trillion mass of Sun. Assuming that cD Galaxy IC1101 dominates the optical cluster within its effective radius (Re = 52".76h70-1kpc) a total mass to light ratio M/LV ≈ 12(MO/LO) at r < 20h70-1kpc rises rapidly to >100(MO/LO) beyond r = 200 h70-1kpc. The consistency with a single NFW mass component and the large M/L suggest that Cluster is Dark-Matter dominated down to a very small radius (r < 0.005rvir). This is an extreme example of DM.

2 IC1101 is a supergiant elliptical galaxy and occupies the central position in A2029. Its luminosity is 2×1012LO and semi-major axis is 1.2Mpc. Both these attributes make IC1101 the BCG in A2029. This central galaxy is remarkable for its size as well as for its uniformity of its structure. Both these characteristics suggest that IC1101 must have been formed in the earliest phase of clustering and it hosts the heaviest BH in its region.

SC	members	Monarch Cluster
Corona Borealis	A2122,A2092,A2067,A2075,A2061 ,A2089, Abell A2056,A2005,A2065,A2019 Comment: One of a few extremely massive, dynamical isolated galactic system in an initial stage of virialization.	A2065
Hercules	Northern S.C. A2197/A2199,A2162; Southern S.C. A2147,A2151,A2152, A148, A1983, A 2040, A2052, A2063, A2107. The northern and southern S.C are interconnected. A2151(Hercules Cluster) has large spiral, elliptical and lenticular galaxies but no giant elliptical galaxies. A2199 is a rich cluster anchored by an enormous elliptical galaxy at the center.	Center of mass of the N.(A2199) and S.(A2151) superclusters.
Shapley	25 significant clusters	A3558(nearest the centroid of SC,richness4)
Centaurus	4 rich clusters: A3526,A3565,A3574,A3581 major groups with 10 to 20 galaxies per group. Hundreds of small groups of galaxies	A3565
Sculptor	6 clusters in region Phoenix of richness class 0 and 5 clusters in Sculptor region where 4 clusters have richness class 1	?
Leo Sits at the border of Leo and Ursa Major at a distance of 450Mly	A1257, A1228, A1185,A1267, A1177, A1142, A999, A1016	A1185

Perseus-Pisces (compact disc has a dia 300Mly next to a Void of dia.100Mly which has a few galaxies e.g.NGC383, NGC507)	A426 (richness class 2), A347, A262, 15 major groups, Pisces Cluster	A426
Horologium S.C. Nearest is 700Mly and farthest is 1.2Gly distant	40 clusters, 5000 galaxy groups	This extended length of clusters orbiting around a vertical axis with cylinderical symmetry
Bootes (800Mly distant, sits next to Bootes Void-300Mly dia.) Binary S.C	N.Bootes S.C.(1 Gly distant), S.Bootes S.C.(830Mly) N.Bootes consists of A1775, A1800,A1861,A1873, A1898 S.Bootes consists of A1795,A1825,A1828,A1827,A1831	?
Catalog 154(Ref.21)	A2023,A2028,A2066,A2029	A2029
Catalog215(Ref.21)	A2666,A2634	A2666

Table 3: Detailed List of the members of Super-Clusters

Cosmic voids and supervoids are large volumes of space that are devoid of baryonic matter as well as dark matter. Super-Void is a visual entity which is devoid of galaxies regardless of luminosity, size or shape. These are circular in cross-section and apparently closed on all sides by galaxies. The filamentary structure of galactic superclusters surrounds the void. Largest is 100Mpc in diameter.

	Super-void	nature
	Local Void	60Mpc in diametrr. It is surrounded by Virgo SC. Local Group lies at the edge. Dwarf galaxy ESO 461-36 lies within the void but appears to be moving to the boundary at 216Km/s
17,18	Bootes	First to be discovered in 1981. 300Mly in diameter. At the edge of the Void almost 60 galaxies were detected which were unusal or of disturbed morphology.
	Eridanus Supervoid	It is a conjectural void based on the cold spot in WMAP. Its diameter is 150Mpc and lies at a distance of 1.8Gpc to 3Gpc.
	Taurus Void	Figure 12 gives the Taurus Void. Right next to the long dense wall of galaxies of Perseus-Pisces Super-Cluster, lies a large circular void of diameter 100Mly. This is known as the Taurus Void. For all practical purposes it is devoid of galaxies except a few. Prominent among them are UGC 2627 and UGC 2629 as shown in Figure 13.

Table 4: List of Super-voids

Filaments and Walls: Filaments are long, thin structures of galaxies like threads much longer than their cross-section. Walls are much wider but flatter than filaments. Their longest length is 0.5×10^9Mpc.a
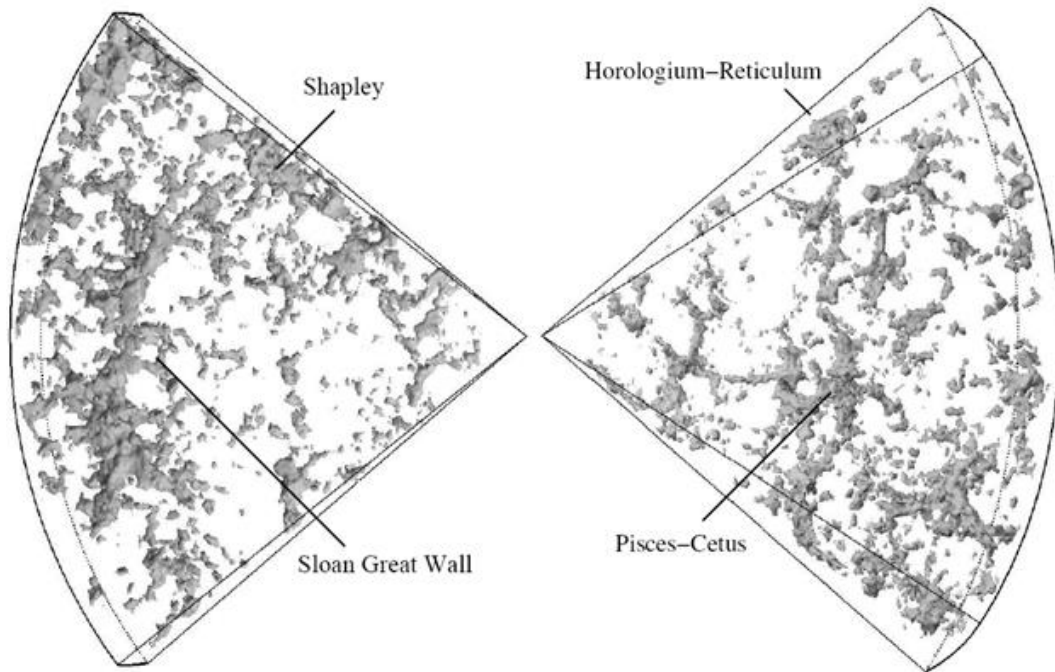
Figure 5: The Sloan Great Wall was first identified in 2003 as part of the Sloan Digital Sky Survey, and is probably the largest structure in the known Universe. It is around 420 Mpc (c. 1.4 billion light years) long, and around 300 Mpc away, though estimates do vary. Some parts of it are not gravitationally bound together and may never be, so in some ways, we should not really consider it as a single coherent structure. Nevertheless, it is impressive. Shown in the image to the right with the Shapley Supercluster, and parts of the Pisces-Cetus filament and Horologium-Reticulum Supercluster.
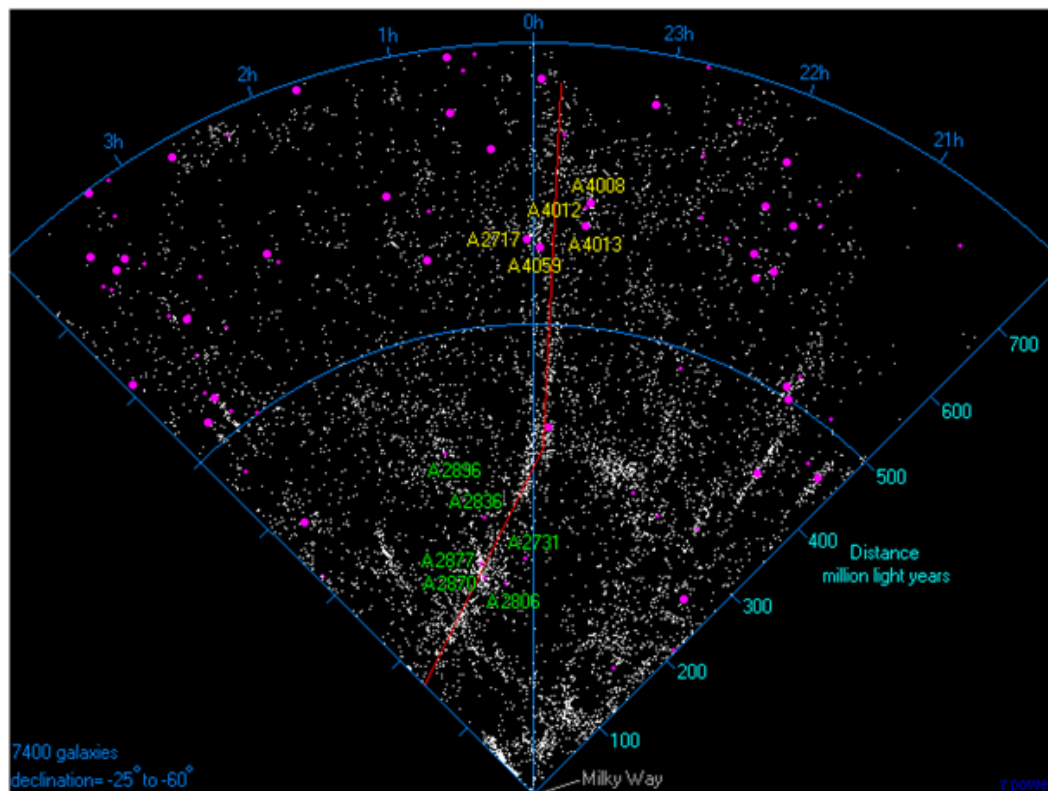

Figure 6: Sculptor Wall (Southern Wall). The map above is a slice of the Universe which shows the Sculptor Wall. The map is a plot 7400 bright galaxies in the vicinity of the Sculptor Wall. Top of the map is 800Mly from the bottom where Milky Way is situated. Red line shows the Sculptor Wall. Nearest part of the wall (Phoenix Super Cluster) lies next to a large rectangular void. This is one of the largest void in the nearby Universe.

Wall	
COMA Great Wall	COMA S.C and Hercules S.C. together form the great wall. Large agglomeration of clusters that shape 3-D Spider web of filaments and sheets surrounding vast empty voids. This gives a foam like structure of the universe at the largest scale.
Pisces-Cetus Filament	This includes Virgo Super cluster or Local Super Cluster. It is 300Mpc long and 50Mpc wide.
Perseus-Pegasus Filament	This lies adjacent to Pisces Cetus Filament. It includes Perseus-Pisces Super Cluster. It is 300Mpc long.
Sloan Great Wall	It is shown in Figure 4. Discovered in 2003. It is situated at 300Mpc and it is 420Mpc long.
Sculptor Wall or Southern Wall	It is shown in Figure 5.Two Super Cluster in the Sculptor and Pheonix regions of the sky mark the position of a very long wall of thousands of Galaxy Groups stretching over nearly 800 Mly. This is probably the longest of the nearby wall of galaxies. Nearest part in the figure lies next to a rectangular void. This is known as the Sculptor Void and is the largest void in the nearby Universe.

Table 5: List of Walls and Filaments

Ref	Monarch Cluster	No. of Galaxies of Richness class 2	Host supercluster	Total mass of the Cluster	Diameter	Monarch Galaxy
A	A2065		Corona Borealis			PGC54888+ PGC54883
B	A426	1000	Perseus-Pisces S.C.		863'	NGC 1277 (LenticularG)
C, D, E	COMof A1656‡+ A1367	1000 galaxies	COMA S.C.	90% mass is the dark matter	800 galaxies accomm-odated in 100×100arc min	NGC4889 (giant elliptical)+ NGC3842 (giant ell.)
F,P	COM of A2151+ A2199 (Hercules Cluster)	100	Hercules S.C.	Rich in spirals		NGC6056+ NGC6166
G	A1060 or Hydra	Richness Class 1 & Lacks hierarchical structure	Hydra S.C.			elliptical NGC3311** (astrometry center)
H,O	A3565	Rich_1-A1060,A3565,A3627	Centaurus S.C.			A3565-BCG
I	A3558 (Shapley S. Cluster)		Shapley S.C.			Enormous Elliptical Galaxy ESO 444-46 with dia.340kly.
J	?	20 galaxies	Pavo-Indus S.C.			?
L, M¶	VIRGO C. Or LSC	2 major clusters (Virgo and Local Group)	Virgo S.C.		15Mly	M87•• at the center.
N	?	Sculptor and Pheonix S.C.	Sculptor S.C.			?
Q	A1185	It is a clumpy cluster	Leo S.C.			NGC3550
R	A1795 (840Mly distant)					A massive elliptical galaxy PGC49005 sits at the center

S	Abell 2666	A2666,A2634				NGC7768 Supermassive cD galaxy
T	Abell 779 (300Mly distant)	30 member galaxy. It is small scale cluster	NGC2832, NGC2830 and NGC2831 form a group.	S.E. edge of Lynx	50'arc	NGC2832 a giant elliptical galaxy
U,V***	Abell 194 (265Mly)	100 galaxies Linear cluster				NGC547 luminous Radio galaxy
X	Abell 2029	A2023,A2028,A2066,A2029				IC1101 Super-giant lenticular cD galaxy
Y	FORNAX					NGC1399

Table 6: List of Clusters

*Clusters with isothermality and lack of central excess emission are simple and lack hierarchical structure. Clusters with hierarchical potential shape have a single dominant galaxy at the center which is cD Galaxy. In contrast Clusters which lack hierarchical potential shape have few galaxies with equal luminosities as is the case with Antilla and A1060.

‡It is said that smaller galaxies(spiral and irregular galaxies) have merged to form large elliptical and lenticular galaxies. Hence we find very few spiral galaxies after billion years. Elliptical and Lenticular galaxies are found in the central region and spiral and irregular galaxies are found in the outer region.

•• M87 has a conical jet of electrons and subatomic particles being propelled out transverse to the equatorial plane of M87. SMBH of mass $6.3 \times 10^9 MO$ at the center of M87[McConell et.al.(2011)] is accreting gas and dust from the surrounding [69]. 50% is concentrated in the accretion disk and 50% is propelled outward by the intense magnetic field.[Pringle 1981] [70].

**The Giant Elliptical Galaxy NGC3311 does not appear to lie close to the Kinematical center of any of the proposed sub-groups [Fitchelt and Merritt 1988] [71]. It is possible that the dominant galaxy lies at the center of the potential well

***There is distortion in the Hubble Flow. There seems to be a large attractor towards Hydra-Centaurus Super Cluster. This produces an anomaly in Local Group Motion. Local Group is affected by Virgo Cluster and by its surrounding Local Super Cluster. Local Group within Local Super Cluster and bulk motion of Local Super Cluster towards Hydra Centaurus Attractor- both these components are 300km/sec.

¶ Milky way is moving with a velocity of 455km/s towards the Great Attractor, 185km/s towards Virgo Cluster and away from the Local Void at a velocity of 260km/s.

Most Clusters are in gravitationally bond clusters of 10 to 10,000 galaxies. Most clusters are poor clusters 1Mpc in size. Rich clusters are 3 to 10Mpc in size. Poor clusters are populated by spiral galaxies and rich clusters are populated by elliptical galaxies. Rich clusters are anchored by 1 massive elliptical galaxy or by the center of mass of a few massive galaxies.

Figure 7: Virgo cluster. It is a moderately rich cluster of galaxies which has 2000 galaxies including giant elliptical galaxy M87. It is 15Mpc distant and 3Mpc in size.M87 is its anchor

Figure 8: COMA Cluster(A1656). It is extremely rich cluster of galaxies. It has 10,000 galaxies. It is 90 Mpc distant and 5Mpc in diameter. Its anchor is NGC4889.

COMA cluster is the densest cluster known. It contains 1000 galaxies and each galaxy has billions of stars. Galaxies in the disk are elliptical and Galaxies in the halo are spiral. Central core formed of NGC4889. It is a giant elliptical of 250kly dia. NGC4889 provides stability and minimum Gibb's Free Energy to the whole configuration. The disk of COMA Cluster is 5Mpc in diameter.

The Cluster contains visible stars and very hot gas distributed evenly through the cluster. Total hot gas mass = 6×mass of the visible stars;
Dark Matter = 6×hot gas mass=6×6×mass of the visible stars=36×mass of the visible stars.
Hence visible star mass constitutes only 2.7% of cluster's total mass in COMA Cluster.
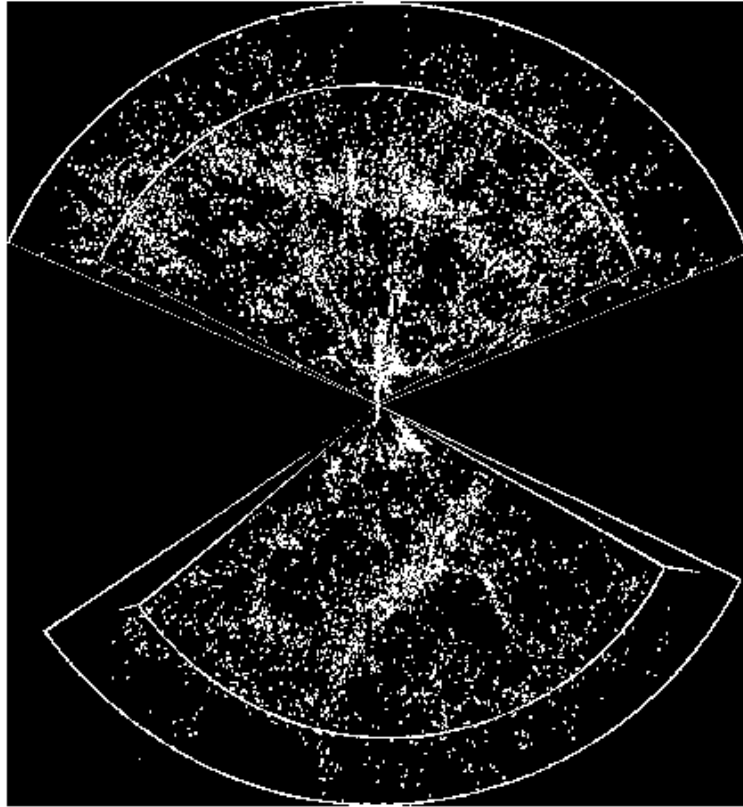
Figure 9: Two Slices of our Universe in North and South hemispheres. Each dot represents a galaxy
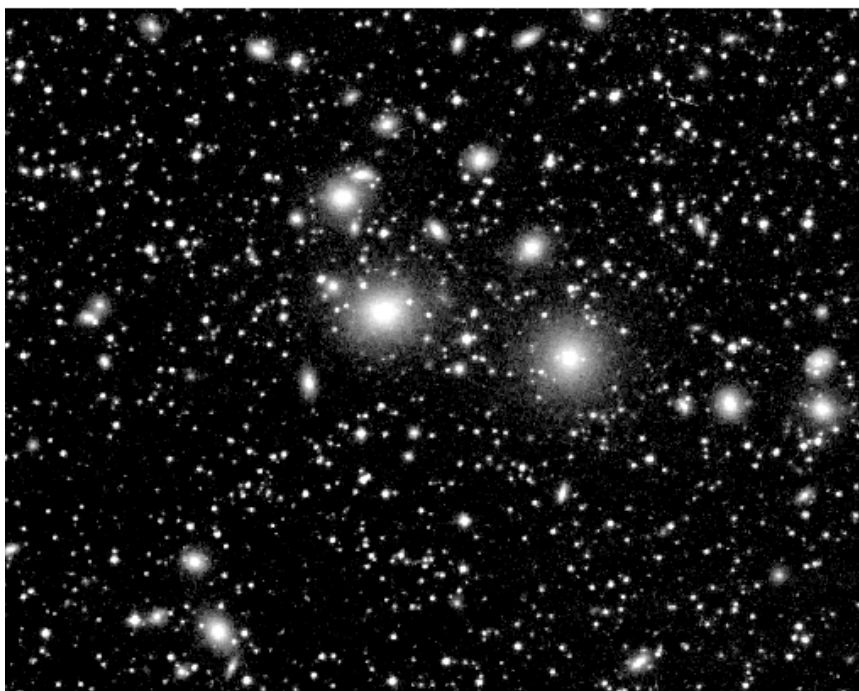

Figure 10: The Perseus Cluster of Galaxies (Abell 426) anchored by NGC1277[Bosch et.al.(2012)] [59].
Credit and Copyright: Digitized Sky Survey

Perseus Cluster of Galaxies by Doppler Shift has a recession velocity of 5366Km/sec. Using Hubble Law:

Distance of this Cluster = d = $v_{recession}$/H

= (5366×10³m/s)/(71×10³m/s/Mpc) = 75.577Mpc = 75.577×3.26Mly

= 246.38Mly.

So Perseus Cluster is 246.38Mly distant from us with a size of arc angle 15°.

The arc angle 15° corresponds to = θ (in radians)×d

=(π/180°)×15°×246.38Mly= 64.5Mly.

So Perseus Cluster has a diameter of 64.5Mly.

It is a cluster of galaxies in the constellation Perseus. It contains thousands of galaxies immersed in a vast cloud of multi-million degree Celsius of gas.Center of the Perseus Cluster is a prodigious source of X-Ray radiation. This source has been called Per XR-1 and is associated with lenticular Galaxy NGC 1277 situated right at the center of Perseus Cluster [Fritz et.al. (1971), Bosch et.al.(2012)] and anchoring and stabilizing Perseus Cluster. Overall Spectral Energy Distribution (SED) displays two peaks: IR peak associated with synchrotron radiation and X-ray/γ-ray associated with Inverse-Compton Emission [59,72].

Previously NGC1275 was mistaken to be the Monarch Cluster. Actually NGC1275 is AGN_Blazer sub-class hosting SMBH of mass greater than 108MSun ~ 1010MSun . There is an accretion disk which is accreting into SMBH with high Eddington Luminosity[See SOM_Appendix F_ Figure F16]. Whenever supply of material for accretion comes within the sphere of influence SMBH is switched on as a powerful X-ray source otherwise it is dormant and quiet SMBH. NGC1277 is not AGN but is hosting the heaviest BH known till date. The mass of the BH is 17 billionMʘ [Bosch et.al.(2012)] [59].

Mass of BH correlates with velocity dispersion of the Galaxy Bulge as well as with Bulge Luminosity. The expected spectrum of an accretion disc around SMBH peaks in Opt-UV band. In addition a corona of hot material formed above the accretion disc. This causes Inverse-Compton Scatter. The photons in Opt-UV band are upward frequency translated to X-Ray Band. This is how it becomes a prodigious source of X-ray. A large fraction of AGN's primary output may be absorbed by interstellar gas and dust close to the accretion disk and this is re-radiated at IR.

There can be an emission of conical beam of energetic charged particles and X-Rays from the north and south pole of AGN due to swirling mass of gas and dust into the rapidly spinning SMBH[See SOM_Appendix F_ Figure F15].
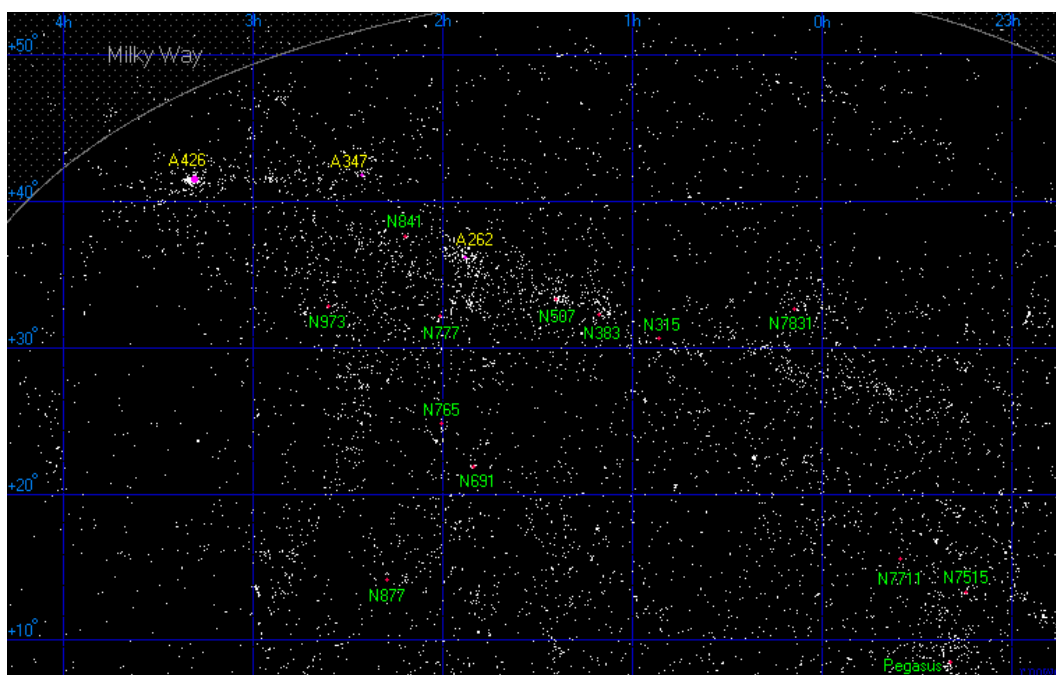

Figure 11: Perseus-Pisces Super-Cluster

Perseus-Pisces Super-Cluster is a long dense wall of galaxies at a distance 300Mly and its length is 300Mly. It is one of the most massive super-clusters within 500Mly.
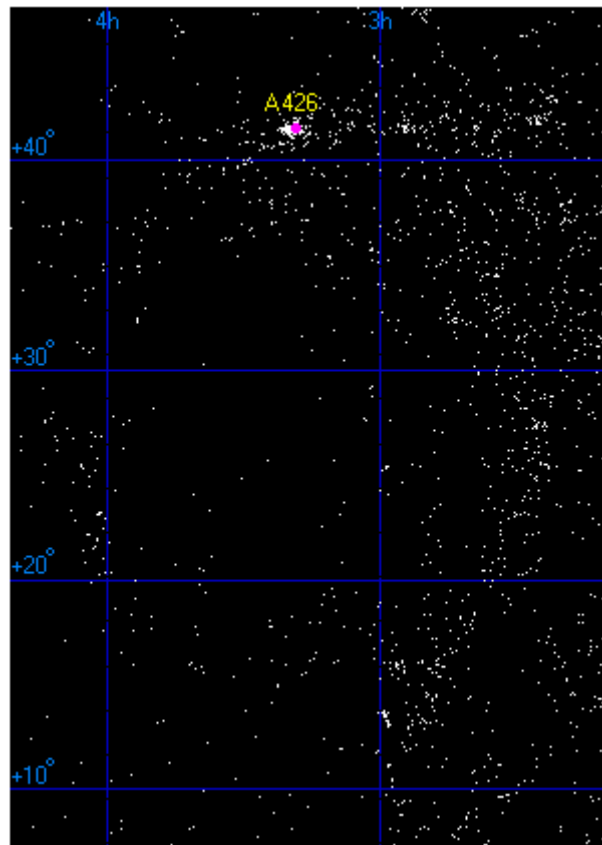
Figure 12: The Taurus Void

Right next to the long dense wall of galaxies of Perseus-Pisces Super-Cluster, lies a large circular void of diameter 100Mly. This is known as the Taurus Void. For all practical purposes it is devoid of galaxies except a few. Prominent among them are UGC 2627 and UGC 2629 as shown in Figure 13.

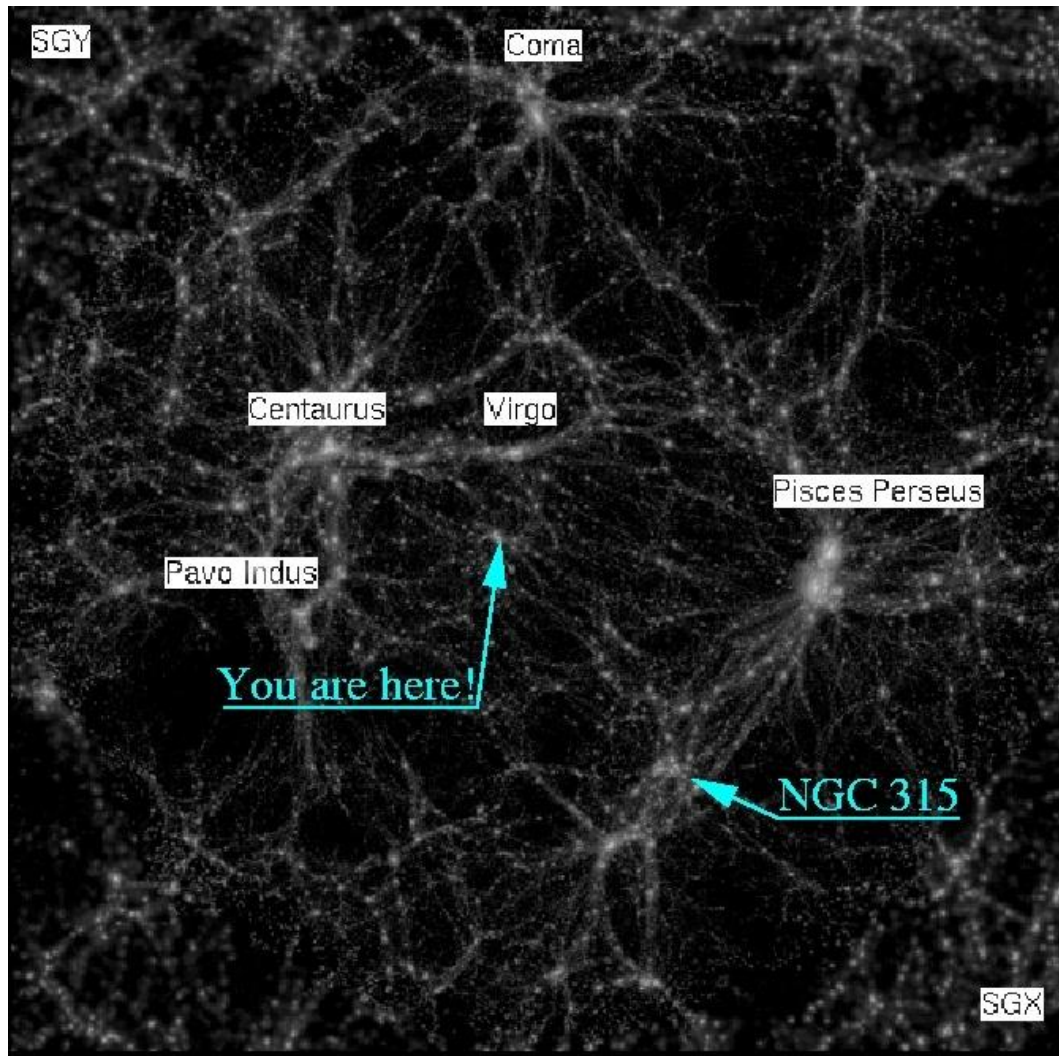**Figure 13:** Few prominent galaxies in the void namely UGC 2627 and UGC 2629

Figure 14: Filament structure of the Universe

5. The first evidence of the evolving Universe.[Pastorella & Patal, 2008]

On Nov.11, 1572, Brahe was a witness to a brilliant new star in the constellation Cassiopeia. The star became as bright as Venus and could be seen for two weeks in broad daylight. After 16 months it disappeared. Brahe documented unlike our Moon and the planets, the light's position did not move in relation to the stars. That meant it lay far beyond the planets of our solar system.

The comtemporary view of the distant heavens was that it was perfect and unchanging. The birth of a new star and its subsequent disappearance came as a rude shock to the commonly held belief that the heavens were static.

6. The detection of Novae, Supernovae and Dark Matter. [Heckman & Kaufmann (2011)] [39].

In 1933, Fritz Zwicky was working on COMA cluster of galaxies. There was too little visible matter to hold together the cluster together. The clusters seemed to be orbiting around a central massive core too fast. Four decades later this kind of missing mass was found in Galaxies also. So it was postulated that each galaxy is embedded in a vast clump of dark matter known as 'halo'. Dark Matter is inferred from the gravitational effects and from the gravitational lensing of the Cosmic Microwave Background Radiation (CMBR).

In a work by Klypin,Anatoly et al (2003) it was shown that if $Y\bullet = MO/LO$ for Sun-like-Star the mass to luminosity ratio for Galaxies and Clusters comes out to be $Y\bullet = K.(MO/LO)$ where K = 2 to 10 [73]. For Local SuperCluster 'K' come out to be 300 and for Milky Way it comes out to be 2.7. This variation in 'K' is the clinching evidence in favour of the dark matter.

Wilkinson Microwave Anisotropy Probe (WMAP) measured Big Bang's after-glow "Cosmic Microwave Background Radiation". The temperature was found to vary even so slightly. The pattern of hot and cold spots reveal the hetrogenity at the age of 400,000 years after the Big Bang. This wee bit hetrogenity could explain the present large scale stuctures of the COSMIC WEB only if Universe has 4% ordinary matter, 23% dark matter and 73% dark energy, all interacting through gravity. This dark matter can be explained in one of the following manners:

i. If space has miniscule extra dimension then dark matter could

exist;

ii. Or it could be introduced to patch up the conceptual hole in the theory of strong force that binds the protons together in the nucleus;

iii. Or it could exist acording to super-symmetry predictions. Super-symmetry predicts that every particle has a heavier super partner. The lightest among them is $100m_p$. These are called Weakly Interacting Massive Particle (WIMP).

Super symmetry of matter predicts that Big Bang should leave right amount of WIMP after the Big Bang which will correctly account for the 23% of dark matter required for maintaining the Cosmic Web of the visible matter intact.

7. Group of Galaxies and Cluster of Galaxies

Universe displays a hierarchical structure. Stars are not random but are clumped together in galaxies. Galaxies are not scattered randomly but are clumped together as Clusters. A Cluster may typically contain 10 to 10,000 galaxies. Clusters of Galaxies are similarly clumped in superclusters. The evidence is there that super-clusters are in turn clumped as hyper-clusters. It is more appropriate to say that stars are gravitationally coupled in higher order binary called Galaxy anchored by SMBH and Galaxies are gravitationally coupled in higher order binary called Cluster anchored by cD Galaxy and Clusters are gravitationally coupled in higher order binary called Super Cluster and anchored by the heaviest cluster in the group. This goes ad-infinitum.

Our Milky Way has a diameter of 100,000ly. Solar system is situated at 25,000ly from the galactic center. Orbital period of our Solar System around the primary is 240My. This gives a tangential velocity of 220km/sec. As seen by Hubble Ultra Deep Field (HUDF) telescope we have 10,000 galaxies in our field of view. Since there are 107 fields of view to cover the sky. Therefore there are 107×10,000=1011 visible galaxies. There are 100billion stars in our galaxy. Therefore the total number of stars in the visible Universe is =1011galaxies×1011stars per galaxy= 1022stars. Just as Galaxy grows around SMBH to develop a stable configuration ensuring minimum Gibb's free energy. In a similar way every cluster has a massive cD Galactic core to ensure stability and minimum Gibb's free energy. The center of mass of Milky Way and Andromeda Galaxy acts as the central massive core and anchor of the Local Group.

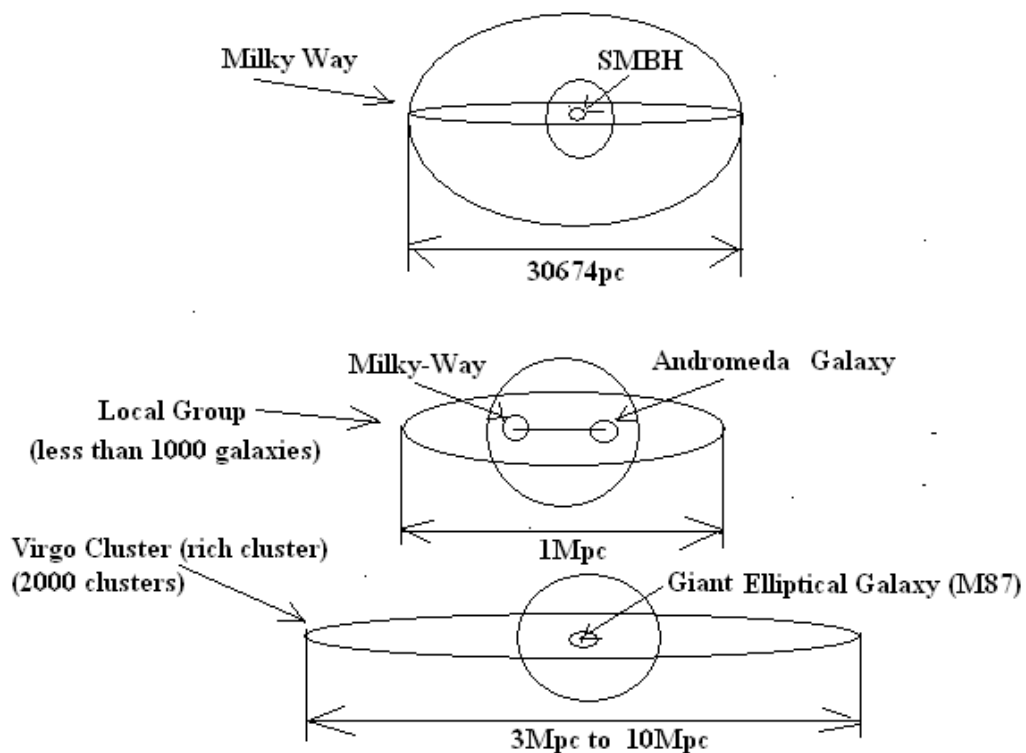In Figure 15, the schematic of Milky Way, Local Group and Virgo Cluster is given.

Figure 15: A comparatiuve study of Galaxy and a Cluster of Galaxies.

8. Super-Cluster of Clusters

Clusters clump into Super-clusters. Our Local Group belongs to Virgo Super Cluster also known as Local Super Cluster. This is a large scale structure in the Universe. The center of mass of the local group and Virgo Cluster occupy the core of the Super cluster imparting stability to the large scale structure . The collective mass of the Virgo Super Cluster is 1015×MO and its flattened disk diameter is 34Mpc.

Superclusters are not spherical but form flattened walls or elongated filaments as much as 50Mpc in length. Superclusters are seperated by enormous spherical voids. These voids are 100Mpc in diameter and contain very few galaxies.

Galaxy filaments consist of Super Cluster Complexes or Great Walls. These are masive, thread-like structure with a typical length of 50 to 80 Mpc that form boundaries between the voids.

9. Hypercluster and Filaments

Hyperclusters are composed of local groups of superclusters and this will require 100by to form. Voids are turbulent magnetic fields between super clusters. These connect to hyperclusters by gigantic filaments. These filaments are longer than SLOAN Great Wall Filament. The gigantic filaments are 420Mpc. Universe must be filled with innumerable hyperclusters that form fractal filamentary structure. Stenflo in "Solar Magnetic Fields" 2008 has identified on the Sun's surface a widespread "fractal-like pattern of voids" that are teeming with turbulent magnetic fields.[Thomas, Abdalla and Aahav (2010)] [74].

Virgo Super Cluster or Local Super Cluster has 100 galaxy groups and clusters. It is 34Mpc in length and it is at the boundary of Southern Local Supervoid which is 600 times as voluminous as Milky Way.

The Universe is filled with vast hyperclusters that challenge the standard Big Bang Cosmological Model. There are aggregation of galaxies streching a length of 920Mpc.

Anolmous Signal given by excess power over large scales imply a large anomaly with a couple of % variation in density from place to place but a huge density contrast that is twice what they predict.

Elliptical Galaxies in a new MegaZDR7 volume Galaxy survey photometric catalogue have the highest photometric redshift. These most distant and oldest known galaxies are forming Hyperclusters.

9.1. Mechanisms of the formation of Hyperclusters.

Just as galaxies form clusters in exactly the same fashion clusters form super clusters and superclusters form hyper clusters. Just as Earth-Moon system is moving towards minimum energy configuration [SOM_Appendix_A], Solar System and Exo-Solar systems move towards minimum energy configuration. In exactly the same fashion Galaxies are always moving towards minimum energy configuration. Anologously Galaxies form clusters. Galaxies may form pair configuration of minimum energy or Galaxies/ Galaxy pairs form minimum energy configuration with the massive core. In all these case a stable configuration may be formed or secondary may merge with primary by getting trapped in a death spirtal.

Identically clusters can be in a stable configuration with respect to the cD Galactic core or can get trapped in a death spiral heading towards a headlong collision with the central core. If it gets trapped in a death spiral it creates hurricane like condition tossing galaxies far from their orbital paths and churning shock waves of 100million Kelvin through out the intergalactic space.
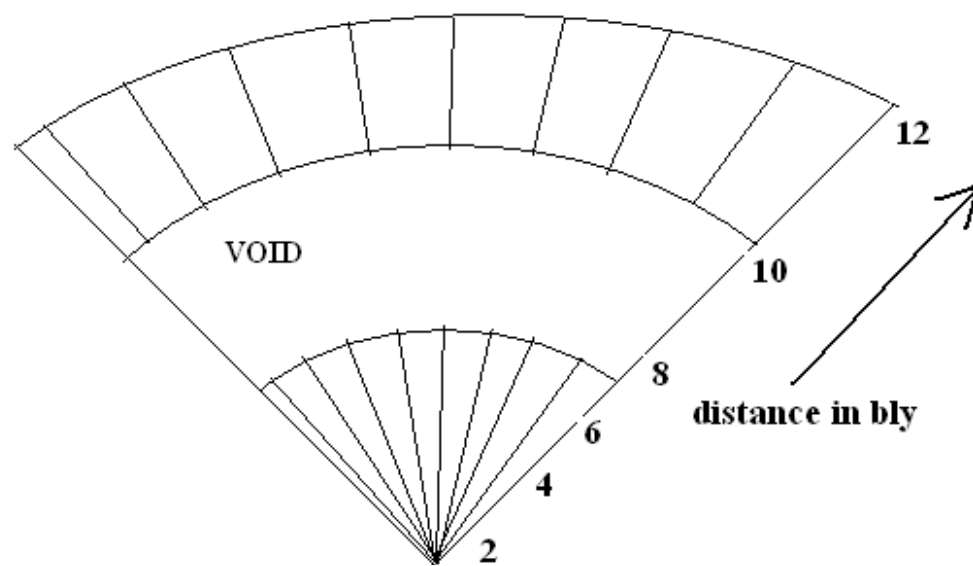

Figure 16: Filamentary Structure in the Cosmic Web

9.2 The Mother of All Pileups.[Phil Berardelli (2009)]

The Cosmic Collision named MACS0717 is qualitatively different from Galactic Collisions and Mergers. Discovered in 2003 and located about 5.4bly away. Composite image Figure 17 shows hot gas from four galaxy clusters converging along a cosmic filament. These four clusters, consisting of 1000 galaxies, are converging along a filament 13.5Mly long. This filament consists of galaxies, gas clouds and mainly dark matter. Such filament of dark matter seem to permeate the Universe and draw in galaxies, clusters and superclusters as well as intergalactic gas clouds from less dense region.
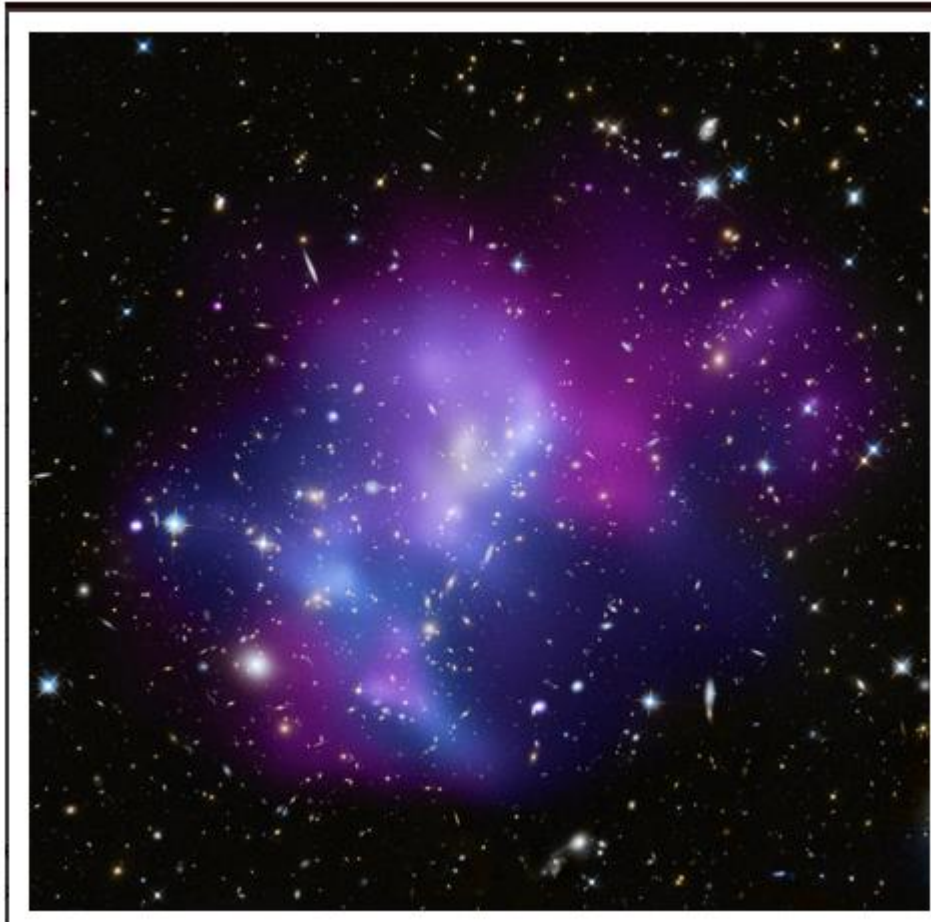
Figure 17: Gridlock This composite image shows hot gas (blue) from four galaxy clusters converging along a cosmic filament. Credit: NASA/CXC/STScI/IfA/C. Ma et

10. Discussion

Discovery of over-massive BHs in Giant Elliptical Galaxies and in compact disk-dominated lenticular galaxy transforms the Primary-Centric Architecture from realm of conjecture to Real-Universe basis of evolution. The three Super-Clusters namely PP SC, LSC and COMA SC hosting NGC1277, M87, NGC3842 and NGC4889 respectively teach us the basic design rules of Large-Scale Universe Architecture.

In this study I have studied 15 SCs. Due to lack of data and due to the complexity of the configuration, I could not arrive at a final primary-centric configuration in four cases namely Pavo-Indus SC, Sculptor SC, Horoligum SC and Bootes SC. The remaining 11 SCs were tentatively analyzed and primary-centric configurations were arrived at. Out of these 11 SCs, 3 SCs configurations mentioned above have been proved to be correct with finality on dynamical considerations. In case of the remaining 8 SCs, the eight Monarch Galaxies need to be tested to see if these galaxies do indeed harbour over-massive BHs as their counterparts.

This study has amply vindicated our original post-copernican conjecture that Universe is multi-level hierarchical higher order binary system (a single primary with multiple secondaries). At every level there is a dominant primary referred to as Monarch Primary which is deciding the stable orbits of its multiple secondaries. This pattern is being repeated at higher level and hence we call it a Fractal Architecture. This ensures minimum Gibb's free energy and hence the dynamical stability of the sub-system. If the secondary deviates from its assigned orbit it is bound to get trapped in a death spiral and eventually be absorbed by the primary. Mass Dominance of the Primary till galactic level was well established from the previous studies. This study has extended this postulate to cluster and super-cluster level. Now what remains to be done is to test the stars orbit around its Primary SMBH in Primary-centric Mathematical Framework. This work has already been done by Schodal et.al.(2001) in Copernican Framework [14].

Copernican Framework does not put any restriction on the permissible orbit semi-major axis for the secondary. It can be any orbit as given by Kepler's Third Law.

Whereas for a given set of orbit-globe parameters, there is only one stable orbit which is the outer Clarke's Orbit (aG2) which happens to be the larger root of the (ω/Ω) Equation 2 namely:

$$\frac{\omega}{\Omega} = E . a^{3/2} - F . a^2 = 1$$

This Kinematics has been applied to umpteen exo-planets, Star-Brown Dwarf binaries, Brown-Dwarf pairs, Star pairs and Pulsar Pairs[Sharma et.al.(2004a, 2004b, 2004c), Sharma(2011)

and Sharma(2011 under review)] and in each case the stable orbit observed is the same as that predicted by Primary-centric Formulation [3,6,7,41]. This is a considerable advance over the Copernican Mathematical Framework.

11. Conclusions

We can confidently conclude that indeed the Universe follows the fractal architecture as predicted by Primary-centric view proposed by me. There was always a curiosity and uncertainty regarding the Kinematics of the orbits of the celestial bodies. This uncertainty has been removed with complete finality. This kinematics can be tested on the various systems we encounter in our astronomical and astrophysical research. In my future work the research of Schodal et.al will be redone in Primary-centric Frame work and then it will be extended to Cluster and Super-Clusters. This will prove the usefulness of Primary-centric framework for future applications.

References

1. Sharma, B. K. (2008). Basic Mechanics of Planet-Satellite Interaction with special reference to Earth-Moon System. arXiv preprint arXiv:0805.0100.
2. Sharma, B. K., Ishwar, B., & Rangesh, N. (2009). Simulation software for the spiral trajectory of our Moon. Advances in space research, 43(3), 460-466.
3. Sharma, B. K. (2011). The Architectural Design Rules of Solar Systems Based on the New Perspective. Earth, Moon, and Planets, 108, 15-37.
4. Krasinsky, G. A. (2002). Dynamical History of the Earth-Moon System. Celestial Mechanics and Dynamical Astronomy, 84, 25-55.
5. Carlberg, J. K., Majewski, S. R., & Arras, P. (2009). The role of planet accretion in creating the next generation of red giant rapid rotators. The Astrophysical Journal, 700(1), 832.
6. Sharma, B. K., & Ishwar, B. (2004a). Planetary Satellite Dynamics : Earth-Moon, Mars-Phobos-Deimos and Pluto-Charon (Parth-I). 35th COSPAR Scientific Assembly, 18-25th July, Paris, France
7. Sharma, B. K., & Ishwar, B. (2004). A new perspective on the birth and evolution of our Solar System based on Planetary-Satellite Dynamics. In 35th COSPAR Scientific Assembly (Vol. 35, p. 635).
8. Dukla, J. J., Cacioppo, R., Gangopadhyaya, A. (2004). Gravitational slingshot. American Journal of Physics, 72(5), 619-621.
9. Jones, J. B. (2005). How does the slingshot effect work to change the orbit of a spacecraft?. Scientific American, 293(5), 116-116.
10. Epstein, K. J. (2005). Shortcut to the slingshot effect. American journal of physics, 73(4), 362-362.
11. Cook, C. L. (2004). Comment on 'Gravitational Slingshot', by Dukla JJ, Cacioppo, R., & Gangopadhyaya. A.[American

12. Mayer, L., Quinn, T., Wadsley, J., & Stadel, J. (2002). Formation of giant planets by fragmentation of protoplanetary disks. Science, 298(5599), 1756-1759.
13. Santos, N. C., Benz, W., & Mayor, M. (2005). Extrasolar planets: constraints for planet formation models. Science, 310(5746), 251-255.
14. Schödel, R., Ott, T., Genzel, R., Hofmann, R., Lehnert, M., Eckart, A., ... & Menten, K. M. (2002). A star in a 15.2-year orbit around the supermassive black hole at the centre of the Milky Way. Nature, 419(6908), 694-696.
15. Jackson, B., Barnes, R., & Greenberg, R. (2009). Observational evidence for tidal destruction of exoplanets. The Astrophysical Journal, 698(2), 1357.
16. Jackson, B., Greenberg, R., & Barnes, R. (2008). Tidal heating of extrasolar planets. The Astrophysical Journal, 681(2), 1631.
17. Hellier, C., Anderson, D. R., Cameron, A. C., Gillon, M., Hebb, L., Maxted, P. F. L., ... & Wheatley, P. J. (2009). An orbital period of 0.94 days for the hot-Jupiter planet WASP-18b. Nature, 460(7259), 1098-1100.
18. Israelian, G., Santos, N. C., Mayor, M., & Rebolo, R. (2001). Evidence for planet engulfment by the star HD82943. Nature, 411(6834), 163-166.
19. Bloom, J. S., Giannios, D., Metzger, B. D., Cenko, S. B., Perley, D. A., Butler, N. R., ... & Van Der Horst, A. J. (2011). A possible relativistic jetted outburst from a massive black hole fed by a tidally disrupted star. Science, 333(6039), 203-206.
20. Levan, A. J., Tanvir, N. R., Cenko, S. B., Perley, D. A., Wiersema, K., Bloom, J. S., ... & Xu, D. (2011). An extremely luminous panchromatic outburst from the nucleus of a distant galaxy. Science, 333(6039), 199-202.
21. Hawking, Stephen. (2005). "The Illustrated on the Shoulders of Giants", Running Press Publications.
22. Gale, Thomson. (2005-2006). "Ptolemic Astronomy, Islamic Planetary Theory and Copernican's Debt to the Maragha School", Science and its Times, Thomson Corporation.
23. Lawson, Russels. (2004). Burns, William Earl,(Editor) " Science in the Ancient World- An Encyclopaedia", History of Science, ABC-Chos, 29-30.
24. Dreyer, J. L. E. (2004). Tycho Brahe: A picture of Scientific Life and Work in Sixteenth Century. Kessinger Publication.
25. Kupperburg, Paul. (2005). "Hubble and the Big Bang",The Rosen Publishing House, 45-46.
26. Srinivasan, G. (Ed.). (2000). From white dwarfs to black holes: the legacy of S. Chandrasekhar. University of Chicago Press.
27. Bethe, H. A. (1997). J. Robert Oppenheimer, 1904-1967: A Biographical Memoir. National Academies Press.
28. Dickey, J. O., Bender, P. L., Faller, J. E., Newhall, X. X., Ricklefs, R. L., Ries, J. G., ... & Yoder, C. F. (1994). Lunar laser ranging: A continuing legacy of the Apollo program. Science, 265(5171), 482-490.
29. Cameron, A. G. W. (1997). The origin of the Moon and the single impact hypothesis V. Icarus, 126(1), 126-137.
30. Cameron, A. G. W. (2002). Birth of a solar system. Nature, 418(6901), 924-925.

Journal of Physics, 72 (5), pp 619–621.

31. Kerr, R. A. (2002). The first rocks Whisper of their origins.
32. Touma, J., & Wisdom, J. (1998). Resonances in the early evolution of the Earth-Moon system. The Astronomical Journal, 115(4), 1653.
33. Ward, W. R., & Canup, R. M. (2000). Origin of the Moon's orbital inclination from resonant disk interactions. Nature, 403(6771), 741-743.
34. Canup, R. M., & Esposito, L. W. (1996). Accretion of the Moon from an impact-generated disk. Icarus, 119(2), 427-446.
35. Canup, R. M., & Asphaug, E. (2001). Origin of the Moon in a giant impact near the end of the Earth's formation. Nature, 412(6848), 708-712.
36. Williams, G. E. (2000). Geological constraints on the Precambrian history of Earth's rotation and the Moon's orbit. Reviews of Geophysics, 38(1), 37-59.
37. Leschiutta, S., & Tavella, P. (2001, January). Reckoning time, longitude and the history of the earth's rotation, using the moon. In Earth-Moon Relationships: Proceedings of the Conference held in Padova, Italy at the Accademia Galileiana di Scienze Lettere ed Arti, November 8–10, 2000 (pp. 225-236). Dordrecht: Springer Netherlands.
38. Cattaneo, A., Faber, S. M., Binney, J., Dekel, A., Kormendy, J., Mushotzky, R., ... & Wisotzki, L. (2009). The role of black holes in galaxy formation and evolution. Nature, 460(7252), 213-219.
39. Heckman, T. M., & Kauffmann, G. (2011). The coevolution of galaxies and supermassive black holes: a local perspective. science, 333(6039), 182-185.
40. Sharma, B., & Ishwar, B. (2002). Lengthening of day (lod) curve could be experiencing chaotic fluctuations with implications for earthquake predictions. In 34th COSPAR Scientific Assembly (Vol. 34, p. 3078).
41. Sharma, B. K., & Ishwar, B. (2006). Jupiter-like Exo-Solar Planets confirm the Migratory Theory of Planets. Celestial Mechanics: Recent Trends, 225.
42. Tsiganis, K., Gomes, R., Morbidelli, A., & Levison, H. F. (2005). Origin of the orbital architecture of the giant planets of the Solar System. Nature, 435(7041), 459-461.
43. Morbidelli, A., Levison, H. F., Tsiganis, K., & Gomes, R. (2005). Chaotic capture of Jupiter's Trojan asteroids in the early Solar System. Nature, 435(7041), 462-465.
44. Gomes, R., Levison, H. F., Tsiganis, K., & Morbidelli, A. (2005). Origin of the cataclysmic Late Heavy Bombardment period of the terrestrial planets. Nature, 435(7041), 466-469.
45. Dunlop, J. S. (2011). The cosmic history of star formation. Science, 333(6039), 178-181.
46. Seife, C. (2003). Illuminating the dark universe.
47. Goldhaber, G., & Perlmutter, S. (1998). A study of 42 Type Ia supernovae and a resulting measurement of Ωm and $\Omega\Lambda$. Physics Reports, 307(1-4), 325-331.
48. Walsh, K. J., Richardson, D. C., & Michel, P. (2008). Rotational breakup as the origin of small binary asteroids. Nature, 454(7201), 188-191.
49. Courtland, Rachel. (2008). Controversial dwarf planet finally named 'Haumea, New Scientist, 18th September.
50. Petit, J. M., Kavelaars, J. J., Gladman, B. J., Margot, J. L., Nicholson, P. D., Jones, R. L., ... & Taylor, P. A. (2008). The extreme Kuiper belt binary 2001 QW322. Science, 322(5900), 432-434.
51. Semeniuk, Ivan. (2008). Huge haul of Earth-like planets found, New Scientist, 02 June.
52. Reynolds, C. S. (2008). Bringing black holes into focus. Nature, 455(7209), 39-40.
53. Filippenko, A. V., & Riess, A. G. (1998). Results from the high-z supernova search team. Physics Reports, 307(1-4), 31-44.
54. Yuan, F., Quataert, E., & Narayan, R. (2003). Nonthermal electrons in radiatively inefficient accretion flow models of Sagittarius A. The Astrophysical Journal, 598(1), 301.
55. Ibata, R., Gibson, B. (2007). The Ghost of Galaxies Past. Scientific American, 40-46.
56. Purcell, C. W., Bullock, J. S., Tollerud, E. J., Rocha, M., & Chakrabarti, S. (2011). The Sagittarius impact as an architect of spirality and outer rings in the Milky Way. Nature, 477(7364), 301-303.
57. Bhattacharjee, Y. (2011). Milky Way Researchers' Home Away From Home.
58. Merritt, D. (1985). Relaxation and tidal stripping in rich clusters of galaxies. III-Growth of a massive central galaxy. Astrophysical Journal, Part 1 (ISSN 0004-637X), vol. 289, Feb. 1, 1985, p. 18-32., 289, 18-32.
59. van den Bosch, R. C., Gebhardt, K., Gültekin, K., van de Ven, G., van der Wel, A., & Walsh, J. L. (2012). An over-massive black hole in the compact lenticular galaxy NGC 1277. Nature, 491(7426), 729-731.
60. Kormendy, J., Bender, R., Magorrian, J., Tremaine, S., Gebhardt, K., Richstone, D., ... & Lauer, T. R. (1997). Spectroscopic evidence for a supermassive black hole in NGC 4486B. The Astrophysical Journal, 482(2), L139.
61. McConnell, N. J., Ma, C. P., Gebhardt, K., Wright, S. A., Murphy, J. D., Lauer, T. R., ... & Richstone, D. O. (2011). Two ten-billion-solar-mass black holes at the centres of giant elliptical galaxies. Nature, 480(7376), 215-218.
62. Jordán, A., Blakeslee, J. P., Côté, P., Ferrarese, L., Infante, L., Mei, S., ... & West, M. J. (2007). The ACS Fornax Cluster Survey. I. Introduction to the survey and data reduction procedures. The Astrophysical Journal Supplement Series, 169(2), 213.
63. Jordán, A., Côté, P., West, M. J., Marzke, R. O., Minniti, D., & Rejkuba, M. (2004). Hubble space telescope observations of cD galaxies and their globular cluster systems. The Astronomical Journal, 127(1), 24.
64. Einasto, M., Einasto, J., Tago, E., Müller, V., & Andernach, H. (2001). Optical and X-ray clusters as tracers of the supercluster-void network. I. Superclusters of Abell and X-ray clusters. The Astronomical Journal, 122(5), 2222.
65. Boylan-Kolchin, M., Ma, C. P., & Quataert, E. (2006). Red mergers and the assembly of massive elliptical galaxies: the fundamental plane and its projections. Monthly Notices of the Royal Astronomical Society, 369(3), 1081-1089.
66. Hopkins, P. F., Bundy, K., Hernquist, L., & Ellis, R. S. (2007). Observational evidence for the coevolution of galaxy mergers, quasars, and the blue/red galaxy transition. The Astrophysical Journal, 659(2), 976.

67. Gregory, S. A., & Thompson, L. A. (1978). The Coma/A1367 supercluster and its environs.

68. Pringle. (1981). Eddington Accretion. Annual Review Astronomy and Astrophysics, 19,1-4.

69. Fitchett, M., & Merritt, D. (1988). Dynamics of the Hydra I galaxy cluster. Astrophysical Journal, Part 1 (ISSN 0004-637X), vol. 335, Dec. 1, 1988, p. 18-34., 335, 18-34.

70. Fritz, G., Davidsen, A., Meekins, J. F., & Friedman, H. (1971). Discovery of an x-ray source in perseus. Astrophysical Journal, vol. 164, p. L81, 164, L81.

71. Klypin, A., Hoffman, Y., Kravtsov, A. V., & Gottlöber, S. (2003). Constrained simulations of the real universe: The local supercluster. The astrophysical journal, 596(1), 19.

72. Thomas, S. A., Abdalla, F. B., & Lahav, O. (2011). Excess clustering on large scales in the MegaZ DR7 photometric redshift survey. Physical review letters, 106(24), 241301.

73. Abell, G. O., Corwin Jr, H. G., & Olowin, R. P. (1989). A catalog of rich clusters of galaxies. Astrophysical Journal Supplement Series (ISSN 0067-0049), vol. 70, May 1989, p. 1-138., 70, 1-138.

74. Bonta, E. D., Ferrarese, L., Corsini, E. M., Miralda-Escudé, J., Coccato, L., & Pizzella, A. (2007). The black hole mass of Abell 1836-BCG and Abell 3565-BCG. arXiv preprint arXiv:0706.1959.

75. Sharma, B. K. (2008). Basic Mechanics of Planet-Satellite Interaction with special reference to Earth-Moon System. arXiv preprint arXiv:0805.0100.

76. Benz, W., Slattery, W. L., & Cameron, A. G. W. (1987). The origin of the Moon and the single-impact hypothesis, II. Icarus, 71(1), 30-45.

77. Phil, B. (2009). The Mother of All Pileups, ScienceNOW.

78. Bottches, M. (2007). Modelling the emission processes in Blazers, Astrophysics and Space Sciences, 309, 95.

79. Brunzendorf, J., & Meusinger, H. (1999). The galaxy cluster Abell 426 (Perseus). A catalogue of 660 galaxy positions, isophotal magnitudes and morphological types. Astronomy and Astrophysics Supplement Series, 139(1), 141-161.

80. Cain, F. (2009). What Is Intergalactic Space? Universe Today Website.

81. Fraser, C. (2003). New Evidence of Cold Dark Matter, Universe Today.

82. Chapman, G. N. F., Gellar,M. J., Huchra,J. P. et.al. (1988). Linear cluster of galaxies-A194. Astronomical Journal, 95, 999-1022,

83. Chatzikos, M., Sarazin, C. L., & Kempner, J. C. (2006). Chandra observation of abell 2065: An unequal mass merger?. The Astrophysical Journal, 643(2), 751.

84. Chincarini, G., Thompson, L. A., & Rood, H. J. (1981). Supercluster bridge between groups of galaxy clusters. Astrophysical Journal, Part 2-Letters to the Editor, vol. 249, Oct. 15, 1981, p. L47-L50. Research supported by the University of Oklahoma, 249, L47-L50.

85. Chincarini, G., Tarenghi, M., Sol, H., Crane, P., Manousoyannaki, I., & Materne, J. (1984). The Horologium region. I-The data. Astronomy and Astrophysics Supplement Series (ISSN 0365-0138), vol. 57, July 1984, p. 1-21. Research supported by the University of Oklahoma., 57, 1-21.

86. Cho, A., & Stone, R. (2007). Racing to capture darkness. Science, 317(5834), 32-34.

87. Conselice, C. J., & Gallagher III, J. S. (1998). Galaxy aggregates in the Coma cluster. Monthly Notices of the Royal Astronomical Society, 297(2), L34-L38.

88. Clery, Daniel "Galaxy Evolution", Science, 333, 173-175, 8th July (2011).

89. Cruzen, S. T. (1995). Photometry of the galaxies in the Bootes Void. University of Nevada, Las Vegas.

90. Cucchiara, A., Levan, A. J., Fox, D. B., Tanvir, N. R., Ukwatta, T. N., Berger, E., ... & D'Avanzo, P. (2011). A Photometric Redshift of z□ 9.4 for GRB 090429B. The Astrophysical Journal, 736(1), 7.

91. Da Costa, L. N., Numes, M. A., Pellegrini, P. S., Willmer, C., Chincarini, G., & Cowan, J. J. (1986). Redshift observations in the Centaurus-Hydra supercluster region. I. Astronomical Journal (ISSN 0004-6256), vol. 91, Jan. 1986, p. 6-12. Research supported by the University of Oklahoma., 91, 6-12.

92. da Costa, L. N., William,C; Pellegrini, P. S., Chincarini, G. (1987). Red Shift observation in the Centaurus-Hydra Supercluster region II. Astronomical Journal, v93, 1338-1349

93. Da Costa, L. N., Geller, M. J., Pellegrini, P. S., Latham, D. W., Fairall, A. P., Marzke, R. O., ... & Kurtz, M. J. (1994). A complete southern sky redshift survey. The Astrophysical Journal, 424, L1-L4.

94. Darwin, G. H. (1879). XIII. On the precession of a viscous spheroid, and on the remote history of the Earth. Philosophical Transactions of the Royal Society of London, (170), 447-538.

95. Darwin, G. H. (1880). On the secular changes in the elements of the orbit of a satellite revolving about a planet distorted by tides. Nature, 21(532), 235-237.

96. Di Nella, H., Couch, W. J., Paturel, G., & Parker, Q. A. (1996). Are the Perseus—Pisces chain and the Pavo—Indus wall connected?. Monthly Notices of the Royal Astronomical Society, 283(2), 367-380.

97. Fossati, G. A., Maraschi, L., Celotti, A., Comastri, A., & Ghisellini, G. (1998). A unifying view of the spectral energy distributions of blazars. Monthly Notices of the Royal Astronomical Society, 299(2), 433-448.

98. Genstenkorn, H. (1995). Uber Gezeitenreibung beim Zweikarpenproblem. Z. Astrophysics, 26, 245-274, 1955.

99. Goldreich, P. (1966). History of the lunar orbit. Reviews of Geophysics, 4(4), 411-439.

100. Gregory, S. A., & Thompson, L. A. (1984). The A2197 and A2199 galaxy clusters. Astrophysical Journal, Part 1 (ISSN 0004-637X), vol. 286, Nov. 15, 1984, p. 422-436., 286, 422-436.

101. Gursky, H., Kellogg, E., Murray, S., Leong, C., Tananbaum, H., & Giacconi, R. (1971). A strong X-ray source in the Coma cluster observed by UHURU. Astrophysical Journal, vol. 167, p. L81, 167, L81.

102. Ettori, S., Fabian, A. C., & White, D. A. (1997). On the mass distribution in the Shapley Supercluster inferred from X-ray observations. Monthly Notices of the Royal Astronomical Society, 289(4), 787-800.

103. Hlavacek-Larrondo, J., Fabian, A. C., Edge, A. C., & Hogan, M. T. (2012). On the hunt for ultramassive black holes in brightest cluster galaxies. Monthly Notices of the Royal Astronomical Society, 424(1), 224-231.

104. Craig, J. H. (1996). Primordial Deutrium and the Big Bang. Scientific American.

105. Ida, S., Canup, R. M., & Stewart, G. R. (1997). Lunar accretion from an impact-generated disk. Nature, 389(6649), 353-357.

106. Ikebe, Y., Ohashi, T., Makishima, K., Tsuru, T., Fabbiano, G., Kim, D. W., ... & Kondo, H. (1992). X-ray study of NGC 1399 in the Fornax cluster of galaxies. Astrophysical Journal, Part 2-Letters (ISSN 0004-637X), vol. 384, Jan. 1, 1992, p. L5-L8., 384, L5-L8.

107. Kaula, W. M. (1964). Tidal dissipation by solid friction and the resulting orbital evolution. Reviews of geophysics, 2(4), 661-685.

108. Kopylova, F. G., & Kopylov, A. I. (1998). Structure and dynamic state of the Corona Borealis supercluster. Astronomy Letters, 24, 491-496.

109. Kipp, M. E., Melosh, H. J. (1986). Origin of the Moon. edited by Hartmann, Phillip and TaylorPublishers: Lunar & Planetary Sciences, Houston, 643-647,

110. Kirshner, R. P., Oemler Jr, A., Schechter, P. L., & Shectman, S. A. (1987). A survey of the Bootes void. The Astrophysical Journal, 314, 493-506.

111. Lewis, A. D., Buote, D. A., Stocke, J. T. (2002). Chandra Observation of 2029: The Dark Matter Profile down to < 0.01RVIR in an unusually relaxed Cluster", Astrophysical Journal,586 (1),135-142.

112. Lucey, J. R., Currie, M. J., & Dickens, R. J. (1986). The Centaurus cluster of galaxies–II. The bimodal velocity structure. Monthly Notices of the Royal Astronomical Society, 221(2), 453-472.

113. Lucey, J. R., & Carter, D. (1988). Distances to five nearby southern galaxy clusters and the absolute motion of the Local Group. Monthly Notices of the Royal Astronomical Society, 235(4), 1177-1201.

114. Macdonald, G. J. F. (1964). Tidal Friction. Review Geophysics, 2, 467-541.

115. Mahdavi, A., Geller, M. J., Fabricant, D. G., Kurtz, M. J., Postman, M., & McLean, B. (1996). The lumpy cluster abell 1185. Astronomical Journal v. 111, p. 64, 111, 64.

116. Maurellis, A., Fairall, A. P., Matravers, D. R., & Ellis, G. F. R. (1990). A two-dimensional sheet of galaxies between two southern voids. Astronomy and Astrophysics (ISSN 0004-6361), vol. 229, no. 1, March 1990, p. 75-79., 229, 75-79.

117. Maraschi, L., & Tavecchio, F. (2003). The jet-disk connection and blazar unification. The Astrophysical Journal, 593(2), 667.

118. McNamara, B. R., & Nulsen, P. E. J. (2007). Heating hot atmospheres with active galactic nuclei. Annu. Rev. Astron. Astrophys., 45, 117-175.

119. Melosh, H. J. & Kipp, M. E. Lunar Planetary Science Conference XX, 685-686, (1989).

120. Mieske, S., Hilker, M., Jordán, A., Infante, L., & Kissler-Patig, M. (2007). A search for ultra-compact dwarf galaxies in the Centaurus galaxy cluster. Astronomy & Astrophysics, 472(1), 111-119.

121. NASA/IPAC Extra Galactic DataBase(NED) operated by Jet Propulsion Laboratory, California Institute of Technology under contract with NASA.

122. Nakazawa, K., Makishima, K., Fukazawa, Y., & Tamura, T. (2000). ASCA Observations of a Near-by Cluster in Antlia. Publications of the Astronomical Society of Japan, 52(4), 623-630.

123. Optical Gravitational Lensing Experiment (OGLE) Collaboration Udalski A. 13 Szymański MK 13 Kubiak M. 13 Pietrzyński G. 13 14 Poleski R. 13 Soszyński I. 13 Wyrzykowski Ł. 15 Ulaczyk K. 13. (2011). Unbound or distant planetary mass population detected by gravitational microlensing. Nature, 473(7347), 349-352.

124. Panter, B., Jimenez, R., Heavens, A. F., & Charlot, S. (2007). The star formation histories of galaxies in the Sloan Digital Sky Survey. Monthly Notices of the Royal Astronomical Society, 378(4), 1550-1564.

125. Digital Sky Survey", Monthly Notices of Royal Astronomical Society, 378, 1550-1564.

126. Pastorello, A., & Patat, F. (2008). Echo from an ancient supernova. Nature, 456(7222), 587-589.

127. Gamow, G. (1948). The evolution of the universe. Nature, 162(4122), 680-682.

128. Postman, M., Geller, M. J., & Huchra, J. P. (1988). The dynamics of the Corona Borealis supercluster. Astronomical Journal (ISSN 0004-6256), vol. 95, Feb. 1988, p. 267-283., 95, 267-283.

129. spirality and outer rings in the Milky Way", Nature, 477, 301-303.

130. Rubincam, D. P. (1975). Tidal friction and the early history of the Moon's orbit. Journal of Geophysical Research, 80(11), 1537-1548.

131. van den Bosch, R. C., Gebhardt, K., Gültekin, K., van de Ven, G., van der Wel, A., & Walsh, J. L. (2012). An over-massive black hole in the compact lenticular galaxy NGC 1277. Nature, 491(7426), 729-731.

132. Rydan@astronomy.ohio-state.edu_ Lecture 34, Cluster and Super-Cluster by Prof. Barbara Rydan.

133. Schilling, G. (2001). The first split second. New Scientist, 169(2284), 26-9.

134. Sharma, B. K. (2008). Theoretical Formulation of the Phobos, moon of Mars, rate of altitudinal loss. arXiv preprint arXiv:0805.1454.

135. Sharma, B. K. (2008). Theoretical Formulation of the Origin of Cataclysmic Late Heavy Bombardment Era based on the New Perspective of Birth & Evolution of Solar Systems. arXiv preprint arXiv:0807.5093.

136. Sharma, B. (2012). Enigma of the Birth and Evolution of Solar Systems May Be Solved by Invoking Planetary-Satellite Dynamics. In Space Science (p. 83). IntechOpen.

137. Silvestrini,S., Krizman,C.,Ceretti,G. et.al. (2010). Analysis of Abell 779-photometry and spectroscopy of the cluster. 11Cido come Labaratorio, 1.

138. Steinmetz et.al. "Huge elliptical galaxy of 13th Magnitude".

139. Tallin, Estonian SSR, "The Large Scale Structure of the Universe", Proceedings of the Symposium, Sept

12-16,1977;Publishing Co, 1978,pp 241-250, discussion 250,251. [Ref.No.6 of the Text]

140. Tarenghi, M., Tifft, W. G., Chincarini, G., Rood, H. J., & Thompson, L. A. (1979). The Hercules supercluster. I-Basic data. Astrophysical Journal, Part 1, vol. 234, Dec. 15, 1979, p. 793-801., 234, 793-801.

141. Tarenghi, M., Chincarini, G., Rood, H. J., & Thompson, L. A. (1980). The Hercules supercluster. II-Analysis. Astrophysical Journal, Part 1, vol. 235, Feb. 1, 1980, p. 724-742., 235, 724-742.

142. Tully, R. B. (1982). The local supercluster. Astrophysical Journal, Part 1, vol. 257, June 15, 1982, p. 389-422., 257, 389-422.

143. Tully, R. B. (1982). Unscrambling the Local Supercluster. Sky and Telescope, 63, 550.

144. Tully, R. B., & Fisher, J. R. (1977). A new method of determining distances to galaxies. Astronomy and Astrophysics, vol. 54, no. 3, Feb. 1977, p. 661-673., 54, 661-673.

145. Ulrich, M. H., Maraschi, L., & Urry, C. M. (1997). Variability of active galactic nuclei. Annual Review of Astronomy and Astrophysics, 35(1), 445-502.

146. Uson, J. M., Boughn, S. P., & Kuhn, J. R. (1990). The central galaxy in Abell 2029: an old supergiant. Science, 250(4980), 539-540.

147. Urry, M. (1999). BL Lac Objects and Blazars: Past, Present and Future. In BL Lac Phenomenon (Vol. 159, p. 3).

148. Van den Bergh, S. (2000). Updated information on the Local Group. Publications of the Astronomical Society of the Pacific, 112(770), 529.

149. Walker, S. A., Fabian, A. C., Sanders, J. S., George, M. R., & Tawara, Y. (2012). X-ray observations of the galaxy cluster Abell 2029 to the virial radius. Monthly Notices of the Royal Astronomical Society, 422(4), 3503-3515.

150. Zwicky, F. (1979). On the Masses of Nebulae and of Clusters of Nebulae. In A Source Book in Astronomy and Astrophysics, 1900–1975 (pp. 729-737). Harvard University Press.

Supplementary On-line Materials(SOM)
Appendix A.

The two Clarke's Orbits Stability and Energy Budget Estimate of Gravitational Sling Shot Model.

In order to determine the stability of the two Clarke's Orbits we will have to analyze total Energy Formulation of a binary system for instance Earth-Moon System and determine its maxima & minima points.

Total Energy of Earth-Moon System = Rotational Kinetic Energy + Potential Energy + Translational Kinetic Energy.

A.1

Translational Kinetic Energy of the order of 1×10^8Joules due to recession of Moon for all practical purposes is negligible as compared to Rotational Kinetic Energy of the order of 1×10^{30}Joules . Hence Translational Kinetic Energy is neglected in future analysis.

Moon is trapped in potential well created by the Earth.

Moon's potential energy = $- GM_{Earth}M_{Moon}/a$

G =Gravitational Constant=6.673×10^{-11} N-m^2/Kg^2;

M_{Earth} = mass of the Earth = 5.9742×10^{24} Kg;

M_{Moon} = mass of the Moon = E/81 = 7.348×10^{22} Kg;

a= semi-major axis of Moon's orbit around the Earth= 3.844×10^8 m;

Rotational Kinetic Energy of Earth-Moon System = Spin Energy of the Earth + Orbital Energy of the Earth-Moon System + Spin Energy of the Moon =

$$\frac{1}{2}C\omega^2 + \frac{1}{2}\left(\frac{M_{Moon}}{1+\frac{M_{Moon}}{M_{Earth}}}\right)a^2 \times \Omega_{orbital}^2 + \frac{1}{2}\times(0.4M_{Moon}R_{Moon}^2)\Omega_{spin}^2 \quad A.2$$

Where C = moment of inertia around polar axis = $0.3308M_{Earth}R_{Earth}^2 = 8.02\times10^{37}$ Kg-m^2;

Equatorial Radius of Earth=6.37814×10^6 m;

Equatorial Radius of Moon=1.738×10^6 m;

Earth angular spin velocity = $\omega = 2\pi/TE = [2\pi/(86400)]$radians/sec;

In this analysis we will consider all rates of rotation to be in Solar Days. We will consider one solar day as the present spin-period of Earth. Similarly while calculating Earth-Moon orbital angular momentum we will use present sidereal month expressed in 27.3 solar days.

Earth-Moon Orbital Angular Velocity = $\Omega = [2\pi/(27.3\times86400)]$radians/sec where sidereal month =27.3 d;

Since Moon is in synchronous orbit i.e. it is tidally locked with the Earth hence we see the same face of Moon and Moon's Orbital Angular Velocity = Moon's Spin Angular Velocity = Ω;

Therefore total rotational Kinetic Energy Equation 1 reduces to:

$$\frac{1}{2}C\omega^2 + \frac{1}{2}\left(\frac{M_{Moon}}{1 + \frac{M_{Moon}}{M_{Earth}}}\right)a^2 \times \Omega^2 + \frac{1}{2} \times (0.4M_{Moon}R_{Moon}^2)\Omega^2 \quad A.3$$

Similarly total angular momentum of Earth-Moon System is as follows:

$$J_T = C\omega + \left(\frac{M_{Moon}}{1 + \frac{M_{Moon}}{M_{Earth}}}\right)a^2 \times \Omega + (0.4M_{Moon}R_{Moon}^2)\Omega \qquad A.4$$

Substituting the numerical values in Eq.A.4 we obtain:
J_T = 3.44026×10³⁴ Kg-m²/sec ;
From [Sharma (2011)], we have the following relation between Length of Sidereal Month and Length of Sidereal Day:

$$\frac{LOM}{LOD} = \frac{\omega}{\Omega} = E \times a^{1.5} - F \times a^2 \qquad A.5$$

$$Where \; E = \frac{J_T}{BC} \; and \; F = \left(\frac{M_{Moon}}{C(1 + \frac{M_{Moon}}{M_{Earth}})}\right)$$

$$Here \; B = \sqrt{G(E + m)}$$

Substituting the numerical values we get:
B=20.08884482×10⁶ m³/²/s;
E=2.13531×10⁻¹¹ m⁻³/² ;
F = 9.05036×10⁻¹⁶ m⁻² ;
If the numerical values of E and F are substituted in Eq.A.5. and the present value of 'a' is substituted we get LOM/LOD = 27.2 we should get 27.3. This is because Eq.A.5 has been derived based on Keplarian Approximation. If LOM/LOD was derived from exact analysis we would get LOM/LOD in the present epoch as 27.3.

$$\frac{LOM}{LOD} = \frac{\omega}{\Omega} = E \times a^{1.5} - F \times a^2 = 1 \qquad A.6$$

Equation A.6 defines geosynchronous orbits of Earth-Moon system when both are tidally interlocked and are in triple synchrony state:
$T_{orbit} = T_{spinmoon} = T_{spinearth}$
If Equation B.6 is solved we get two roots:
aG1 =1.46177×10⁷ m and a_{G2} = 5.52656×10⁸ m;
If expressed as the ratio a/R_{Earth} we get:
a_{G1} = 2.29 and aG2 = 86.65;
Rewriting total rotational Kinetic Energy expression from Eq.A.3 we get:

$$KE = \frac{1}{2}C\omega^2 + \frac{1}{2}\left(\frac{M_{Moon}}{1 + \frac{M_{Moon}}{M_{Earth}}}\right)a^2 \times \Omega^2 + \frac{1}{2} \times (0.4M_{Moon}R_{Moon}^2)\Omega^2$$

Reshuffling the angular velocity terms we get:

$$KE = \frac{1}{2}\Omega^2\left[C\left(\frac{\omega}{\Omega}\right)^2 + \left(\frac{M_{Moon}}{1 + \frac{M_{Moon}}{M_{Earth}}}\right)a^2 + (0.4M_{Moon}R_{Moon}^2)\right]; \quad A.7$$

Substituting Eq.A.6 in Eq.A.7 we get:

$$KE = \frac{1}{2}\Omega^2\left[C(E \times a^{1.5} - F \times a^2)^2 + \left(\frac{M_{Moon}}{1+\frac{M_{Moon}}{M_{Earth}}}\right)a^2 + (0.4M_{Moon}R_{Moon}^2)\right]; \qquad A.8$$

According to Kepler's 3rd Law:

$$a^3\Omega^2 = G(M_{Earth} + M_{Moon}) \qquad A.9$$

Substituting Eq.A.9 in Eq.A.8 we obtain:

$$KE = \frac{1}{2} \times \frac{G(M_{Earth} + M_{Moon})}{a^3}\left[C(E \times a^{1.5} - F \times a^2)^2 + \left(\frac{M_{Moon}}{1+\frac{M_{Moon}}{M_{Earth}}}\right)a^2 + (0.4M_{Moon}R_{Moon}^2)\right]; \qquad A.10$$

Therefore total energy of the E-M System is:

$$TE = KE + PE$$

Therefore:

$$TE = \frac{1}{2} \times \frac{G(M_{Earth}+M_{Moon})}{a^3}\left[C(E \times a^{1.5} - F \times a^2)^2 + \left(\frac{M_{Moon}}{1+\frac{M_{Moon}}{M_{Earth}}}\right)a^2 + (0.4M_{Moon}R_{Moon}^2)\right] - $$

$$\frac{GM_{Earth}M_{Moon}}{a} \qquad A.11$$

To determine the stable and unstable equilibrium points in non-keplerian journey of Moon we must examine the Plot of Eq.A.11 from 'a' = 8×10^6 to 'a' = 6×10^8 m;

$$0.5 \times (G/a)(((m + M)/a^2)(C \times (E \times a^{1.5} - F \times a^2)^2 + (m/(1 + 1/81)) \times a^2 + 0.4 \times m \times R^2) - 2 \times m \times M)/.\{G \to 6.673 \times 10^{-11}, m \to 7.348 \times 10^{22}, M \to 5.9742 \times 10^{24}, C \to 8.02 \times 10^{37}, R \to 1.738 \times 10^6, E \to 2.1353127743727534 \times 10^{-11}, F \to 9.050361900127731 \times 10^{-16}\}$$
$$A.12.$$

$$\frac{1}{a}3.3365 \times 10^{-11}(-8.77968432 \times 10^{47} + \frac{1}{a^2}6.047679999999999 \times 10^{24}(8.8782768448 \times 10^{34} + 7.258390243902439 \times 10^{22}a^2 + 8.02 \times 10^{37}(2.135312774372753 \times 10^{-11}a^{1.5} - 9.050361900127731 \times 10^{-16}a^2)^2)) \qquad A.13$$

$$\text{Plot}\left[\frac{1}{a}3.3365 \times 10^{-11}\left(-8.77968432 \times 10^{47} + \frac{1}{a^2}6.047679999999999\right.\right.$$
$$\times 10^{24}(8.8782768448 \times 10^{34} + 7.258390243902439 \times 10^{22}a^2 + 8.02$$
$$\left.\times 10^{37}(2.135312774372753 \times 10^{-11}a^{1.5} - 9.050361900127731 \times 10^{-16}a^2)^2)\right), \{a, 1.4$$
$$\times 10^7, 1.5 \times 10^7\}, \text{GridLines} \to \text{Automatic}, \text{Frame} \to \text{True}, \text{FrameLabel}$$
$$\to semi - majoraxis(a)\text{meter}, \text{PlotLabel} \to \{\text{Total Energy Plot}\}\Big]$$

$$A.14$$
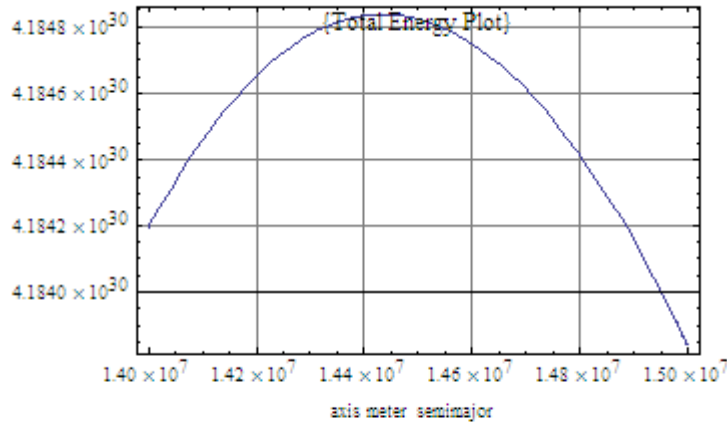
Total Energy Plot from a=1.4*10^{7}m to a=1.5*10^{7}m

Inner Geosynchronous Orbit= aG1=1.46177*10^{7}m

Figure A.1. Plot of total energy in the range 1.4×10^{7}m and 1.5×10^{7}m around the inner geo-synchronous orbit of a = 1.46×10^{7}m.

We find an energy Maxima at inner geo-synchronous orbit hence it is unstable equilibrium point. When Moon is at inner-geosynchronous orbit, any perturbation launches Moon on either a sub-synchronous orbit or on extra-synchronous(or super-synchronous orbit). If it is launched on sub-synchronous orbit then it rapidly spirals in towards the primary body and if it is launched on extra-synchronous orbit then it spirals out from inner to outer geosynchronous orbit. In our case, Moon is fully formed beyond Roches' Limit which is 18,000Km [Ida et.al. 1997] just beyond inner Clarke's orbit or inner Geo-synchronous Orbit hence Moon is launched on expansionary spiral orbit towards outer Clarke's Orbit or outer Geo-synchronous Orbit.

$\text{Plot}[\frac{1}{a}3.3365 \times 10^{-11}(-8.77968432 \times 10^{47} + \frac{1}{a^2}6.047679999999999 \times 10^{24}(8.8782768448 \times 10^{34} + 7.258390243902439 \times 10^{22}a^2 + 8.02 \times 10^{37}(2.135312774372753 \times 10^{-11}a^{1.5} - 9.050361900127731 \times 10^{-16}a^2)^2)), \{a, 5.4 \times 10^8, 5.6 \times 10^8\}, \text{GridLines} \to \text{Automatic}, \text{Frame} \to \text{True}, \text{FrameLabel} \to \text{semimajoraxismeter}, \text{PlotLabel} \to \{"Total Energy Plot"\}]$ A.15
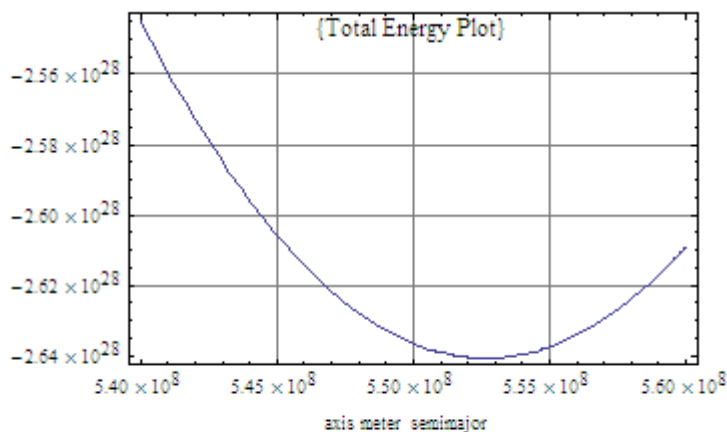
Total Energy Plot from a=5.4*10^8 m to a= 5.6*10^8 m.
Outer geo-synchronous orbir = aG2=5.52656*10^8 m.

FigureA.2. Plot of total energy in the range 5.4×10^{8}m and 5.6×10^{8}m around the outer geo-synchronous orbit of a = 5.527×10^{8}m.

At outer geosynchronous orbit there is energy minima hence it is stable equilibrium point. Secondary body can never move beyond this orbit. Either it is stay-put in that orbit or it gets deflected back into a contracting spiral orbit.

Plot[(1/a)3.3365`*^-11 (-8.779684319999999`*^47+1/a^26.047679999999999`*^24 (8.8782768448`*^34+7.258720964072173`*^22 a^2+8.019999999999999`*^37 (2.1353128`*^-11 a^1.5`- 9.050361900000001`*^-16 a^2)^2)),{a,0.5` 10^7,8` 10^8},PlotStyle->Thick,GridLines->Automatic,Frame->True,FrameLabel->a meter,PlotLabel->{Total Energy Plot}]
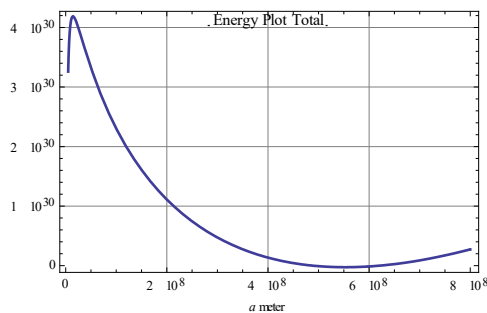
A.16

Figure A.3. Plot of total energy in the range 0.5×10⁷m and 8×10⁸m along the long tidal history of Moon from its inception to its lock-in at outer geo-synchronous orbit.

In a similar work by G.A.Krasinsky (2002) the results obtained are as follows:
"Analytical consideration show that if the contemporary lunar orbit were equatorial the evolution would develop from an unstable geosynchronous orbit of the period 4.42h(in the past) to a stable geosynchronous orbit of the period 44.8 days (in the future). It is also demonstrated that at the contemporary epoch the orbital plane of the fictitious equatorial moon would be unstable in the Liapunov's sense, being asymptotically stable at the earlier stages of the evolution."
In Table A.1, a comparison of results of my analysis and that of Krasinsky is given.

Table A.1. Comparative study of the results obtained by Krasinsky (2002), Sharma [personal communication:arXiv:0805.0100 (2008)]; and Darwin(1879,1880)

	aG1/R$_{Earth}$	aG2/R$_{Earth}$	Orbital period at aG1	Orbital period at aG1
Krasinsky analysis	2.15	83.8	4.42h	44.8days
BKS analysis	2.29	86.65	4.8596h	47.0739days
Darwin Analysis	Not available	90.4	Not available	47days

A.1. Energy Budget of Gravitational Sling –Shot Model of Earth-Moon System.

The Basic Physics of Gravitational Sling-Shot Model is that when there is considerable differential between Earth's Spin Velocity (ω) and Moon's Orbital Velocity (Ω) there is oscillatory changes in the tidal deformation of Earth and Moon. The tidally deformed shape oscillates between extreme oblateness to extreme prolateness. It is this rapid oscillation between the two extremes which leads to dissipation of energy and tidal heating because of anelastic nature of Earth. But at the geo-synchronous orbits ω = Ω and Earth and Moon are tidally interlocked and during the lock-in stage the two bodies are permanently deformed in oblate shape therefore at these two points we have the conservation of energy and the system is a conservative system.
On the basis of the above reasoning, we have assumed the following:
i. From a$_{G1}$ to a$_2$, Earth-Moon System is a conservative system and Moon experiences a powerful sling-shot impulsive torque ;
ii. From a$_2$ to a$_{G2}$, Earth-Moon System is a dissipative system ;
iii. From a$_{G1}$ to 0 , Earth-Moon System is a dissipative system ;
During the conservative phase from a$_{G1}$ to a$_2$ when the secondary tumbles in super-synchronous orbit its tidal drag slows down the spin of Earth and pushes out Moon in an expanding spiral orbit as shown Figure A.1 thereby increasing the orbital period of the Moon and increasing the PE of the E-M system.
At the time Moon is spiraling out three things are happening:
i. The reduction in spin and orbital energy is partially transferred to increase the PE of the system;
ii. Partially transferred to the translational KE of Moon ;
iii. Remaining is dissipated as heat

Hence we can say that :

K×(reduction in Earth Spin Energy +reduction in orbital energy) – increase in Potential Energy = translational Kinetic Energy in the radial direction. A.17

$$2\pi^2 \times C\ [1/(P1)^2 - 1/(P2)^2]\ /.\ C \to 8.02 \times 10^{37}$$ A.18

$$1.583084545934732 \times 10^{39} \left(\frac{1}{P1^2} - \frac{1}{P2^2} \right)$$ *A*.19

$$1.583084545934733`*^39\ (1/P1^2 - 1/P2^2)/.\{P1 \to 0.2023 \times 86400, P2 \to 0.214067 \times 86400\}$$ A.20

Spin Rotational Energy given up by Earth = 5.54023*10^29Joules   A.21

P1 and P2 are the spin period of the Earth when the system are in aG1 and a2 configuration.

At a_{G1} = 1.46177×10^{7}m , the Orbital Period of Moon is P1 = 0.2023d (4.9hr) by Kepler's Third Law.

At a_2 =2.40942×10^{7}m , the Orbital Period of Moon is P2 = 0.4218d (10.1hr). This is 2:1 Mean Motion Resonance Point.

While Moon's orbital period increases from 0.2023d (4.9hr) to 0.4218 d (10.1hr). Since a2 is 2:1 MMR position hence Earth's spin period is half of 0.4218d. Therefore Earth's spin period increases from 0.2023d (4.9hr) to 0.214067d (5.14hr).

Both these slowing down or de-spinning lead to the transfer of rotational KE from the Earth and Moon to the Earth-Moon System. This transfer increases the PE of the system and simultaneously imparts the maximum radial velocity to our Moon. It is this recessionary radial Velocity which enables our Moon to coast on its own from a_2 to a_{G2} orbit. At a_{G2} , radial velocity becomes zero and the spiral path terminates at a_{G2} orbital radius. Our Moon will be deflected back into collapsing spiral path due to Sun's tidal interaction.

$$\mathbf{2\pi^2 \left(I + m^* \times x_1^2 \right) \times \frac{1}{P_1^2} - 2\pi^2 \left(I + m^* \times x_2^2 \right) \times \frac{1}{P_2^2}\ /.\{m^* \to 7.258721 \times 10^{22}, I \to 8.878277 \times 10^{34}\}}$$

A.22

In the above equation, m*= M_{Moon}/(1+M_{Moon}/M_{Earth}) = reduced mass of our Moon = 7.258721×10^{22}Kg.
I = moment of inertia of our Moon around its spin axis= 0.4$M_{Moon}R_{moon}^2$ =
8.878277×10^{34}Kg-m^2.
The parameters x1 and x2 are a_{G1} and a_2 and P1 and P2 are the orbital period of Moon 0.2023d and 0.4281d at a_{G1} and a_2.

2 ×[Pi]^2 ((8.87828*10^34+7.25872*10^22 x1^2)/P1^2-(8.87828*10^34+7.25872*10^22 x2^2)/P2^2)
A.23

2 \[Pi]^2 ((1/(P1^2))(8.878277000000001`*^34+7.258721000000001`*^22 x1^2)-1/P2^2
(8.878277000000001`*^34+7.258721000000001`*^22 x2^2))/.{x1->1.46177*10^7,x2->2.40942*10^7}
A.24

2 (1.5599*10^37/P1^2-4.22279*10^37/P2^2) \[Pi]^2   A.25

2 (1.5599011168063421`*^37/P1^2-4.2227870171506146`*^37/P2^2) \[Pi]^2/.{P1->0.2023*86400,P2->0.4281*86400}   A.26

Orbital energy given up by E-M system = **3.986053971911033 × 10^{29}** Joules.   B.27

Gain of PE=
G*E*m(1/x1-1/x2)/.{G->6.673*10^-11,E->5.9742*10^24,m->7.348*10^22}   A.28

2.92934*10^37 (1/x1-1/x2)   A.29

2.9293416733679992`*^37 (1/x1-1/x2)/.{x1->1.46177*10^7,x2->2.40942*10^7}   A.30

Increase in the PE of E − M system = $7.88181870890782 \times 10^{29}$ Joules A.31

If all the rotational energy given up by Earth and Moon are conserved during conservative phase then:
Rotational Energy given up by Earth + Orbital energy given up by E-M system = **Increase in the PE of E − M system + increase in translational KE in radial direction** **A.32**

Solving Eq.A.32 we get:

5.540225834158889`*^29+3.986053971911033`*^29-7.88181870890782`*^29= **$1.644461097162102 \times 10^{29} = 0.5 \times m \times v_{max}^2$** A.33

Solving Eq. A.33 we get the solution for v_{max} :

Sqrt[2*1.644461097162102`*^29/m]/.m->7.348*10^22 A.34

v_{max} = 2115.64 m/sec A.35

By Lunar Laser Ranging present velocity of recession is 3.8 cm per solar year [Alley et al 1965, Faller et al 1969, Dickey et al 1994] and at MMR 2:1 from primary-centric analysis we have v_{max} = 1.7178 m/solar year = 5.4435×10^{-8} m/s.

This velocity tells us that increase in translational KE in radial direction = 1.08867×10^{8} Joules.
A.36
Solve[K(5.540225834158889`*^29+3.986053971911033`*^29)-7.88181870890782`*^29==1.08867*10^8,K]
A.37

{{K->0.827376}} A.38

Eq.A.38 tells us that 82.7376% of spin and orbital energy given by Earth, Moon and E-M system are transferred to the increase in PE and translational KE and remaining part of the rotational energy is lost as heat.

$$TE = \frac{1}{2} \times \frac{G(m+M)}{a^3}\left[C(E \times a^{1.5} - F \times a^2)^2 + \left(\frac{m}{1+\frac{m}{M}}\right)a^2 + (0.4mR_{Moon}^2) \right] - \frac{GMm}{a}$$ A.39

When Eq.(A.39) is solved:
At maxima i.e. at a_{G1} , TE = 4.18477×10^{30} J. A.40
At minima i.e. at a_{G2} , TE= -2.64045×10^{28} J. A.41

TE cuts the zero axis at 4.87914×10^{8} m and at 6.2136×10^{8} m. A.42

When our Moon recedes from 2:1MMR position
i.e. from $a_2 = 2.40942\times10^{7}$ m to a = 4.87914×10^{8} m:

i. Earth's spin energy released is 4.59781×10^{30} J by solving Eq. A.18 while Earth de-spins from 0.214067 d (5.14hrs) to 2.658 d because at a = 4.87914×10^{8} m, LOM/LOD=14.6785 and LOM=39.0145d therefore LOD=2.658d ;
ii. E-M orbital energy and Moon's spin energy released is 5.79252×10^{29} J by solving Eq.A.22 while Moon spin and orbital period de-spins from 0.4218d (10.1hrs) to 39.0145d ;
iii.Gain in PE=1.15575×10^{30} J ;

Following is the energy budget equation:
Solve[K*4.59781*10^30+5.79252*10^29 ==1.15575*10^30,K]   A.43

{{K->0.125385}}   A.44

This means only 12.5% of Earth's spin energy is transferred to E-M system . 88.5% of energy released goes for tidal heating of our Earth. This is an expected result.
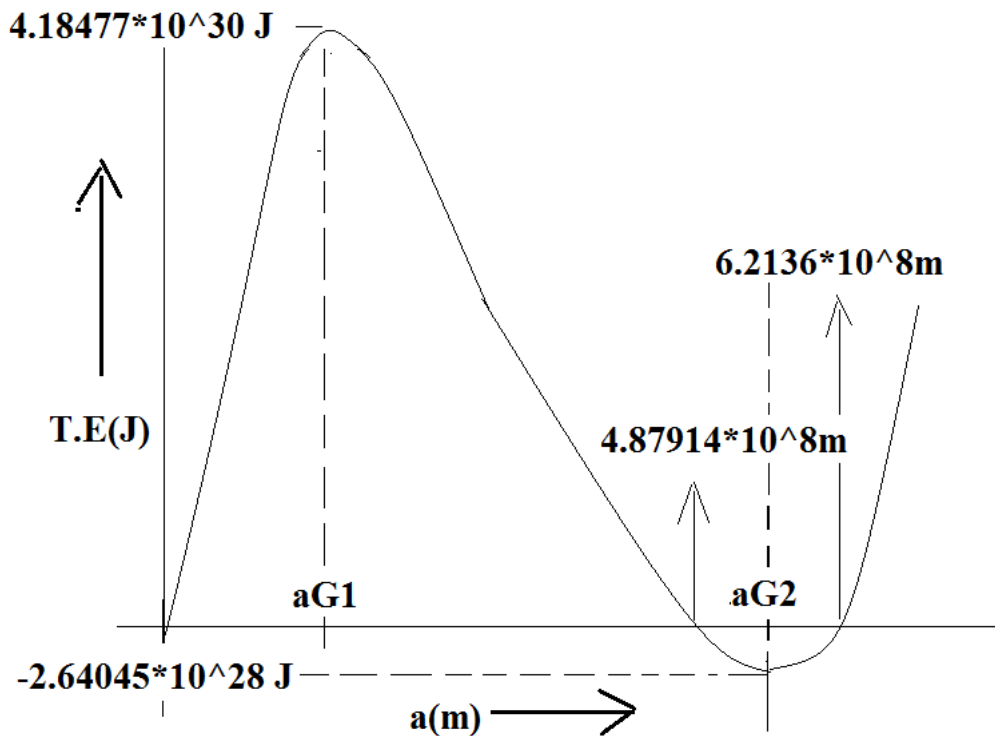

Figure A.4. Total Energy Plot of E-M system with respect to 'a'm.

Appendix B
Birth and Evolution of Stars
['Cosmic History of Star Formation', James S. Dunlop, Science 333,178(2011); 'Galactic Paleontology', Eline Tolstoy, Science 333, 176(2011)]
B.1.Physics and life cycles of Stars.
All stars have one thing in common and that is nuclear fusion. When a solar nebula is born then it can give rise to asteroids, planets, brown dwarfs or stars or a combination of these objects.
An accretion of gas and dust is a planet if the mass is below 13mJ .A typical planet is either a Gas-Giant, an ice-Giant or a rocky planet like Earth.
An accretion of gas and dust between 13mJ and 75 to 80mJ is a Brown Dwarf. It is called a sub-stellar body but technically it is a failed star where hydrogen fusion cannot be sustained.
Above 80mJ , a full fledged star is born where the gravitational collapse leads to Helmholtz Compression and heating, leading to Nuclear Fusion of Hydrogen. The energy released during the nuclear fusion checkmates the further collapse and the fusing star mass reaches a temporary equilibrium.
When the core reaches 15MegaKelvin temperature Hydrogen fusion starts. Through Carbon-Nitrogen-Oxygen cycle Hydrogen is converted into Helium.
When Hydrogen , the reactor fuel, is exhausted then energy release is stopped and gravitational collapse sets in until a core temperature of 100MKelvin is reached. At this point Helium fusion into Carbon by Triple-Alpha Process is ignited.
When Helium , the reactor fuel, is exhausted then energy release is stopped and gravitational collapse sets in again until a core temperature of 600MKelvin is reached. At this point Carbon fusion into Neon by Carbon Burning Process is ignited.
When Carbon, the reactor fuel, is exhausted then energy release is stopped and gravitational collapse sets in again until a core temperature of 1200MKelvin is reached. At this point Neon fusion into Oxygen by Neon Burning Process is ignited.

When Neon , the reactor fuel, is exhausted then energy release is stopped and gravitational collapse sets in again until a core temperature of 1500MKelvin is reached. At this point Oxygen fusion into Silicon by Oxygen Burning Process is ignited.

When Oxygen , the reactor fuel, is exhausted then energy release is stopped and gravitational collapse sets in again until a core temperature of 2700 to 3500MKelvin is reached. At this point Silicon fusion into Nickel by Silicon Burning Process is ignited.

Once Silicon is exhausted a gravitational collapse again sets in which is unchecked because no newer type of Fusion Reaction can set in.

The star at this point achieves a onion like multi-layer structure with Hydrogen-Helium in the outer most layer and Nickel-Iron at the core.

Heavier stars have a short span because they quickly burn way their fuel whereas lighter stars have long life span like our Sun which has life span of 10Gy. It has survived for 5Gy and it will survive for another 5Gy.Universe age is 13.7Gy. Our Milky Way is a spiral galaxy which is 10Gy old. In the Milky Way Sun is probably third generation star. The solar nebula was born 4.567Gy ago. From this Solar Nebula, Sun , Planets, Asteroids, Comets and Kuiper Belt Objects (KBO) were born.

In Table B.1 we give the final three alternative destinations which the stars can achieve.["We are cosmic dust but you are everything to me", Kelly Oakes, July 21, 2011]

Table B.1. The three alternative fates of a star in its death.

Mass of the star	Type of Explosion	Mass after the explosion	The process which checkmates the collapse	Type of remnant.
Sun-like	Nova	Less than $1.4M_\circ$	Electron degeneracy	White Dwarf
Less than 20 $M_\circ$	Supernova	$1.4M_\circ$ to $3M_\circ$	Neutron degeneracy	Neutrinos take away the heat hence a stable Neutron Star is formed with 30km dia.
20 $M_\circ$>M>50 $M_\circ$	Supernova	Greater than$3M_\circ$	Quark degeneracy /?	Black hole
M>50 $M_\circ$	Directly collapses into BH	Greater than$3M_\circ$	?	Black hole
M>140 $M_\circ$	Pair-instability SN	?	?	No Black Hole

Table B.2. The properties of White Dwarf, Neutron Star and Black Hole.

Type of remnant	Matter density	Mass	Diameter	
White Dwarf	$10^9 Kg/m^3$	Less than $1.4M_\circ$	12000km	
Neutron Star	$10^{17} Kg/m^3$(density of the nucleus)	$1.4M_\circ$ to $3M_\circ$	20km	
Black Hole	?	Greater than$3M_\circ$	Event horizon	

B.2. Evolution of Stars and Galaxies.

The earliest stars and galaxies were made of pristine materials and they are called Population III stars. They primarily had Hydrogen and Helium with traces of Lithium and Deutrium.

After the death of Population III stars , heavier elements were introduced through Novae explosions and Super-Novae explosions. Carbon, Neon, Nitrogen, Oxygen, Silicon, Nickel and Iron are introduced in the Universe through Novae explosions. These elements have been nucleosynthesized in the cores of all stars during their Main-Sequence existence.

Calcium, Magnesium and Titanium and other radioactive elements were synthesized in Super-novae explosions and strewn around the Universe subsequently.

In 1950 , M. Burbidge, G. Burbidge, W. Fowler, F. Hoyle expounded the theory of Nucleosynthesis.

It became clear by theory as well as by careful observations also that as we move from Population III to Population II and now in Population I stars we find that over time with each successive generation of stars and their novae or supernovae deaths the gas in galaxies, from which the stars are formed , become enriched in heavy elements. Hence we conclude that matallicity [%of heavier elements as well as alpha elements abundance= α/Fe =(Ca+Mg+Ti)/Fe] have steadily improved.

Through the study of nearby galaxies it has been concluded that Milky-way and its like can retain the enriching products of Super-novae explosions and rapidly build up metals and alpha elements in its disk, bulge and halo. This is not the case with nearby Dwarf Galaxies.

Our neighboring dwarf Galaxies have difficulty retaining gas and products of star formation. This results in large scatter in abundance ratios as well as much slower build-up in alpha elements in Dwarf Galaxies.

We also conclude that the bulk of stellar mass of Population I and II galaxies cannot have come from the merger of two galaxies but that most have come from the gas within the bulge of the galaxy. This means that in first 1 Gy (that is at z , redshift,= 5 or larger- see Appendix C) after the Big-Bang according to the current theory of hierarchical structure formation smaller structures(dwarf galaxies) may have merged to form the larger galaxies but in Population I and II smaller galaxies merger is an exception.

B.3. The results of the studies conducted by Sloan Digital Sky Survey(SDSS).

Sloan Digital Sky Survey Programme has calibrated the optical spectra of 1 million galaxies in the Local Universe. Most massive galaxies are the oldest, generally elliptical, have very little recent star formation histories and the spectra of the galaxy can be explained in terms of one to three distinct stellar populations namely bulge, disk and halo population.

Typical masses of galaxies have younger average stellar ages, more complicated star formation histories and the overall spectra can be explained in terms of five distinct stellar populations namely extreme disc, thin disc, thick disc, bulge and halo.

This means star formation rate was very high initially and then it monotonically declined. Star formation has in effect moved from most massive galaxies to less massive galaxies.

Here the question arises as to why star formation has stopped in most massive galaxies ?

In last twenty years we have built a large number of ground-based giant telescopes of 8 to 10 m diameter. We also have space telescopes such as Hubble Space Telescope, Spitzer Space Telescope and Herschel Space Observatory. Study of young massive stars provide the most useful tracers of star formation activity as enumerated in Table B.3.

Table B.3. The useful tracers of star formation activity in Young Massive Stars.

Tracer number	1	2	3	4
Propertry of the tracer	Bright optical-UV continuous light from star themselves	Brigth H_2 & O_2 emission lines from the surrounding gas ionized by the hot stars	Enhanced emission at Mid & Far infra Red from the dust warmed by UV light from the stars.	Radio-emission from the relativistic electrons acelerated by the shock waves produced by Supernova explosions.

B.4. Star Formation Rate through the cosmic times. [Peebles et.al. (1994), Hogan (1996)]

After extensive studies particularly those of Sloan Digital Sky Survey(SDSS) we have arrived at the Figure B.1 and concluded the following results in Table B.4:

Table B.4. The Cosmic History of Star formation.

Time after BB	Z† (redshift) Or T(Kelvin)	Event	Comment
0 year	Infinite	Big Bang occurs	Time is born with Big Bang
10^{-43}s	3.16×10^{31}K	1st Symmetry breaking	Quantum Gravitation to GUT phase transition. Relic gravitons left out. Density of matter = 10^{93}gms/cc.
10^{-10}s	10^{15}K, 100GeV	2nd Symmetry breaking	GUT to Electro-Weak Phase transition, weak force decouples, relic intermediate vector bosons left out, Universe filled with a soup of quarks, leptons, photons
10^{-6}s	10^{13}K, Less than 1GeV	Fission of nuclear particle stops	Quark-nucleon phase transition. Universe filled with a soup of leptons, nucleons, photons. Relic quarks left out. Density of matter = 10^{18}gms/cc.
10^{-4}s	10^{12}K 1000×the core temp of Sun	Instability of leptons lead to instability of baryons.	Continuous transmutation taking place between proton and neutron. Density of matter = 10^{14}gms/cc.(nuclear density)
4sec	5×10^9K	Leptons become stable hence baryons stabilize.	p, n stabilizes to 7:1
3min	745×10^6K		75%H ions,25% He ions
15mins	333.3×10^6K	Nuclear fusion first stage completed.	Matter in plasma form stabilized at 75%H ions,25% He ions or 92% and 8% by atomic number density with traces of Lithium

From here onward Universe enters the Dark Ages. But the matter is not uniformly distributed as confirmed by the study of Cosmic Microwave Background Radiation through COBE and WAMP. The denser part of matter shows up as red in CMBR map and rarefied part shows up as blue. The denser part are the seeds of stars, galaxies and clusters. CMBR carries the imprint of the matter distribution at the time of decoupling which will occur at 380,000 years after the BB because temperature cools below 4000K which allows plasma to neutralize.

380,000yrs	4000K	Plasma recombines into cold, neutral, dark universe.	Temperature of the Universe falls to 4000K where all ions recombine to form neutral atoms and molecules of H_2 and He. Gravity will dominate from now on.
The stage is set for the formation of Population III stars and galaxies.			
500My	Z=8.5	?	?
600My	Z=7	Dark age ends and the epoch of re-ionization begins	Population III stars and galaxies are formed and these re-ionize the cold, neutral and dark universe.(detected by near-IR Wide Field Camera3 mounted on Hubble Space Telescope).
Population III stars were massive and hence short lived however through internal fusion followed by supernova explosion they must have commenced the process of chemical enrichment through recycling in the interstellar matter. This produced the successive generations of Population II and Population I stars with progressively higher metallicity and alpha elements.			
1Gy	Z=6	Rapid build-up of low metallicity stars.	Here heavier elements reside in cool gas and dust grains within the Galaxies.
2Gy	Z=3	Metallicity increases through nuclear synthesis. Star formation Rate $= \rho = 0.2*$	Heavier elements reside in stars , planets and interstellar gas. There is possibly a peak in Star Formation Rate.
3Gy	Z=2	Half the stars were in place and $\rho \geq 10\, \rho_0$	Population II & Population I stars and Galaxies are born. Milky Way is born at this time. It is the third Generation Galaxy(Population I).
4Gy	Z=1	Rate of star formation is $10\, \rho_0 = 0.1*$	
9.133Gy		Our Solar Nebula is born.	Our Sun is Population I star.
13.7Gy (present)	Z=0	Rate of star formation is $\rho_0 = 0.01*$	

*Units of star formation rate is $(M_{SUN}) \times y^{-1} \times Mpc^{-3}$, ρ_0 = present day star formation rate;

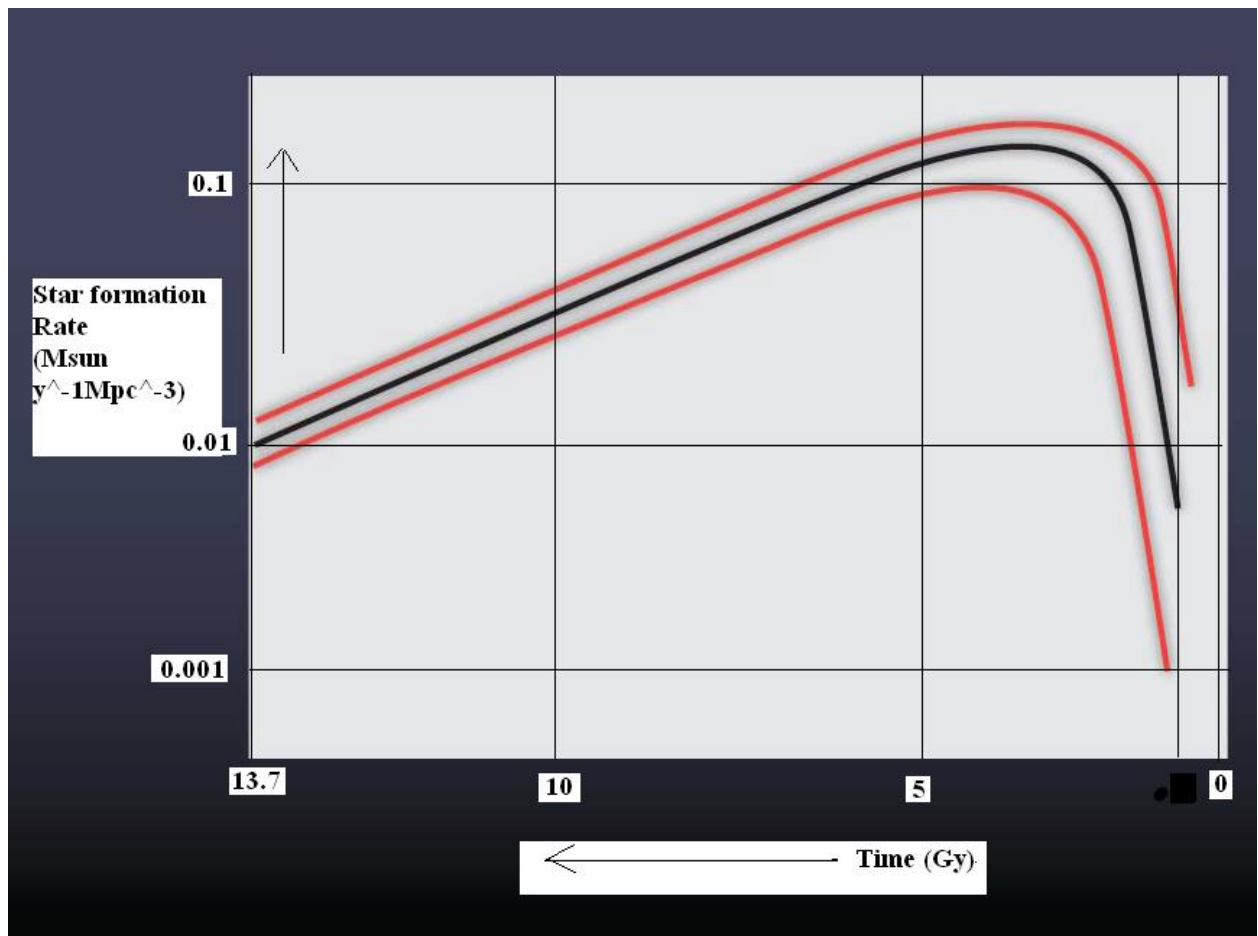†Distance calculation from Redshift (z) is given in the Appendix.C.

Fig. B.1. A simple representation of our current knowledge of the rise and fall of globally averaged star-formation activity over the 13.7 billion years of cosmic history. The black line indicates our best estimate of how the density of star formation (in solar masses formed
per year per unit of co-moving volume) grew rapidly in the first 2 billion years after the Big Bang, stayed roughly constant for a further ~2.5 billion years, then has declined almost linearly with time since the universe was ~5 billion years old. The red lines indicate the typical current uncertainty in the measurement, which rises to approximately an order of magnitude at the earliest times.

APPENDIX C.
Formation and Evolution of Galaxies [Milky Way Researchers (2011), Heckman & Kauffman (2011)]
Through the advancement of γ-Ray and X-Ray astronomy it has been possible to peer into the nucleii of several galaxies and through the study of the last decade it is confirmed that probably all the Galaxies have Super Massive Black Holes(MBH). It is confirmed that the lives of Galaxies and MBHs are inextricably intertwined. It can also be said that as the galaxies grow so do the MBH at the center.

Quantum Mechanical fluctuations in the Universe emerging from the Big Bang gave rise to the small inhomogenities which will act as the future seeds of the super clusters, cluster and galaxies. These inhomogenities attracted the surrounding matter gravitationally and grew into lumps called haloes. In these haloes there is gravitational heating as we see in Pre-Main Sequence Stars and there is radiative expansion and cooling. The two are trying to compensate each other. If gravitational heating dominates there will be subdued star formation and if radiative cooling takes place then there will be rapid star formation.

In low-mass haloes below critical mass 10^{12}MO, cooling dominates and there is a star formation burst due to cold gas inflow. This is how the spiral galaxies grow by gas accretion.

In high-mass haloes above 10^{12}MO , heating dominates and growth stops by accretion. Halo mergers take place leading to large haloes. Within the large haloes galaxy mergers take place and spiral galaxies disks are scrambled into bulgy elliptical galaxies.
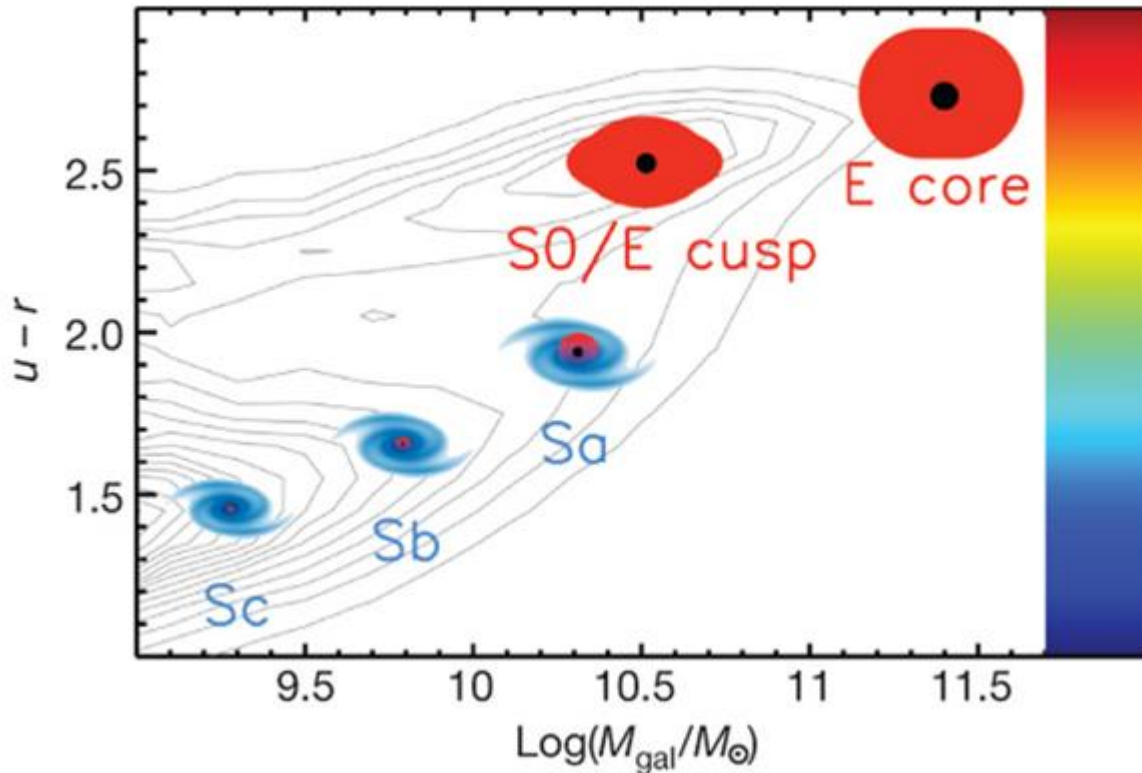
Figure C.1. The contours show the galaxy distribution on a stellar mass (M_{gal}) – colour diagram[92]. The difference between ultraviolet luminosity and red luminosity, quantified by the magnitude difference u - r, is a colour indicator; larger values of u - r correspond to redder galaxies. The colour bar has been inserted to convey this notion visually and has no quantitative meaning. Galaxies are classified into two main types: spirals that mainly grew through gas accretion ('S', shown in blue) and ellipticals that mainly grew through mergers with other galaxies ('E', shown in red). 'S0' galaxies are an intermediate type, but we assimilate them to ellipticals. Spirals have central bulges, shown in red, that resemble miniature ellipticals. All ellipticals and bulges within spirals contain a central black hole, shown with a black dot. Moreover, ellipticals and bulges within spirals have the same black-hole mass to stellar mass ratio, of the order of 0.1%. This is why we call them 'bulges' indiscriminately. In contrast, there is no connection between masses of black holes and masses of disks (the galactic component shown in blue). Spirals and ellipticals are separated by a colour watershed at u - $r \approx 2$ and a mass watershed at $M_{gal} \approx M^* \approx 10^{10.5} M_O$. M^* is of the order of $f_b M_{crit}$, where M_{crit} $10^{12} M_O$ is the critical halo mass for gas accretion and f_b 0.17 is the cosmic baryon fraction. Spirals form a sequence where the bulge-to-disk ratio tends to grow with Mgal (Sc, Sb, Sa). Ellipticals have two subtypes: giant ellipticals with smooth low-density central cores formed in mergers of galaxies that have long finished their gas ('E core') and lower-mass ellipticals with steep central light cusps formed in mergers of galaxies that still have gas ('E cusp'). Whereas core ellipticals formed all their stars over a short time span at high redshift, the formation of the lower-mass cuspy ellipticals from the 'quenching' and reddening of blue galaxies continues to low redshift.[This Figure is from the article: "The role of black holes in galaxy formation and evolution",
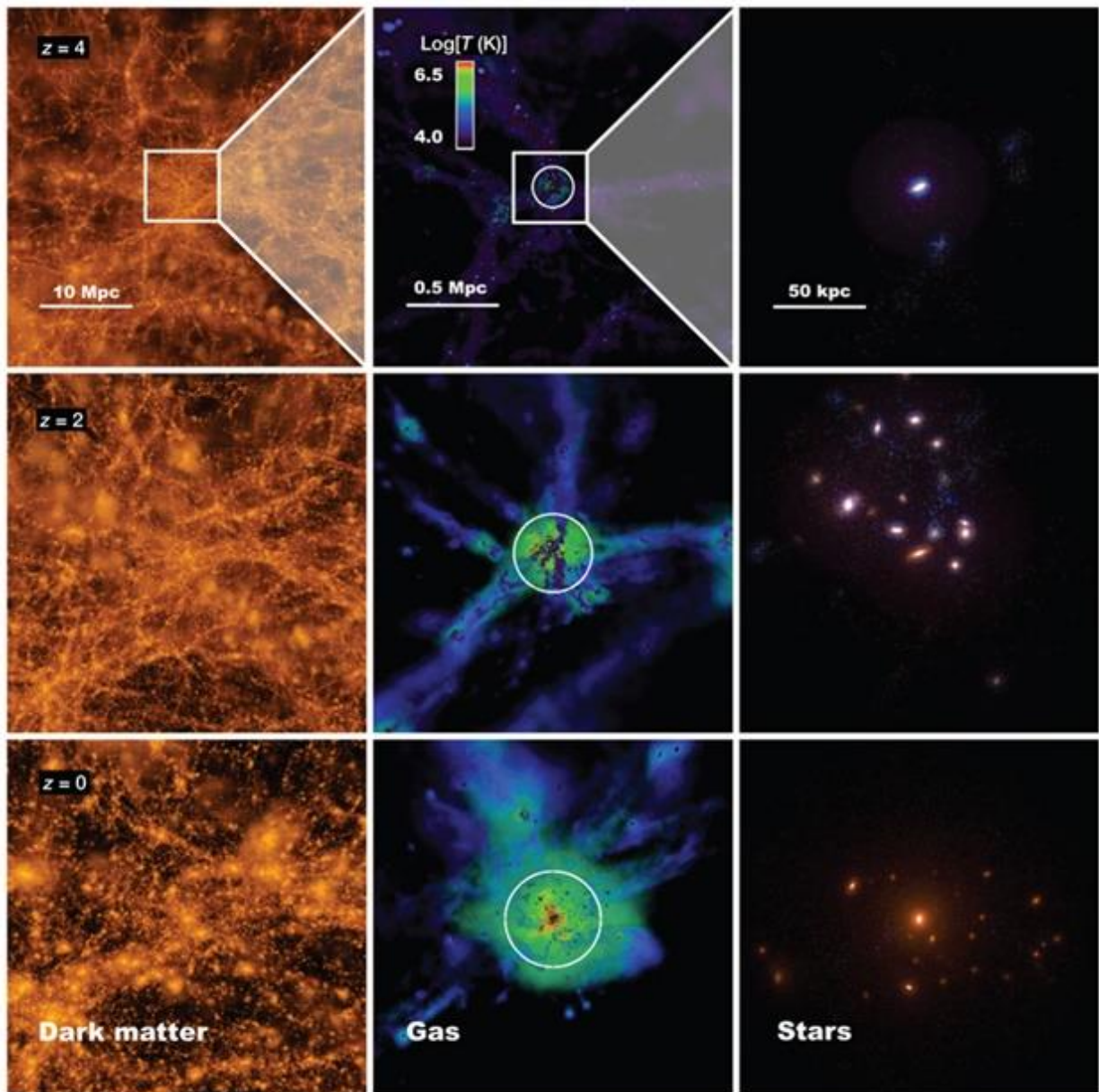
Figure C.2. A computer simulation of the formation of an elliptical galaxy. The nine panels illustrate the formation of an elliptical galaxy by showing how the dark matter (left column), the gas (centre column) and the stars (right column) are distributed at three epochs in the expansion of the Universe: when the Universe was 1/5 of its current size (redshift $z = 4$), when the Universe was 1/3 of its current size ($z = 2$), and today ($z = 0$). The gravity of the dark matter dominates the evolution on large scales (left column). As time passes, the Universe becomes lumpier because the dark matter clumps via gravity into haloes (bright orange spots in the left panels). The centre column zooms into the region around and inside a halo to show what happens to the gas. The halo radius is shown as a white circle, and the gas is colour-coded according to its temperature: blue is cold, green (and red) is hot. Initially the halo is small, and the gas streams into the halo down to its centre in cold flows. When the halo reaches the critical mass Mcrit $\approx 10^{12}$ M_O ($z = 2$), the gas begins to form a hot atmosphere (green); eventually, all the gas within the halo is hot ($z = 0$). The right column zooms in even further to show the visible galaxy formed by the gas fallen to the centre. The galaxy is initially a blue spiral ($z = 4$). It starts to become red when the halo gas starts to be hot ($z = 2$). By then, its halo has merged with neighbouring haloes to form a galaxy group. Mergers with companions eventually transform the galaxy into an elliptical ($z = 0$).[ibid]

Most MBHs are turned off or dormant. But if there is a disc of accretion , the gas and dust within the radius of influence will be sucked into the BH just as a vortex in a river sucks in the surrounding water. When the reservoir of gas and dust is exhausted this accretion will stop and BH will shut-off.

In-falling gas and dust emits radiation in γ_ray, X-Ray, Ultra-Violet and optical part of the spectrum. These AGN are seyfert galaxies [Fritz et.al.(1971)].

Apart from these emissions there are conical relativistic jets being emanated from the poles of the BH [McNamara et.al. (2007)]. Unsteady accretion flow gives rise to variable AGN. The most variable AGN are a sub-class called Blazers with typical masses of 108 to 109 MO. It is radio and optically bright but luminosity is dominated by X-ray and γ-ray. Doppler beam emitting region within a jetted outflow moving relativistic ally causes changes on minutes- to hours- time scale. The high energy emission is caused by Inverse Compton Up-Scattering of accretion disk photons. The conical emanation takes place in Super Massive Black Hole engulfing a large amount of surrounding gas and dust[Ulrich et.al.(1997), Maraschi et.al.(2003), Bottcher et.al.(2007), Fossati et.al. (1998)]. The same kind of jets can be emanated from Massive Black Hole which is tidally shredding the star launched on a death spiral towards the nucleus of the Galaxy [Bloom et.al.(2011), Levan et.al. (2011)]. The two conical jets are very narrow streams of particles travelling in opposite directions at relativistic speeds. These relativistic jets travel out to distances across the Galaxy.

As they emerge out of the two poles of the galaxy they finally decelerate as they interact with the interstellar gas and dust and they turn on two radio-emitting lobes. This kind of Active Galactic Nucleus(AGN) is called QUASERS as shown in the Figure C.3.

Figure C.1. Twin jets produced by the supermassive black hole in the galaxy Messier 84 are strongly interacting with the hot tenuous gas in the galaxy's halo. The black hole is located at the center of the brightest region in this image. The jets are traced by their radio emission (shown in red) as mapped with the Very Large Array (VLA), and the hot gas is traced by its x-ray emission (shown in blue), as mapped with the Chandra X-ray Observatory. The jets decelerate as they travel out into the halo and light up as two lobes of radio emission. These lobes form two cavities in the hot gas as they push it out of their way. [Source: x-ray, NASA/Chandra X-ray Center (CXC)/Max Planck Institute for Extraterrestrial Physics/A. Finoguenov; radio, NSF/National Radio Astronomy Observatory/VLA/European Southern Observatory/R. A. Laing; optical, Sloan Digital Sky Survey]

The Star population converts 0.7% of Solar Nebular Matter into energy by nuclear reaction from which it has been born. In contrast SMBH in AGN accretes 10% of the rest mass in the bulge of the Galaxy and converts it into energy. Hence they stand out as distinct cosmic beacons clear across the Universe. Through such beacons, distance estimate can be made for the far flung Galaxies . Detection of GRB090429B, the most distant GRB, is a case in point [Cuchiara et.al. (2011)] and these beacons will also let me know how the SMBH have evolved across the entire span of cosmic time. We have different categories of AGN and accordingly we have different categories of Galaxies such as Seyfert Galaxies, Blazers and QUASERS. All these three play an important role in anchoring Clusters and Super-Clusters.

Even a tiny fraction of (<1%) of this energy released within each bulge could heat and blow away the entire gas content from the bulge and completely stop star formation..

C.1. The results of Galaxy Classification by Galaxy Zoo [Clery (2011)].

Galaxy Zoo was an online classification program for all the galaxies catalogued by Sloan Digital Sky Survey(SDSS) over a period of 11years. The results have been tabulated in Table(C.1).

Table C.1. Classification of Galaxies based on the Galaxy Zoo program.

	Blue (indicative of star formation)	Red (star formation quenched)	
Spiral Galaxy	80% Here gas component is large hence star formation is high.	20%_these are barred red spirals. Hydrogen is being siphoned off from the halo and star formation is retarded	
Elliptical Galaxy	20%_these are recently formed small galaxies and are undeeregoing vigorous star formation.	80% These lack gas hence star formation has stopped. Only old light mass stars are there	
Little Green Galaxies			Compact galaxies. These undergo extreme star formation and emit light at a wavelength that is characteristic of highly ionized oxygen . In SDSS images these appear green.

Astronomers have concluded that galaxies are formed when dark matter clusters together under its own gravity and then pulls gas, dust, stars and smaller galaxies to form the flat extended disk of a spiral galaxy. Dark matter stays in the spherical "halo" that surrounds the whole galaxy. In spiral galaxies, stars keep forming in the disk as neutral gas rains down from halo into the spiral arms. Elliptical galaxies result when two galaxies of comparable masses collide- if one or both are spiral galaxies, the spiral structure is destroyed and stars are left in random orbit around the galactic center. The collision also slam together gas clouds causing burst of intense star formation that flares and burns out quickly using up all the hydrogen gas. The end result is a structure less blob of a galaxy with no gas clouds and few young stars.

Galaxies grow by accretion of surrounding cool gas in the halo or the merger between two or more galaxies. This merger takes place in seven distinct steps:

i. Two galaxies merge together as shown in Figure F.11, Appendix F. Thin and highly ordered disk components are scrambled together.

ii. Tidal forces between the two galaxies drain away angular momentum from the cold gas in the disk of the galaxy, allows the cold gas to flow into the inner region and then fuels an intense burst of star formation. This flow delivers a fresh supply of gas to SMBH as shown in Figure F.12..

iii. The scrambled disk material settles into a newly created bulge.

iv. If the two progenitors had their own BH then the two also merge to give rise to a new BH as shown in Figure F.13.

v. The release of energy from the merger induces a star formation burst so intense that it may blow away most or all remaining gas in a powerful outflow.

vi. Relativistic conical jets from SMBH will pump energy into the surrounding gas preventing it from cooling and falling into the galaxy thus quenching star formation.

vii. Finally we have a single Galaxy with a larger bulge and a larger SMBH as shown in Figure F.13.

viii. Living Galaxy has reached its limit of growth and it becomes passive. Star formation stops.BH growth also stops.

Growth rate of Galaxies and SMBH depend strongly on mass.[Panter et.al.(2007)]. As we see in Figure F.17 ,in Appendix F, most massive galaxies and their respective SMBHs grew rapidly early in the cosmic history and then they stopped growing after reaching a limit. In contrast as seen in Figure F.18, lower mass galaxies and their respective BHs have grown at a lower uniform rate throughout the entire cosmic history.

Apart from these major mergers there are minor mergers. Our Milky Way has assembled itself from a kit of hundred of Galactic building blocks. Whenever a small galaxy or a star cluster passes by too close, our Galaxy's gravity tears it apart and draws it into the main galaxy [Ibata et.al. 2007, Purcell et.al. 2011]. Our Milky Way's , and so Galaxy's in general, tangled history of merging and accreting have brought new stars, gas and dark matter within the halo of our Milky Way. In fact merger and accretion are processes which have become the main driver of Galaxy formation and evolution. These minor mergers have also revealed the nature of dark matter- its hydro-static equilibrium shape and its granuality.

C.2 Different classes of Galaxies according to the mass of BH.[Heckman et.al. (2011)]
Table C.2. Classification of Galaxies according to the mass of the BH.

Mass of BH	Accretion disc	Spin Rotation	spectrum	Name of the galaxy
$10M_\circ$		?	?	This is not the fulcrum of the galaxy and is the result of the death of a massive star of mass $> 20M_\circ$
10^5 to $10^6 M_\circ$(moderateBH)	No	Little or no	quiet	Fulcrum of light weight Galaxy
10^5 to $10^6 M_\circ$(moderateBH)	Yes	Yes	IR to γ-Ray continuous	Fulcrum of Seyfert galaxy.
10^6 to $10^8 M_\circ$(MBH)	Yes. Rate of BH growth/ρ_{SFR}* = 1:1000	Yes	More luminous and radio loud.	Fulcrum of Intermediate galaxies.
10^8 to $10^{10}M_\circ$(SMBH)	No Lack cold, dense gas.	?	Switched off	Fulcrum of massive galaxies. Buried in aged Galaxies with little or no reservoir of cold, dense gas.
10^8 to $10^{10}M_\circ$(SMBH)	Mass ratio of SMBH/Mass of the bulge = 1:1000 Surrounded by a halo of hot and tenuous gas		Switched on.	Fulcrum of massive galaxies. Active Galactic Nuclei(AGN)†.It has relativistic jet and strong emissions. It heats the surrounding gas. This shuts off the star formation

*ρ_{SFR} = star formation rate.†AGN can be a sub-class of Blazer or it can be QUASER.

There is a strong connection between Star Formation Rate(ρSFR) in the bulge and the growth rate of SMBH. When there is a sufficiently large reservoir of cold, dense gas then both processes are supported.
The self-regulating process which keeps Mass ratio of (SMBH/Mass of the bulge) = 1:1000 or which keeps Rate of BH growth/ ρSFR= 1:1000 is by feedback mechanism as given below:
i. In Galaxies hosting 108 to 1010M∘(SMBH), powerful relativistic conical jets are created which prevent the in-fall of cool gas into the bulge. Hence star formation is quenched and growth of SMBH is stopped.
ii. In intermediate mass Galaxies hosting 106 to 108M∘(MBH), SN explosions due to the death of newly formed massive stars causes an out-flowing galactic wind. This sweeps away Galactic gas into the halo where it is in hot form. This also regulates the availability of cool gas in the bulge thereby regulating the star formation rate and growth rate of MBH to the ratio 1000:1.
 In a living galaxy or young galaxy, stars formation is going on and accretion of gas and dust on the BH is also going on. The accretion by BH leads to Gamma Ray Burst (GRB) and relativistic Jets. Gamma Ray Bursts are the Universe's most luminous explosions emitting more energy in a few seconds than our Sun will during its energy producing life-time.
Massive stars collapse into Black Holes surrounded by a dense hot disk of gas. The in-falling matter is diverted into a pair of high energy jet particles that tear through the collapsing star. The jets move upward at 99.9% of the speed of light. The jet of particles strikes the gas beyond the star to produce after glows. "Catching these afterglows before they fade is the key to determine the distances of the bursts. "
GRB090429B has qualified as the most distant galaxy till date [Cucchira et.al. 2011]. It was detected by its Gamma Ray Burst. It is at 13.14 billion light years distance with date of occurrence at 520My after the Big Bang when the Universe was 4% of the present age and 10% of the present size. This is the first galaxy to form after the Big Bang.
James Well Space Telescope due to launch in 2017 has been carefully engineered for studies in the early Universe. An after glow

spectrum from this facility would be an unique and valuable source of data.

Penn State University, South West Research Institute, Cornell University have proposed JANUS explorer to be launched by 2017. This will be used for understanding the first galaxies and the various processes guiding their formation.

By discovering and observing the most distant GRBs and QUASERS and measuring their distances autonomously without the need for follow up observation, JANUS would provide a steady stream of rewarding targets to James Well Space Telescope and ground based telescopes.

Nothing else illuminates the conditions in the early Universe like its brightest lights the GRB and QUASERS.

Massive stars are dying , leading to SN explosions. The strong emissions from SN explosions and relativistic jets are heating up the gas in the halo and SN explosions are powering an outward galactic wind that can sweep out the Galaxy's gas and sweep it into the halo. For a given black hole mass, there is a maximum AGN luminosity, called the Eddington limit, above which the radiation-pressure force outwards exceeds the gravitational force inwards, suppressing the gas flow onto the black hole. The velocity dispersion is the bulge property that is most closely linked to the black hole because it determines the depth of the potential well from which the gas has to be expelled, and thus the minimum black hole mass for feedback. At the Eddington Limit , star formation is halted as well as the growth of black hole is stopped and Galaxy is switched off. Young and living Galaxy is turned into aged and passive galaxy. This self-regulating process has kept the mass ratio pinned down to 1:1000 in the early galaxies and keeps Rate of BH growth/ρSFR= 1:1000 in the present day galaxies.

There is always fresh cool and dense gas coming in the bulge from the outer disk subsequently. There is also the remnants of the dying stars being fed into the bulge. Both these factors eventually may rejuvenate the dormant galaxy.

Table 3.Classification of AGN.

90%	No conical jet of energetic particles		
10%	Have conical jet	Radio Galaxies, Quasers and Blazers	

Different orientation of observation also gives rise to different galaxies.

If we look down the conical barrel of emission then we have Quasers and Blazers,

If we look broadside then we have Seyferts Galaxies

Table 4. Classification of Seyferts, QUASERS and Blazers.

	Nucleus brightness variation time scale	Spectrum	At the nucleus	Total luminosity
Seyferts Appendix F. Figure F.14	months	Continuous, absorption lines, strong emission lines of H and also of O	Shoot out narrow beams of energetic electrons producing synchrotron radiation.	$10^{10}L_0$
QUASER Figure C.1	X-ray variation in days, hours ,mins	Continuous, absorption lines, strong emission lines of H and also of O	It outshines the stars. It has relativistic conical jets and two radio lobes	$10^{12}L_0$
Blazers Appendix F. Figure F.15	Optical vari. Over days.	High radio brightness,high optical polarization Widest range of frequencies from radio to γ-Ray.	It has relativistic jets pointed to Earth	

• Two sub-groups of Blazers:
i. Sources showing strong and broad emission lines, such as those of quasars (called Flat Spectrum Radio Quasars)
ii. Sources showing a featureless optical spectrum (called BL Lac objects) . [Urry (1998)]

APPENDIX C.
Galactic distances are measured using the Hubble relationship:
v = Hd   C.1
where H = 71Km/(sec.Mpc) [7-year release in 2010 from WMAP data alone]
and 1Mpc = 3.26 ly(light-year).
Velocity of recession has to be determined from Z (red shift).
Z (Doppler shift) has to be determined by spectroscopy. Observed Wavelength (λOBS) are determined by observation and Emitted Wavelength (λEMITTED) are determined by spectroscopy science.

$(\lambda_{OBS}) = (\lambda_{EMITTED}) \times (1+z)$ C.2

$Z(red\ shift) = \Delta\lambda/\lambda =$

$(\lambda_{OBS} - \lambda_{EMITTED})/(\lambda_{EMITTED}) = (1+v/c)/\sqrt{(1-v^2/c^2)} - 1$ C.3

From Eq.C.3, velocity of recession of the given Galaxy is determined.

Receding galaxies spectrum suffer from Doppler Red Shift.

Velocity of recession gives distance in light-years using Hubble relationship Eq.C.1.

Distance of Galaxies and QSO(quasi stellar objects) based on Z measurement

Velocity of recession (m/second)	Z shift	Distance of the given obje time by light.
1×10^8	0.414	4.591Gy
1.5×10^8	0.732	6.887Gy
2×10^8	1.2361	9.183Gy
2.5×10^8	2.3166	11.478Gy
2.7×10^8	3.3589	12.397Gy
2.8×10^8	4.38516	12.856Gy
2.9×10^8	6.68	13.3Gy
2.95×10^8	9.91	13.545Gy
2.99×10^8	23.47	13.728Gy

APPENDIX D

cD Galaxies are Supergiant Galaxy and Diffuse type. It is also known as Central Dominant Galaxy. These are Super Giant Elliptical Galaxies with 1 trillion stars. In the Table A a comparative study of cD Galaxy and Milky Way is made.

Table A. A comparative study of cD Galaxy and Milky Way.[Fraser Cain (2009)]

Galaxy	Luminosity	Mass	Diameter of the disk	Total number of stars
Milky Way	L*	M*	100,000ly	100 billion
cD Galaxy	10×L*	100×M*	6,000,000ly	1 trillion

APPENDIX E

ABELL 2029 consists of thousands of Galaxies enveloped in hot gas and dark matter. Total Mass of the dark matter is 100×1012MO. X-Ray data shows that the dark matter increases smoothly all the way to the centre of the Galaxy Cluster. This distribution of dark matter matches the predictions of Cold Dark Matter. This cluster is at 1 bly from us. At the center there is an enormous, elliptical Galaxy acting as the anchor of the system.

a tidally disrupted Star", Joshua S. Bloom, Dimitrios Giannios, Brian D, Metzger, S.Bradley **APPENDIX F**

Extension of the New Perspective as the principal formative process in shaping the Universe - GRB110328 comes as a grand vindication of the New Perspective based on Gravitational Sling-Shot Model of Earth-Moon System.

["An extremely Luminous Panchromtic Outburst from the Nucleus of the distant Galaxy", A.J. Levan, N.R.Tanvir,S.B.Cenko et al, Science 333, 199-202(2011),

"A possible Relativistic Jetted Outburst from a Massive Black Hole fed by Cenko et al, Science 333,203-206(2011)]

A long duration Gamma Ray Burst(GRB110328) was picked up by Burst Alert Telescope (BAT) aboard SWIFT Gamma Burst Mission Spacecraft. Emission of X-Rays and Gamma Ray is persisting. It seems a Super Massive Black Hole(SMBH) situated at the center of a Galaxy 3.8 b lighyears away with a red-shift of 0.3534 was ripping apart a star of about sun's mass($M\odot$) and SMBH was gobbling it up gradually. It was the biggest and the brightest event in the series of GRB and QUASERS observed till now. Earth was in line with the Jet emissioin. SWIFT was looking down the conical barrel of X-Rays and γ-Rays. This conical barrel is normal to the plane of the star's orbit of death spiral. This event was reported by Joshua S.Bloom et al of University of California and by Andrew Levin et al of University of Warwick in 8th July 2011 Science Vol 333.

This long duration GRB may not be rare but SWIFT falling in line of sight of the conical barrel of this stupendous emission is a very rare event. This happens 1-in-108 ~ 109 events.

Gamma-ray bursts (GRBs) are the most powerful explosions the Universe has seen since the Big Bang. They occur approximately once per day and are brief, but intense, flashes of gamma radiation. They come from all different directions of the sky and last from a few milliseconds to a few hundred seconds. So far scientists do not know what causes them. Do they signal the birth of a black hole in a massive stellar explosion? Are they the product of the collision of two neutron stars? Or is it some other exotic phenomenon that causes these bursts?

With SWIFT, a NASA mission with international participation, scientists have a tool dedicated to answering these questions and solving the gamma-ray burst mystery. Its three instruments give scientists the ability to scrutinize gamma-ray bursts like never before.

It has three instruments aboard:1.BAT-Burst Alert Telescope;2.XRT-X-Ray Telescope:3.UVOT-Ultra-Violet/Optical Telescope. BAT scans 1/6 of the sky at one time. Within seconds of detecting a burst, it directs XRT and UVOT to lock on the GRB and study the afterglow in X-Ray, UV and Visible range of the electromagnetic spectrum. Swift relays its location to ground stations, allowing both ground-based and space-based telescopes around the world the opportunity to observe the burst's afterglow. Swift is part of NASA's medium explorer (MIDEX) program and was launched into a low-Earth orbit on a Delta 7320 rocket on November 20, 2004.

With better luck, or more advanced facilities, it should be possible in the future to use the bright afterglows of bursts like GRB 090423 and GRB 090429B to explore the conditions of star and galaxy formation at these early cosmic epochs in detail. "Discovering extremely distant bursts is pretty fun," says Fox, "but we suspect there is a whole lot more information in the bursts, waiting for us, that we have yet to access."

GRB as indicated by the above two events are extremely bright and these are detectable at long distances . GRB090423 spectra gave a red-shift of z=8.2 indicative of 13.04biliion light years distance and GRB090429B gave a red shift of z=9.4 indicative of 13.14 billion light years. Gamma Ray Burst is short lived event lasting less than 10 seconds. They have a faint after-glow in X-Ray region and in IR region but give no glow in optical region.

Visible region "Drop Out" behavior is a distinctive signature of the most distant objects and has been used in initial identification of all the most distant quasers, galaxies and GRB.

The center of the image recorded contains an extraordinary gamma-ray burst (GRB) called GRB 110328A, observed with NASA's Chandra X-ray Observatory. This Chandra observation confirms the association of GRB 110328A with the core of a distant galaxy and shows that it was an exceptionally long lived and luminous event compared to other GRBs.

The position of a faint galaxy - located about 3.8 billion light years from Earth - observed with NASA's Hubble Space Telescope and the Gemini-North telescope on the ground. Allowing for experimental errors, the position of the galaxy is indistinguishable from that of the X-ray source, showing that the source is located close to the middle of the galaxy. This is consistent with the idea, suggested by some astronomers, that a star was torn apart by a supermassive black hole at the center of the galaxy. This idea differs from the usual interpretation for a GRB, involving the production of a jet when a black hole or neutron star forms after the collapse of a massive star (30M$\odot$ or more)   or a merger between two neutron stars.

http://chandra.harvard.edu/resources/illustrations/blackholes2.html

Figure F.1. Sun-size star, after being born at aG1 the first geo-synchronous orbit, is launched on a collapsing spiral orbit around the nucleus of the Super Massive Black Hole. (Illustration: NASA/CXC/M.Weiss)

The first illustration in this sequence shows a doomed star (orange circle) that is launched on a death spiral around SMBH. The black hole's enormous gravity stretches the star until it is torn apart. Some of the disrupted star's mass (indicated by the white stream) is swallowed by the black hole, while the rest is flung away into the surrounding galaxy.
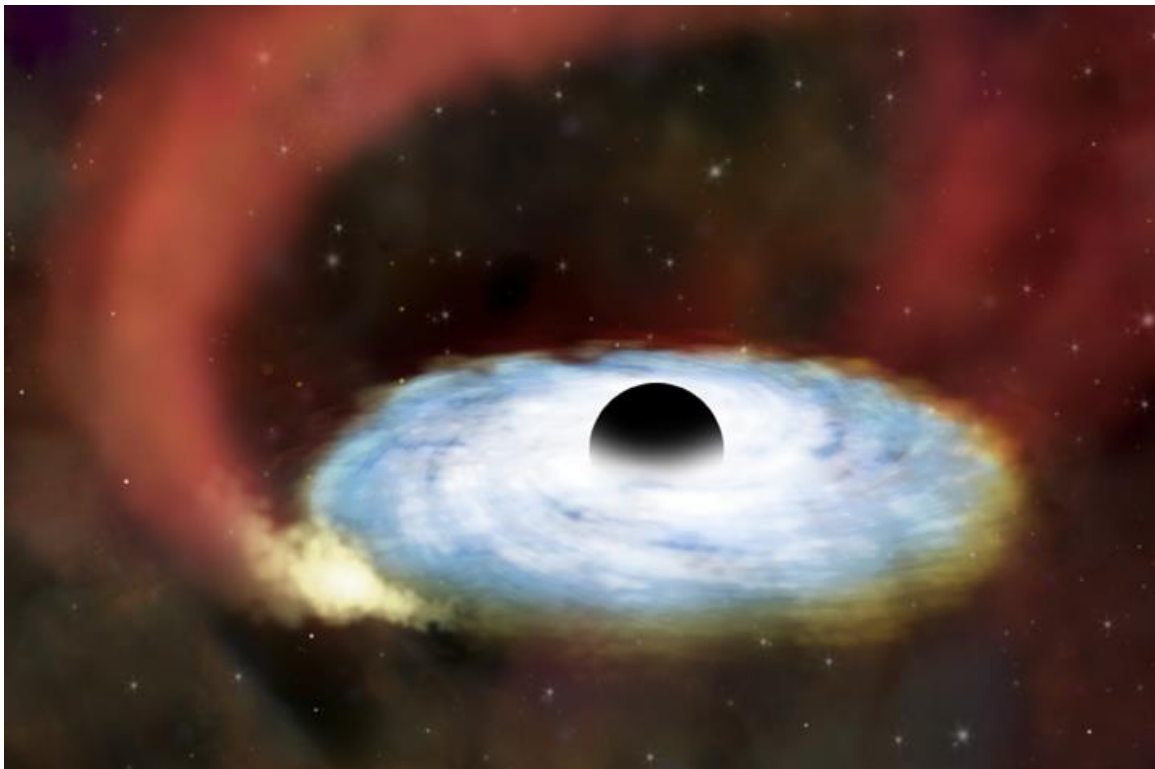
Figure F.2.Fraction of the star's mass which is gobbled up by the SMBH is spread into a disk around the SMBH. (Illustration: NASA/CXC/M.Weiss)

The second illustration shows how the gas that was pulled towards the black hole forms a disk and is heated before being swallowed by the black hole.

Figure F.3. The much fainter disk after about ten years have passed when most of the gases has been swallowed up. (Illustration: NASA/CXC/M.Weiss)

The third illustration shows a much fainter disk, after about ten years have elapsed, when most of the gas has been swallowed by the black hole.
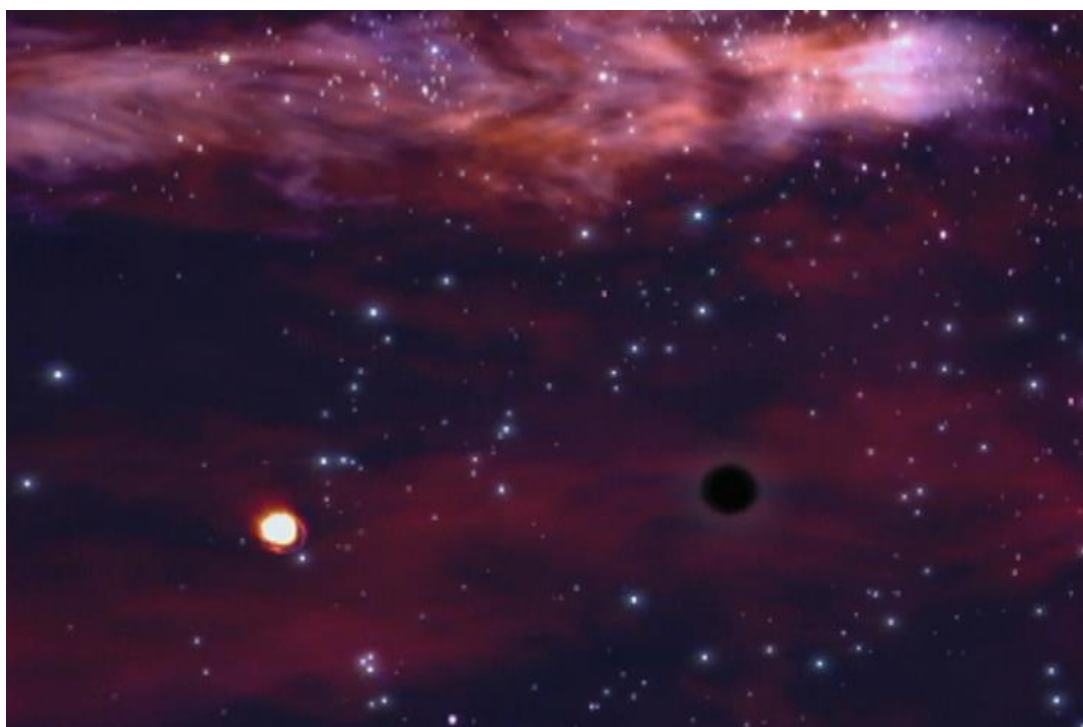

Figure F.4. A normal star in the given Galaxy after being born at aG1 is launched on a death spiral around the black hole. (Illustration: NASA/CXC/M.Weiss)

Figure F.5. The doomed star spirals inward on a collapsing spiral orbit around the SMBH. (Illustration: NASA/CXC/M.Weiss)
As the doomed star nears the SMBH, the star is stretched by tidal forces exerted by the black hole and is quickly torn apart.

Figure F.6.Most of the yellow gaseous debris of the shredded star escapes on parabolic orbits as can be seen in the spread of the yellow debris spiraling in anticlockwise direction. (Illustration: NASA/CXC/M.Weiss)

Most of the yellow gaseous debris from the star escapes the black hole in parabolic orbits.

Figure F.7. A small fraction of the shredded star swirls into the vortex created by the rapidly spinning SMBH. As the remnents of the shredded star is sucked in a swirling motion it gets heated up and emits X-Ray. (Illustration: NASA/CXC/M.Weiss)

However, a small amount of material is captured by the black hole and then forms a rotating disk of gas. X-rays are emitted as the gas in the disk is heated (as shown by the blue color) and is gradually swallowed by the black hole, eventually emptying the disk.
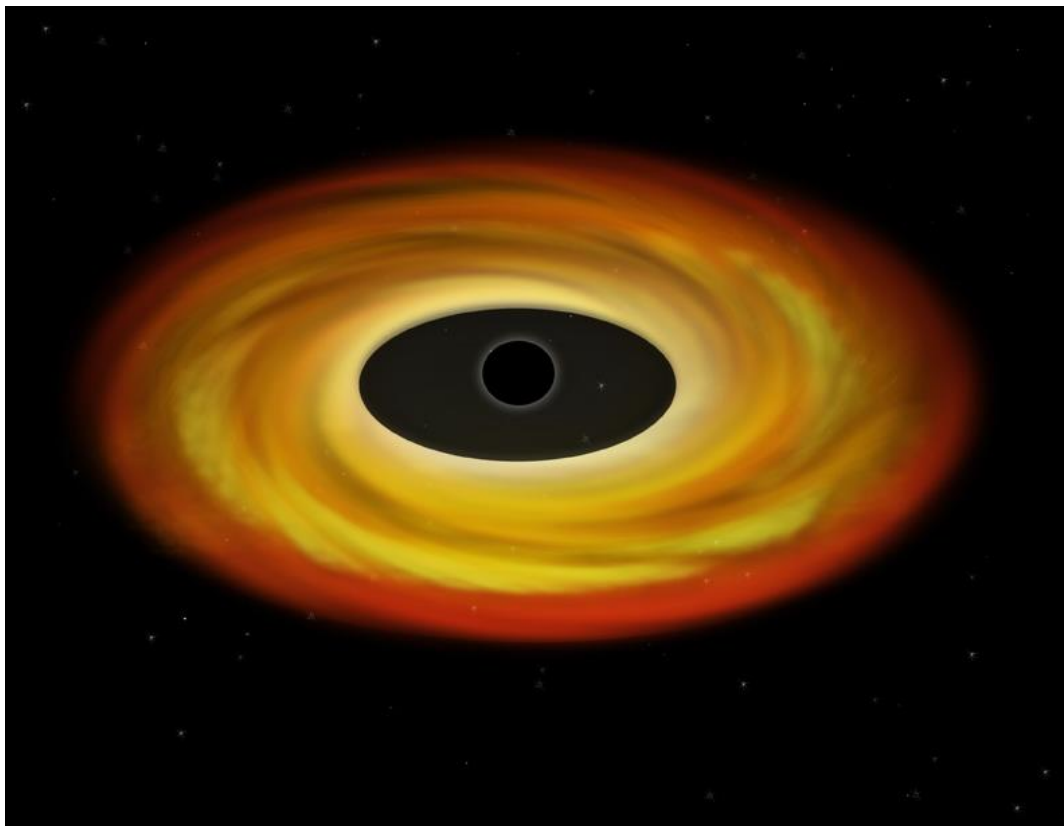
Figure F.8. A non-spinning SMBH a consequence of zero inward spiral. (Illustration: NASA/CXC/M.Weiss)

When there is little or no inward spiraling debris, SMBH has little or no spin.
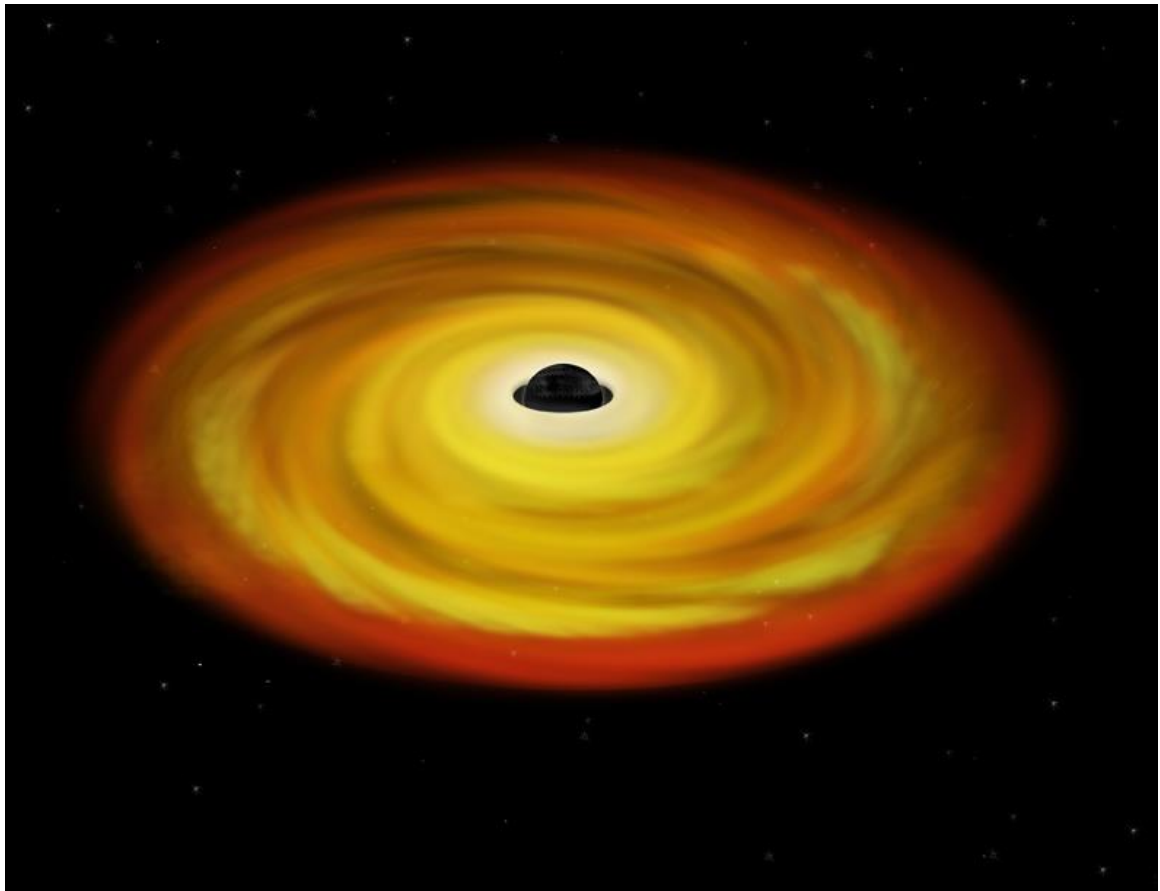
Figure F.9. A rapidlyspinning SMBH because of enormous inward spiraling debris. (Illustration: NASA/CXC/M.Weiss)

As shown in Figure 7 and Figure 8, the gravity of a black hole shifts X-rays from iron atoms to lower energies, producing a strongly skewed X-ray signal. Figure 7 has black hole that is depicted as not spinning , and a second black hole in Figure 8 is depicted as spinning rapidly . One consequence of Einstein's theory of relativity is that spinning black holes drag space with them as they spin, making it possible for particles to orbit nearer to the black hole. A possible explanation for the differences in spin among stellar black holes is that they are born spinning at different rates. Another is that the gas flowing into the black hole spins it up.
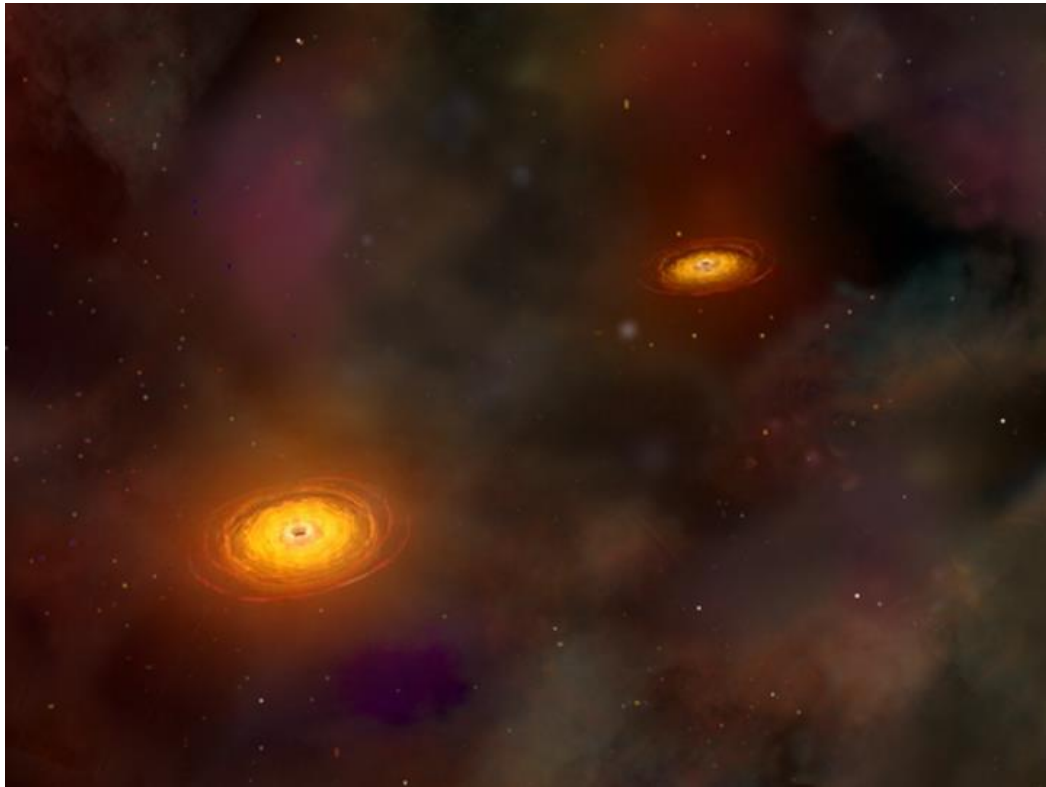
Figure F.10. First stage in the merger of two Spiral Galaxies. (Illustration: NASA/CXC/M.Weiss)

The first stage in the merger of two spiral galaxies. In a cluster, galaxies are hierarchichally arranged just as in a galaxy stars are hierarchically arranged. The heaviest galaxy with the largest SMBH form the nucleus or the primary body and the lighter galaxy forms the secondary body. The secondary Galaxy if it falls short of the inner geo-synchronous orbit is bound to be launched on a collapsing spiral orbit and thereby get trapped in death spiral. These two Galaxies are destined for merger.
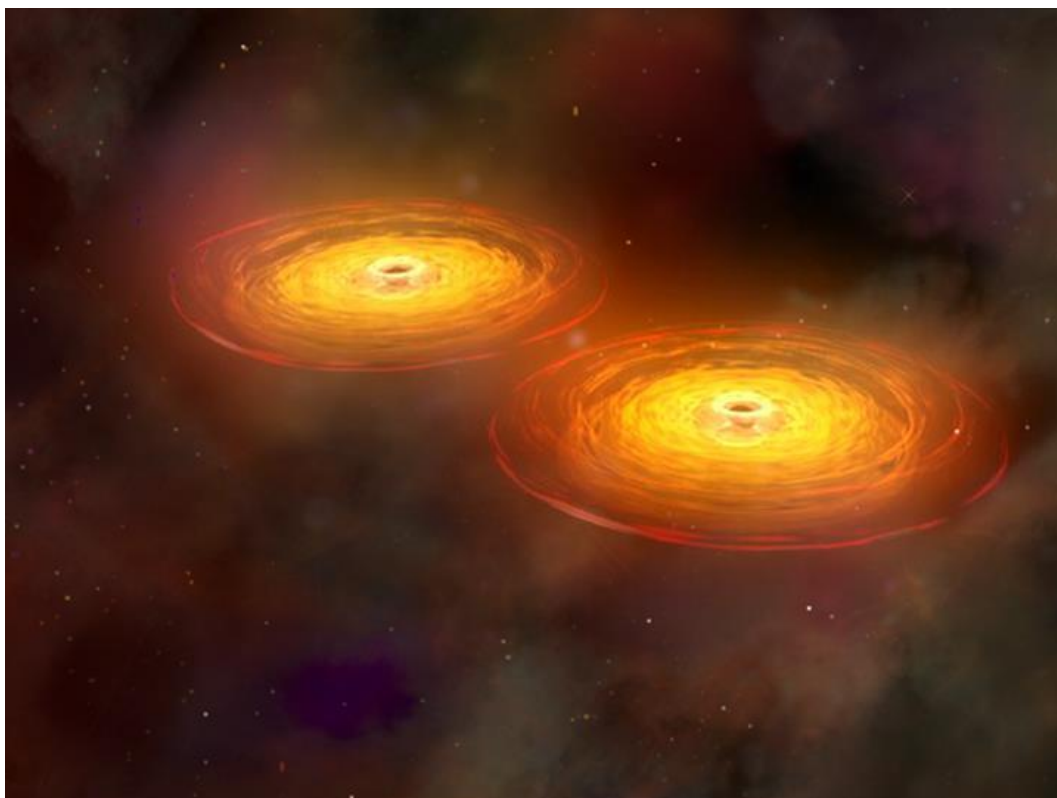

Figure F.11.Second stage in the merger of the primary and secondary Galaxies. The two galaxies are spiraling around the barycenter and moving closer together. (Illustration: NASA/CXC/M.Weiss)
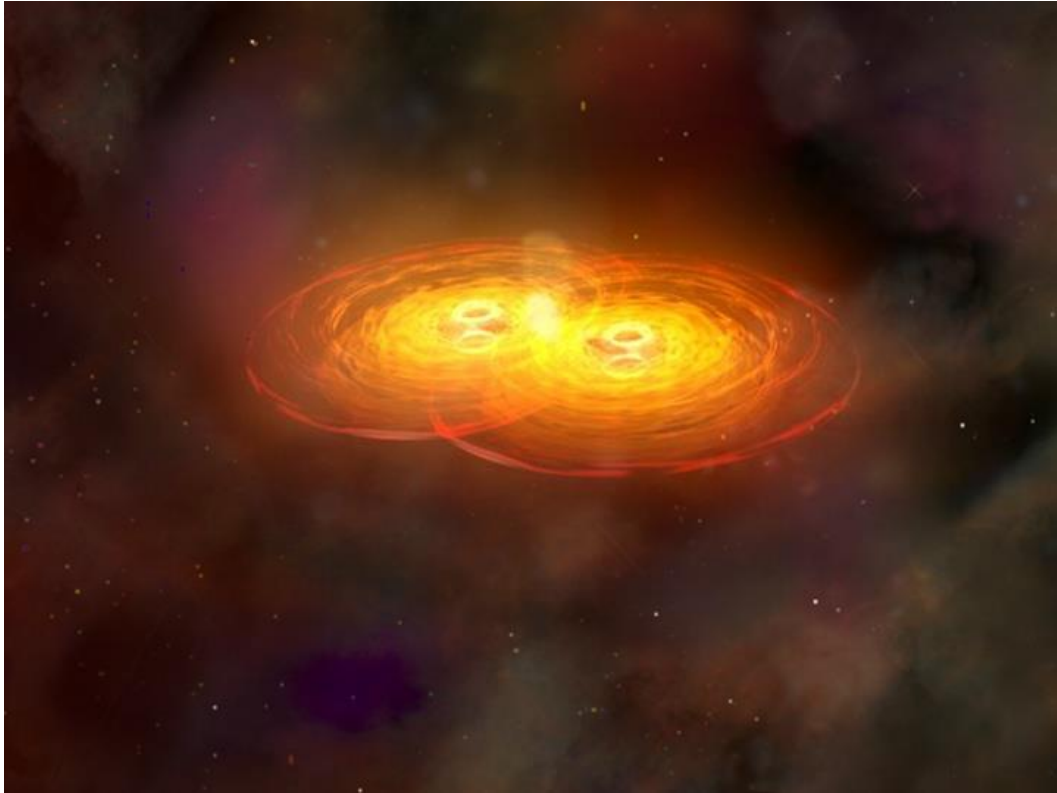
Figure F.12. In the advanced stage of merger when the two Galaxies are overlapping and interpenetrating. The two SMBHs are indistinguishable surrounded by a single merged Galaxy. (Illustration: NASA/CXC/M.Weiss)
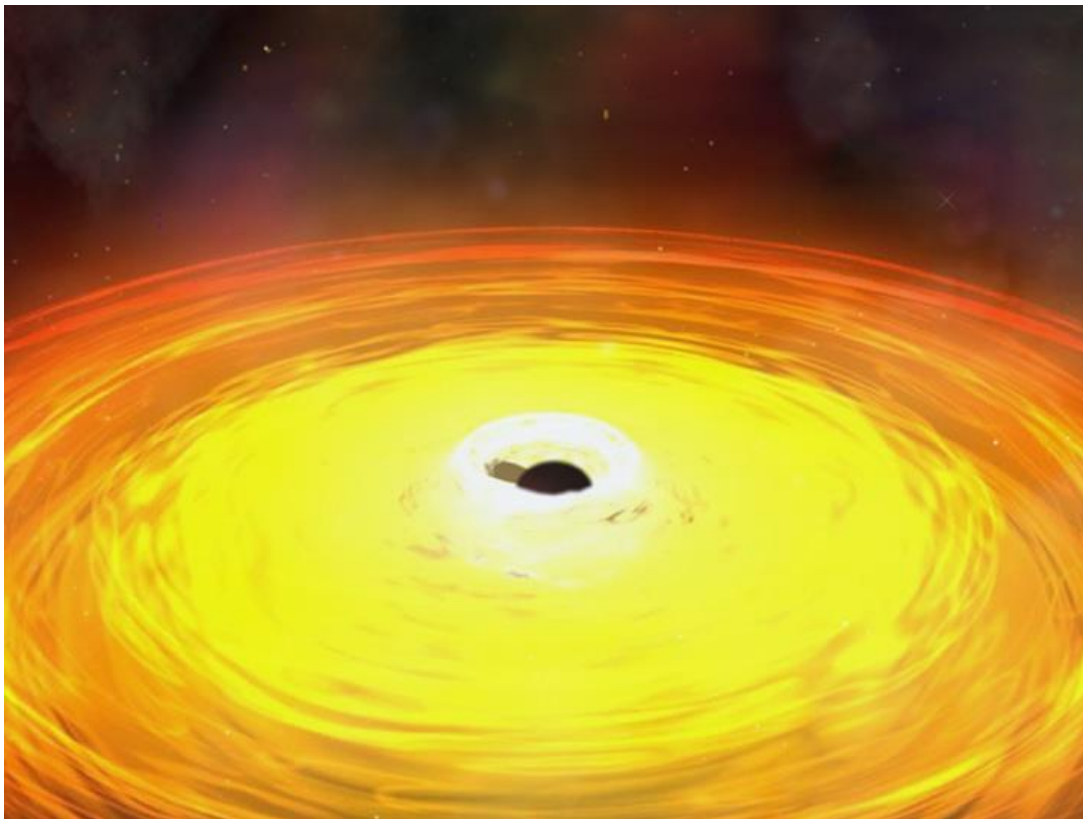

Figure Figure F.13. The two SMBHs spiral around the common barycenter until they coalesce into a single SMBH. (Illustration: NASA/CXC/M.Weiss)

This series of Figures depict 4 stages in a merger of two galaxies (artistic representation) that forms a single galaxy in Figure F.13 with two centrally located supermassive black holes surrounded by disks of hot gas. The two black holes orbit each other for hundreds of millions of years in Figure F.12 before they merge to form a single supermassive black hole in Figure F.13 that sends out intense gravitational waves.
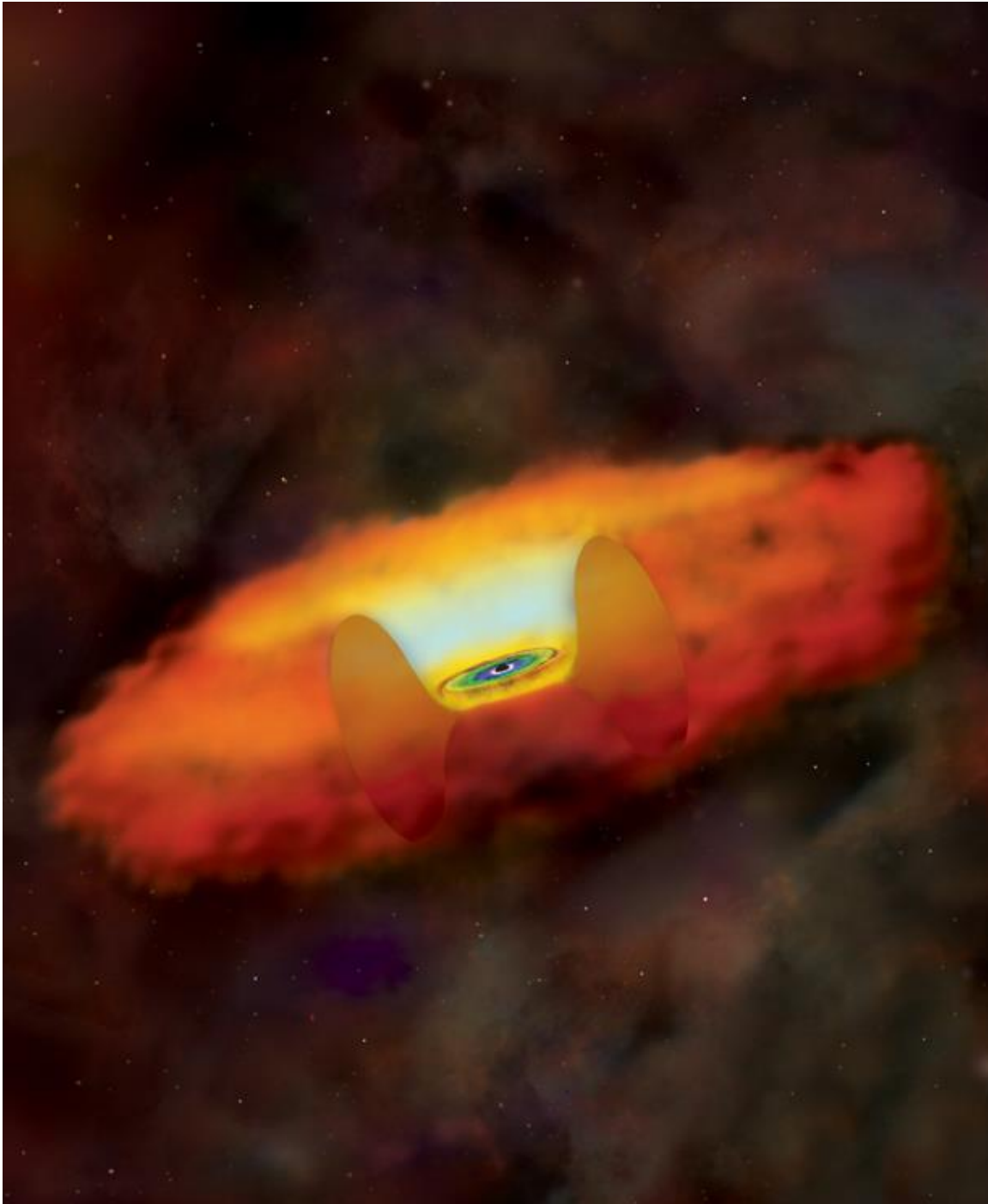

Figure F.14. An active galactic nucleus(AGN) (Illustration: NASA/CXC/M.Weiss)

An artist's conception shows a black hole surrounded by a disk of hot gas, and a large doughnut or torus of cooler gas and dust. The light blue ring on the back of the torus is due to the fluorescence of iron atoms excited by X-rays from the hot gas disk.
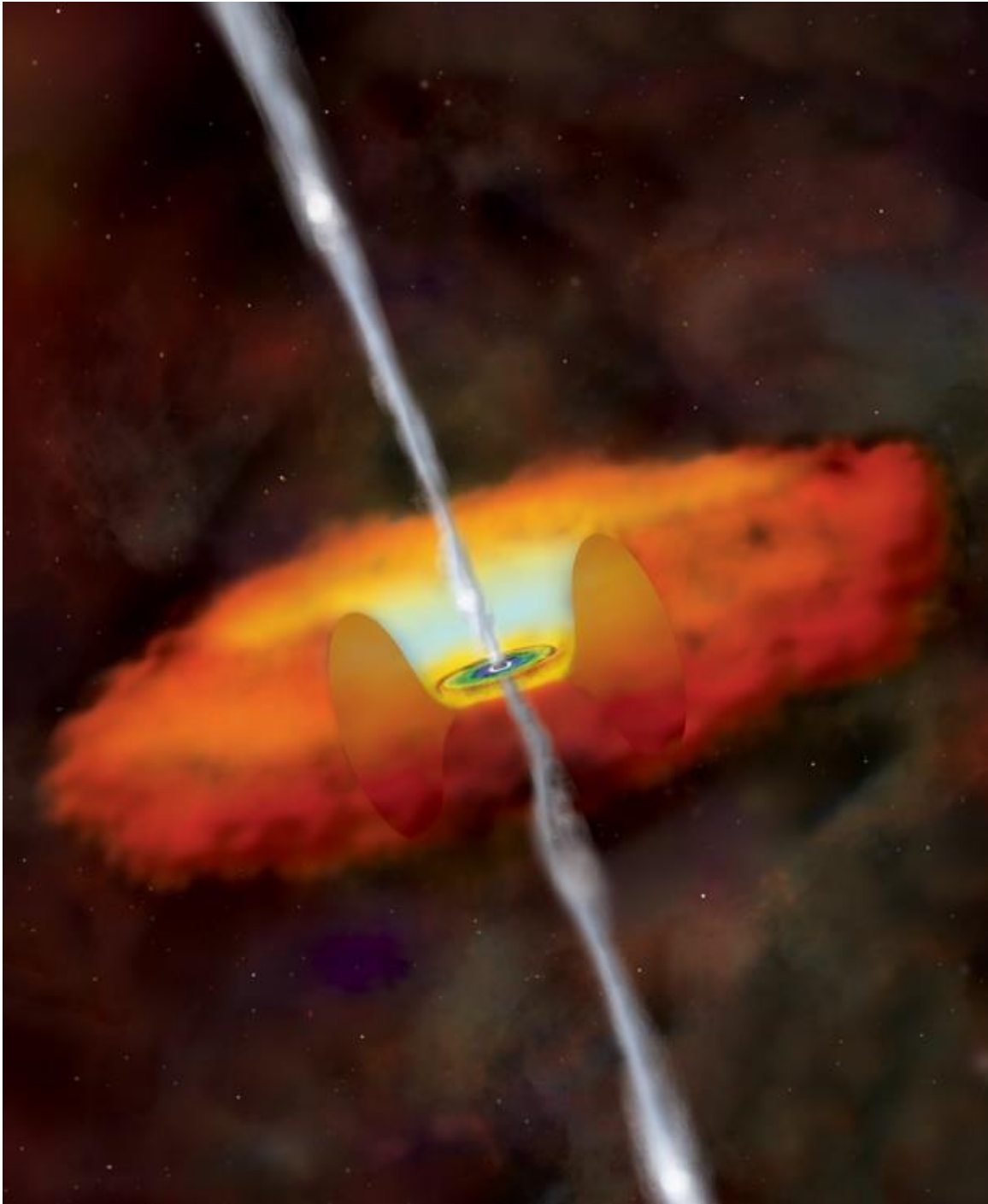
Figure F.15. An emission of conical beam of energetic charged particles and X-Rays from the north and south pole of AGN due to swirling mass of gas and dust into the rapidly spinning SMBH. (Illustration: NASA/CXC/M.Weiss)

An artist's conception shows a black hole surrounded by a disk of hot gas, and a large doughnut or torus of cooler gas and dust. The light blue ring on the back of the torus is due to the fluorescence of iron atoms excited by X-rays from the hot gas disk. Jets of high energy particles (white) are propelled away from the vicinity of the black hole by intense electric and magnetic fields.
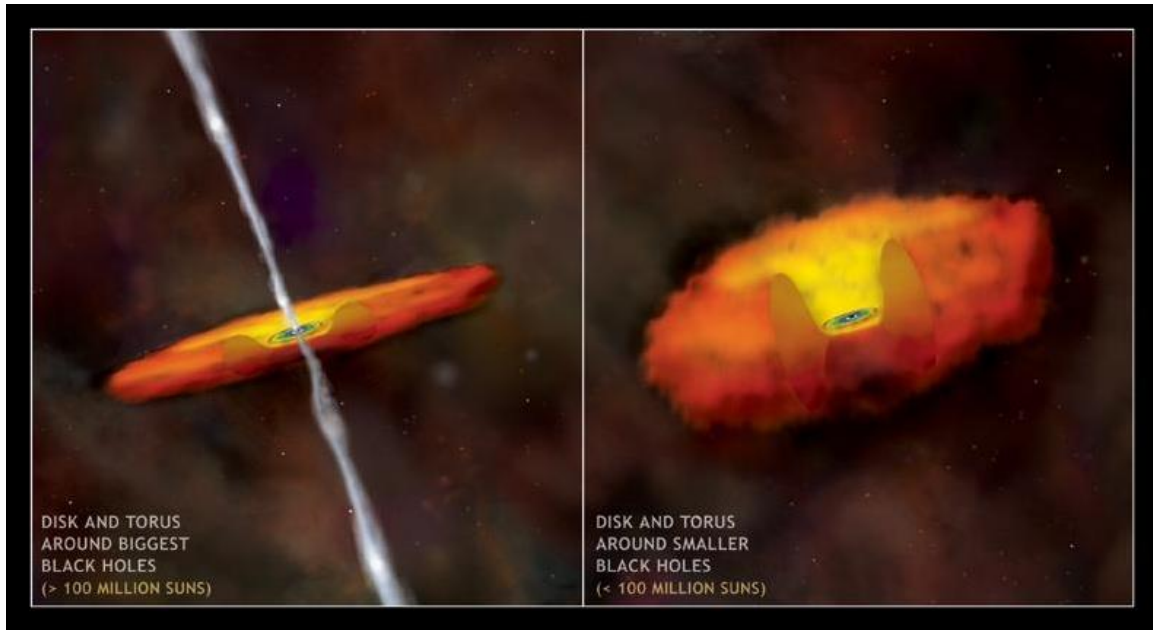
Figure F.16. Left SMBH is greater than 100 Million Suns. It has thinner torous and a powerful beam of energetic particles emanated from the two poles of the SMBH. Right SMBH is between 10 Million Suns and 100Million Suns. It has a much thicker donought of gas and dust and no conical emission from the two poles. (Illustration: NASA/CXC/M.Weiss)

Figure F.16 shows two kinds of AGNs. These two show the difference between the very biggest supermassive black holes in the Universe and relatively smaller ones. In each case, the black hole is swallowing large amounts of gas from a surrounding disk. The first illustration is of a black hole with a mass between about 10 million and 100 million Suns. Here, the central black hole is obscured by a thick donut-shaped cloud of dust and gas. The second shows the growth of a larger black hole, with a mass greater than 100 million Suns. This black hole is surrounded by much a thinner torus of dust and gas and has a powerful beam of conical beam emanated from the two poles of SMBH.

Figure F.17. Black-hole size versus Cosmic time in very early Universe. (Illustration: NASA/CXC/M.Weiss)

In early universe Super Massive Black Holes and Super Massive Galaxies grew synergic ally. Subsequently Massive Black Holes and Massive Galaxies were formed. Figure F.17 shows the typical growth, over cosmic time, of supermassive black holes with masses greater than 100 million Suns (these objects include the largest black holes in the Universe). These large black holes grow quickly in the early Universe but their growth then stops ("hits the wall"), perhaps because powerful winds or jets generated by the feeding frenzy of the black holes clears out any remaining fuel. The rapid, early growth of these large black holes, as observed with Chandra, is similar to the growth of their large host galaxies, as observed with optical telescopes.
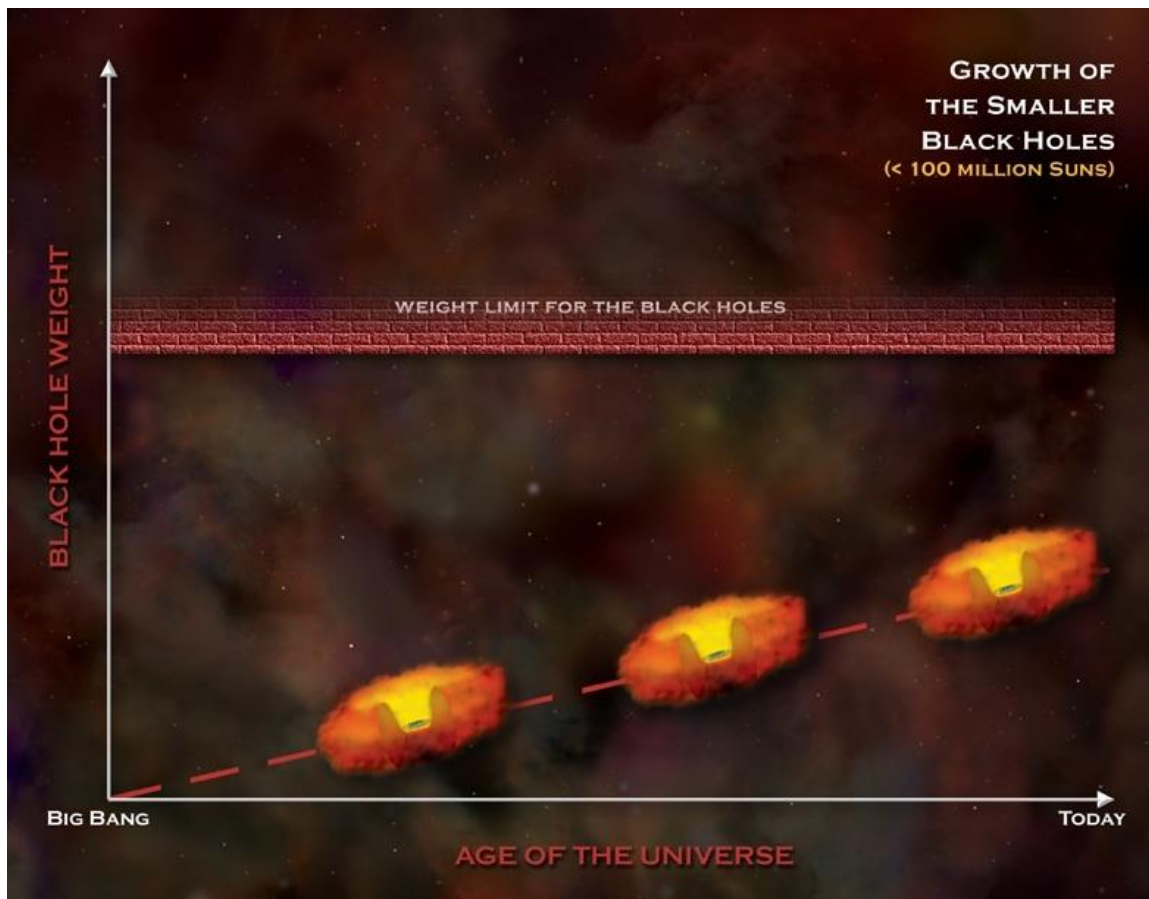

Figure F.18.Black hole size versus Cosmic time in later times. (Illustration: NASA/CXC/M.Weiss)

Figure F.18 shows the typical growth of super massive black holes with masses less than about 100 million Suns. These black holes grow much more slowly than the biggest black holes. Typically they will not reach their weight limit for another several billion years. This slow growth is similar to the growth of the black holes' host galaxies.
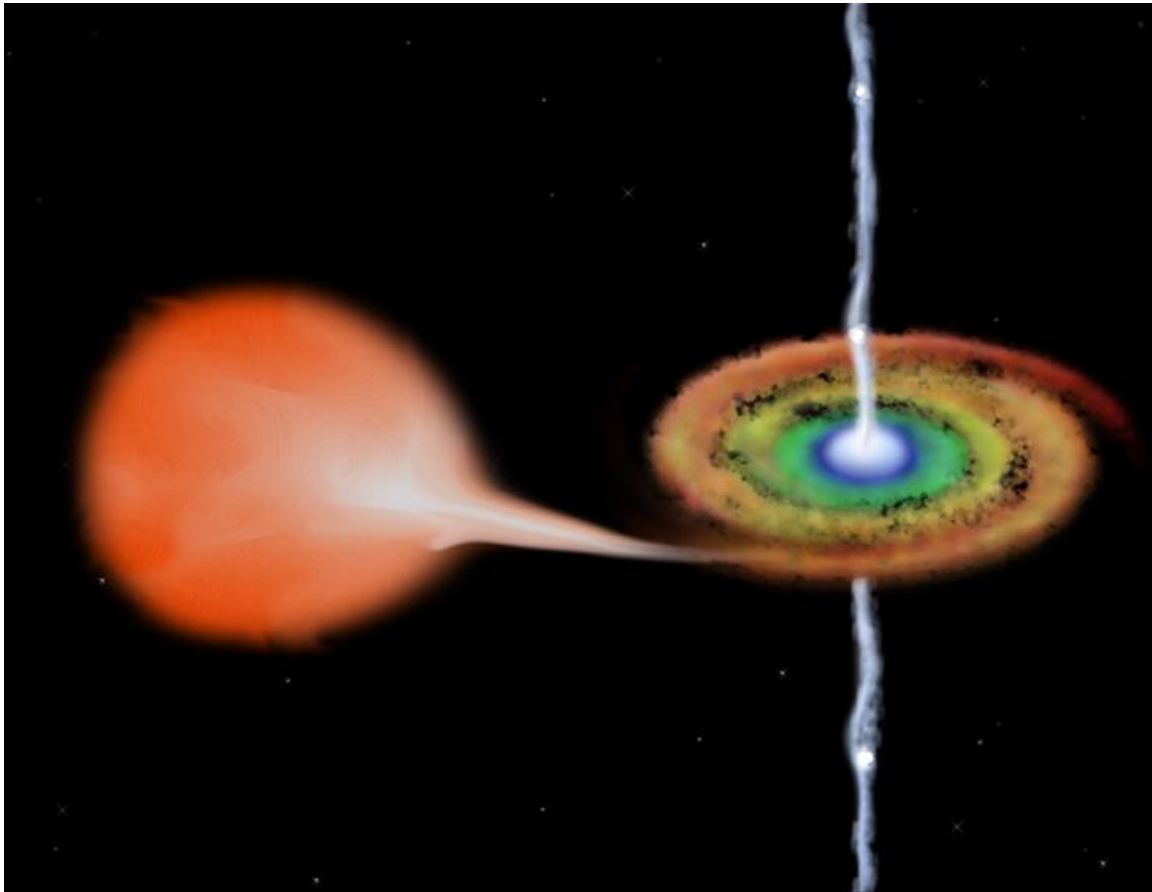
Figure F.19.A double star system of Sun-like star and BH. (Illustration: NASA/CXC/M.Weiss)

In a double-star system of normal star and BH, normal star is a secondary body and BH is primary body. If the secondary is launched on an expanding spiral orbit it rapidly evolves to a stable orbit at aG2. But if it is launched on a contracting spiral the star gets trapped on a death spiral doomed to be shredded and devoured by the SMBH and in the process emnate a powerful cone of energetic particles, X-rays and γ-rays. This is tidally disrupted event accompanied by big , intense and long duration gamma and X-ray burst. A double star system where a normal Sun-like star is in orbit around a black hole. As gaseous matter is pulled from the normal star it spirals toward the black hole, forming a disk, and is heated to temperatures of millions of degrees. Intense electromagnetic forces in the disk can expel jets of high-energy matter.

GRB110328A was of the category shown in Figure F.19. Joshua Bloom sent a email GCN 11847 on GRB Coordinates Network (GCN). He suggested that it was not a typical GRB associated with the collapse of a massive star into a neutron star or into a black hole neither it was a GRB associated with the merger of two neutron stars.. It was an event associated with a tidally disrupted event (TDE) of a sun-sized star by a million sun mass SMBH. GRB was coincident with the nucleus of the Galaxy. This was rechristened as SW1644+57. The Chandra data pinpoints GRB110328A in the core of this galaxy and shows that the associated X-ray source is very bright and long-lived.

A normal GRB can occur anywhere in the galaxy where star formation is active.

Most MBH or SMBH are quiescent or dormant without the swirling mass of gas and dust surrounding it.

MBH can have a disc of gas and dust swirling into the rapidly spinning vortex created by MBH. This swirling mass gets heated up and emits high energy particles, X-Rays and some emit γ-Rays also. These are known as Active Galactic Nuclei (AGN) as shown in Figure F.14 and Figure F.15. These are active because they are continuously fed by gaseous and dust matter. These AGN are also called QUASERS. In about 10% of galaxies we have AGN.

AGN are easy to detect because of their X-Ray emission and some have weak γ-Ray emission also. But SW1644+57 is a class apart. It is 100× brighter than AGN.

Before 28March 2011, Sw1644+57 was quiescent as confirmed from the data of Fermi Satellites Large Area Telescope (LAT). Only when a star spiraled into 'the disruptive radius' sphere of an otherwise quiescent SMBH that long duration GRB was triggered from the relatively slow tidal disruption of the doomed star. 10% of the debris from the shredded star was converted into X-Ray and γ-Ray (typical accretion efficiency of the BH =$\in_{BH}$= 10%).

During TDE UV, X-ray, Visible light have been seen but γ-Ray had never been seen.

Sw1644+57 has unique brightness and variability of X-Rays after-glow. It flared 5 times since April 3,2011. The burst of X-Ray and γ-Ray is stronger than 1000 to 10000 times. This flare up will not happen again because star had been fully swallowed.

Table F.1. Comparison of TDE occurring in SMBH and MBH.

Mass of BH			
$>10^8 M_\circ$	Disruption Radius<Event horizon	TDE will be hidden	No relativistic cone
$<10^8 M_\circ$	Disruption Radius>Event horizon	TDE will be seen	Relativistic cone is detectable
$\sim 10^8 M_\circ$	Disruption Radius>Event horizon	TDE will be seen	Relativistic cone is detectable

Sw1644+57 shows that there is a new class of TDE. Though it was detected because of Gamma burst its behaviuor at X-Ray and IR was unique. It stayed at a high flux level for days to weeks. This puts it in a class apart from known high energy transients.

Remarkably, this "tidal disruption" event may have been caught in real time, rather than detected later from analyzing archival observations. However, this X-ray source is about a hundred times brighter than previously observed tidal disruptions. One possible explanation for this very bright radiation is that debris from the disrupted star fell towards the black hole in a disk and the swirling, magnetized matter generated intense electromagnetic fields that created a powerful jet of particles. If this jet is pointed toward Earth it would boost the observed brightness of the source. This scenario has already been suggested by observers to explain the bright and variable X-ray emission observed by NASA's Swift telescope.

This observation was part of a so-called target of opportunity, or TOO, led by Andrew Levan from the University of Warwick in the UK. A TOO allows the telescope to react quickly to unpredictable cosmic events, within 24 hours in some situations. Chandra scientists and engineers can decide to alter the scheduled observations and instead point the telescope to another target if the circumstances warrant it. This process was put into place once the discovery of GRB 110328A with Swift was announced on March 28th, 2011. The Chandra team was able to reset the telescope's schedule to observe GRB 110328A early in the morning of Monday, April 4th for a period of just over four hours.

1. Results of Levan Group.

An extremely luminous panchromatic outburst, a high-energy transient, was seen on the night of 28 March 20111. This will be referred to as Sw1644+57. There are several candidates which can produce sufficiently bright bursts of high radiation such as :

i. Electrical discharges associated with thunderstorms on Earth;

ii. Some fraction originate from the Milky Way :(a) from isolated neutron stars with intense magnetic field or (b) from binary systems containing neutron stars and black holes;

iii. Some long lived but variable X-Ray and γ-ray emissions originate in active galaxies;

iv. Brightest are the long duration γ-ray bursts (long-GRB) which are detected by SWIFT-mission at a rate of approximately two a week and thought to originate from the collapse of massive stars in the distant Universe.

Even among the long-GRB observed till now, the present candidate Sw1644+57 manifests some unusual properties as shown in Table F.2.

Table F.2. The comparative study of Long-GRB and Sw1644+57.

	Long-GRB	Sw1644+57
	Destrucrtive event and non-repetitive	
Prompt γ Emission duration.	1~10sec	
Subsequent trigger	zero	4 triggers over a period of 48 hours
Late time X-Ray flare	Yes	Quite unlike the afterglow of long-GRB (0.3 to 10keV)
Peak X-Ray flare		3×10^{48}ergs/s Persisted for 1000s.

Light curve of X-Rays emission in 0.3 to 10 keV	Plateau phase of 9 hours	Plateau Phase maintained till 5 weeks
IR light curve	Very faint in afterglow	Plateau Phase for 5 weeks
Luminosity in after-glow for X-Ray and IR	X-Ray luminosity is much less and IR is faint	Persisted at $L_x \sim 10^{47}$erg/s and persisted for 2 weeks. 10-100 times more luminous in X-Ray & IR.*
Total energy emitted in first 10^6sec	Much less than 10^{53}ergs	10^{53}ergs= 10% of the rest energy of SUN
Afterglow Astrometric position	Highly correlated with host galaxy light(particularly with the blue light generated by massive stars)	Coincident with the nucleus of the galaxy

Sw1644+57 is well beyond the bright end of the quaser luminosity function and 100 times more luminous than the brightest Blazer. The overall energetic, long duration, together with order-of-magnitude variation in flux over 100s time scale indicate that we are dealing with a very different class of high energy transient.

These differences show that Sw1644+57 is not a classical long-GRB. Then where does it fit ?

Below in Table F.3, we describe different classes of AGNs.

Table. F.3. Classification of AGNs

Class of AGN	Properties
LINERS & Seyferts	Moderate X-Ray and optical luminosity
Luminous QUASERS & blazers	Brighter AGN
Blazers	X-Ray Luminosity approaches 10^{46}ergs/s and Optical absolute magnitude is -30 or brighter. Light curve has a variability of a factor of 2 hence this is considered as most variable AGN.
Sw1644+57	Peak X-Ray luminosity is in excess of 10^{48}ergs/s. In just a few hundred seconds it has a light curve variability of 100. Extremely X-Ray luminous but optical & IR is much fainter. Spectrally unusal. X-Ray Luminositty/Optical Luminosity$\sim 10^{4 \sim 8}$;

The host galaxy is compact and non-interacting with (half-light radius in the optical range) r_h = 1.04kpc and absolute magnitude of MV = -18.9. This is comparable to Large Magallenic Cloud (LMC) Galaxy. The study of emission lines show that it is normal star forming Galaxy which had a dormant SMBH at the nucleus. The inferred rate of formation of stars is 0.5M$_\circ$ per year.

Peak Luminosity corresponds to Eddington Luminosity of the accretion by 1010M○ mass Black Hole. But Stellar Mass-Black Hole Mass relation indicates that central Black Hole is 107M○. Hence Sw1644+57 is either accreting at a super-Eddington rate or has its total energy modified by a relativistic beaming or both.

2. Results of Bloom Group.
If a star happens to enter the sphere of influence of a centrally located BH in a given galaxy then the star will be tidally shredded and almost half of the shredded star will be accreted by the BH at a typical accretion efficiency of 10% and remaining half will be deflected away tangentially. The disruption radius of the BH is given by Equation F.1.

$$r_d(disruption\ radius) = R_O \times \left(\frac{M_{BH}}{M_O}\right)^{1/3} \qquad F.1$$

Where R$_O$= radius of a Sun-like star = 6.955×10^{8}m;

M$_O$ = mass of a Sun-like star =1.9891×10^{30}Kg;

M$_{BM}$= mass of the central black-hole = 10^M ×M$_O$;

A centrally located BH has an event horizon. The radius of this event horizon is given by Schwarzschild Radius. The escape velocity ($v_{esc} = \sqrt{(2GM)/R}$) from the sphere surrounded by this event horizon is the speed of light 'c' hence even light cannot escape from within this event horizon, Schwarzschild Radius is given by the expression in Equation F.2.

$$r_s(\boldsymbol{Schwarzchild\ radius}) = \frac{2GM_{BH}}{c^2} \qquad\qquad F.2$$

Where G = 6.673×10⁻¹¹m³Kg⁻¹sec⁻² ;

c = velocity of light;

M_{BH}= mass of the central black-hole = 10^M ×M_O ;

In Table F.4, the comparative values of the disruption radius and event horizon radius are given for the various values of the central BH.

Table F.4.Comparative values of Disruption Radius and Schwarzschild Radius for different masses of centrally located BHs.

Mass of BH($\times M_O$)	Disruption Radius(m)	Schwarzschild Radius(m)
10^5	3.2×10^{10}	2.95×10^8
10^6	6.92×10^{10}	2.95×10^9
10^7	1.49×10^{11}	2.95×10^{10}
10^8	3.2×10^{11}	2.95×10^{11}
10^9	6.9×10^{11}	2.95×10^{12}
10^{10}	1.49×10^{12}	2.95×10^{13}
10^{11}	3.2×10^{12}	2.95×10^{14}
10^{12}	6.9×10^{12}	2.95×10^{15}

As can be seen from the Table F.4 for BHs lighter or equal to $10^7\times M_O$, the Event Horizon Radius is much less than the Disruption Radius hence Tidally Disrupted Flare can be recorded and Tidally Disrupted Event is observable. If there was a heavier BH, then possibly the event could not have triggered the Burst Alarm Telescope and the event would have gone unnoticed and unrecorded. Fortunately this was not the case for GRB110328A.

X-Ray after-glow persisted for more than 2 weeks and its peak luminosity was 3×10^{47}ergs/sec. These two features put this event in a class of scaled down version of Blazers which was impulsively fed by a stellar mass of ~1M_O . This event seemed coincident with the nucleus of the host galaxy. This coincidence was confirmed by the following three facts:
i. Astrometric coincidence of the associated X-Ray, Optical, IR and Radio transient with the light centroid of the putative host galaxy is strongly indicative of a positional connection to MBH;
ii. Observed X-Ray variability time scale are consistent with those of an accreting MBH;
iii. Observed X-Ray flux and spectral hardness is similar to that observed in Blazers.

By applying Bulge Mass-BH mass and Bulge Luminosity-BH Mass correlations we arrive at MBH $\leq 10^7$M_O. This is securely under the limit (few$\times10^8$MO) required for tidal disruption of a solar mass to occur outside the event horizon so that the TDE can be recorded and analyzed from outside.
Beaming factor taken into account, the X-Ray luminosity LX = 10^{47}ergs/sec is consistent with Eddington Luminosity (where inward gravitational force is balanced by outward radiation pressure) of 10⁷MO MBH.
Archival searches spanning two decades have yielded no evidence for prior AGN activities from Radio to γ-Ray waveband. This confirms that BH turned-on specifically on 28/03/2011 due to near-Eddington accretion rates at the time of Burst Alert given by BAT of Swift Satellite. This turning-on launched a relativistic outflow of energetic particles and photon.
This sudden increase in accretion cannot result from gas entering the sphere of influence (soi) because the time scale of

$$\sim\frac{R_{soi}}{\sigma} \geq 10^4 years$$

is required to appreciably alter the accretion rate near the horizon.
In the above equation , Rsoi is the radius of the sphere of influence given by the following expression:

$$R_{soi} = \frac{GM_{BH}}{\sigma^2} = 1.3\times10^{17}\ m \sim 1pc$$

Where σ = 100km/sec (typical bulge velocity dispersion); MBH=10^7M$_O$;

G = 6.673×10^{-11}m^{3}Kg^{-1}sec^{-2} ;

Hence this event can only be Tidally Disrupted Flare (TDF)..

The observed energy output is compatible with the mass accreted over a time period of 50days. This can be verified by the following analysis:

The observed X-Ray fluence SX suggests an energy release of EX =1.6×10^{53}f$_b$ ergs over a period of 50 days.

Beam forming factor = f$_b$ = 5×10^{-3} hence the available energy Eav = 8×10^{50}ergs.

This energy is coming from the accretion of the tidally shredded star. We have seen that in such TDE only 50% of the matter is accreted. Hence only 0.5M$_O$ will be converted into energy through matter-energy conversion equation with 10% accretion efficiency($\in_{BH}$). Hence the energy got is:

$$\frac{1}{2}M_O c^2 \times \in_{BH} = 8.95 \times 10^{46}J \times 0.1 = 8.95 \times 10^{52} ergs \sim 10^{53} ergs$$

If we take into consideration that mass gets lost through circularization as well due to disk wind the matter to energy conversion easily accounts for the observed energy of 1051ergs.

This Eddington rate accretion accompanied with matter to energy conversion powers a two-sided jet of relativistic energetic particles and photons. This plows through the interstellar region surrounding BH at a Lorentz Factor Γj. At some later time jet reaches a distance Rj where the forward shock radiates the observed radio and IR light.
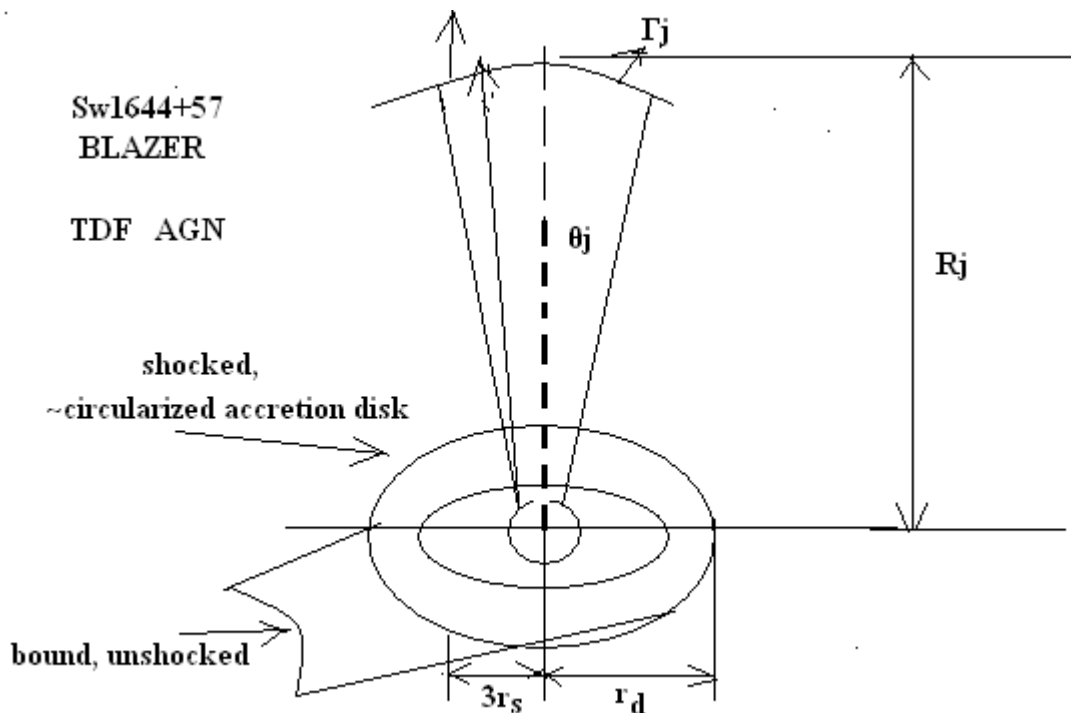

Figure F.20. Schematic representation of the geometry and emission region for Sw1644+57. A star is disrupted at a distance of r$_d$ from a MBH of mass M$_{BH}$ with Schwarschild Radius rs . Half of the mass of the star escapes on unbound orbits while the other half accretes. Shocked circularized fall back mass sets up a temporary accretion disk with inner radius of 3rs .(for a non-spinning BH). A two sided jet is powered starting at the time of accretion and plows through the interstellar region surrounding the BH at a Lorentz factor Γ$_j$. At some later time the jet has reached a distance R$_j$ where forward shock radiates the observed radio and IR light. Emission from the accretion disk is upscattered, giving rise to the observed X-Rays. Different viewing angles (whether the observer is inside θ$_j$ = 1/ Γ$_j$) determines the class of Blazer we observe.

Emission from the accretion disk is Compton Upscattered giving rise to the observed X-Rays. Differing viewing angles (whether the obsever is inside $\theta j \approx 1/\Gamma j$ or not) determine the sort of phenomena we observe.

The duration of X-Ray light curve and the requisite accretion rate also are broadly compatible with the several days fall back time. Overall SpectraL Energy Distribution(SED) displays two peaks: one for IR and the other for X-Ray/γ-Ray. This is reminiscent of Blazers. Low energy is modeled as Synchrotron Emission and high energy is modeled as Inverse Compton(IC) emission.

X-Ray emission shows bright/flaring and a dim/slower flaring(quiescent state). Under TDF hypothesis, the observed SED is explained as follows:

1. Synchrotron origin for Radio Emission;

2. As in Blazers, here IR is synchrotron emission and X-Ray Peaks are IC emission;(vF_v *luminosity of low energy peak*)/(vF_v *luminosity of high energy peak*)=1/10~1/100 . The extreme ratio and relatively low frequency of the synchrotron peak are compatible with Eddington-accreting Blazer emission;

3. Rapid variability of X-Ray emission strongly indicates of internal origin. The Radio-IR emission varies more smoothly and could result from the interaction of the Jet with surrounding interstellar medium. Since there was no previous AGN activity hence the jet must burrow its way through the gas in the central region of the Galaxy. The fast motion of the newly formed jet drives a shock into the external gas (forward shock) while simultaneously a reverse shock slows it down. Particles acceleration at these shocks may power afterglow emission simultaneously with jet formation and yet persisting beyond the fading of internal emission..

This model , shown in the Figure F.20, best accommodates the data and predicts the long term evolution of Radio and IR transient. If TDF hypothesis is correct, emission will fade over the year and will not repeat because all the accreting material would have exhausted by then

The emerging jet from the tidal disruption event appears to accelerate cosmic rays to the highest observed energy (10^{20}eV). The observed rate of jets associated with tidal disruption of stars is dR/dt ~10-11Mpc-3year-1. Energy released per event is $3 \times$EX ~ 5×10^{53}erg. Energy injection rate is dE_{TDF}/dt ~ 5×10^{42} ergs Mpc-3year-1. The injection rate of energy into the tidally powered cone should be 1044 ergs Mpc-3year-1 in order to accelerate the cosmic particles to energy above 1019eV.

There is much evidence that AGN jets are accelerated by Magneto Hydro Dynamics.

APPENDIX G.
Calculation of (Baryonic Matter/Dark Matter)

Launch of COBE(Cosmic Background Explorer) started the era of precision measurement of the Cosmic Microwave Background(CMB) Radiation.

What is CMB ?

According to Big Bang theory, our Universe started from a singularity. It rapidly inflated to a very large size in 10-30 seconds. Its event Horizon expanded faster than light speed. This lasted from 10-43 seconds to 10-35seconds. After 10-30seconds. Universe expanded sedately and monotonically.[Schilling (2001)]

Initially the four forces (Gravitational forces, Strong forces, Weak forces and Electro-magnetic forces) were of equal magnitude as a single Force as shown in Figure G.1.
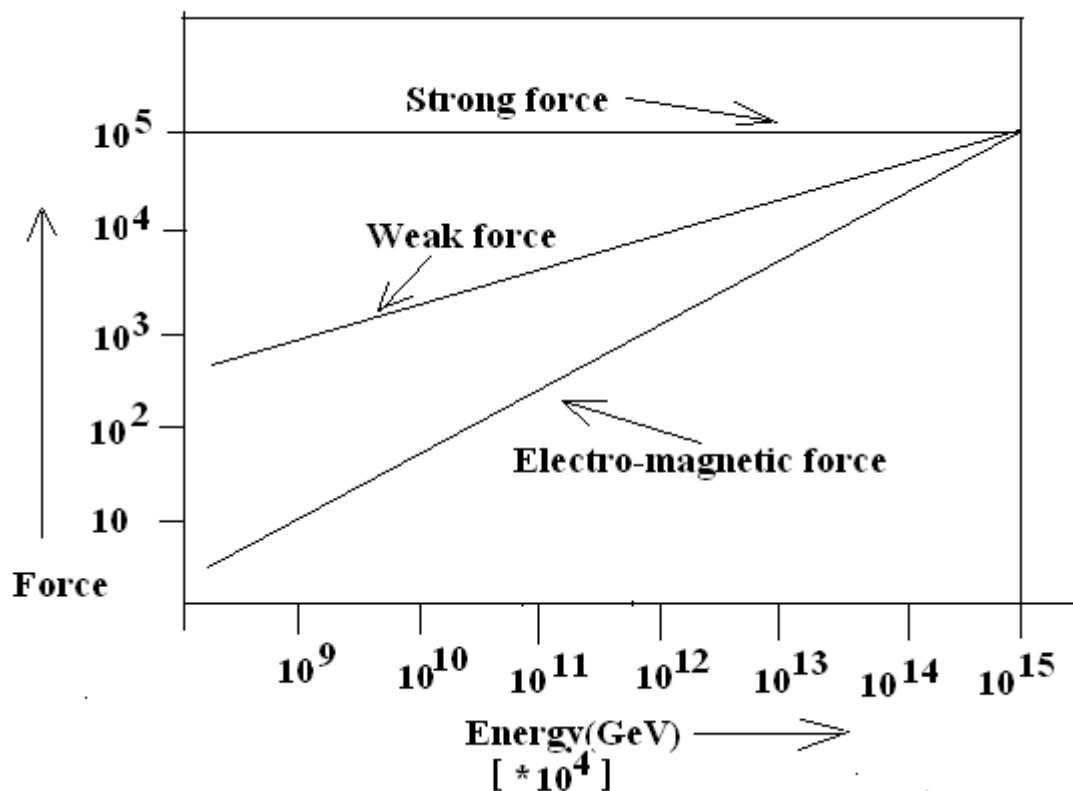
Figure G.1. Comparative plot of Strong, Weak and Electro-magnetic forces.

From 0 second to 10^{-43} second, temperature fell from infinity to 10^{19}GeV, radius of the Universe expanded from 0 to 10-33cm. Below 10^{19}GeV, super symmetry is broken and Universe makes a **phase transition from Quantum Gravitation to Grand Unified Phase.** *Gravitational force decoupled and relic Gravitons were left behind* which we should be able to measure but have not been able to measure till now.

From 10^{-43}sec to 10^{-35}sec, Universe experienced an inflationary expansion. The event horizon surrounding the singularity expanded at a speed greater than the speed of light.

By 10^{-30}sec, Universe expanded from a singularity of zero dimensions to a base ball size sphere. After this, Universe expanded sedately and monotonically. The inflationary phase was over.

At 10^{-10}sec, temperature fell to 100GeV. There is **phase transition from Grand Unified Phase to Electro-weak phase.** *Weak force decouples and relic Intermediate Vector Bosons W^+, W^- and Z^0 are left behind.* Below 100GeV, weak forces and electro-magnetic forces are separated. This phase transition is also known as Salam-Weinberg Transition in honour of Abdus Salam and Steven Weinberg who worked out the electro-weak theory.

At 10^{-6}sec, temperature fell to 1GeV. Below 1 GeV, there is **Quark-Nucleon Phase transition.** *Strong forces get decoupled, quarks are confined to baryons (which are triplets of quarks) and mesons (which are doublets) and relic quarks are left behind.* Baryons are the nuclear particles like protons and neutrons and mesons mediate the strong force within a nucleon. In this decoupling residual quarks are left behind as relic quarks which should be detected with its abundance as high as that of gold but till date no relic quark has been detected.

At 380,000 years after the Big-Bang the temperature of the hot soup known as plasma, the fourth state of matter, consisting of proton, neutrons and electrons falls to 4000K. Below 4000K, plasma gets neutralized into a neutral gaseous mixture of H2 and He. Radiation decouples leaving behind relic photons. Today after 13.7Gy, these Relic Photons have cooled to 2.7K Black Body Radiation. This 2.7K Black Body Radiation is known as Cosmic Microwave Background Radiation(CMB radiation).

For 380,000years after the Big Bang, matter was in a plasma state and , through Compton Scattering, matter and photon were kept in thermal equilibrium though they had different adiabatic indices. Because of Compton Scattering, photons had the same density distribution as the matter density distribution. When temperature fell below 4000K, matter and radiation got decoupled and matter changed from ionized state to neutral state. Since the two cooled independently, Temperature of matter fell inversely as the square of

the Radius of the Universe and temperature of radiation fell inversely as the Radius of the Universe. But the Black body Radiation carried the imprint of the matter density distribution at the time of parting at 380,000 years after the Big Bang.

Subsequently matter has evolved as a very differentiated and non-homogeneous system of super-clusters, clusters, galaxies and as exo-solar systems. If today we have such a non-uniformity of matter distribution then at 380,000years after the Big Bang we should have the seeds of this non-uniformity and this imprint should be present as ripples in CMB radiation.

In 1960's AT & T, Bell Lab used a radiometer in a telescope that would track the early communication satellites namely Echo-1 and Telster. This radiometer was being tested by Arno A. Penzias and Robert W. Wilson. In course of this testing they detected a background noise in microwave spectrum. It corresponded to 2.776K Cosmic Microwave Background Radiation(CMBR). They were led to this idea by the news that Robert H. Dick had suggested in 1940 that a radiometer would detect this CMBR.

The discovery firmly established the Big Bang Theory. In 1978 the Nobel Prize in Physics was awarded to Arno A Penzias (American), Robert Woodrow Wilson (American) and P.L. Kepiteza (Russian) for the discovery of Cosmic Microwave Background Radiation. In 1990, a satellite called COBE (Cosmic Background Explorer) measured the spectrum and temperature variations in the radiation pattern. The spectrum was exactly as expected for 2.7K Black Body radiator. The temperature variation was 1 in 100,000. Till then CMB radiation had appeared as perfectly isotropic and isotropic radiation pattern cannot explain the galaxies, clusters and super-clusters formation. Therefore the achievement of COBE marked the correctness of the Big Bang Theory.

To refine the CMB radiation pattern studies, in 2001 Wilkinson Microwave Anisotropy Probe was launched (WMAP). This is in a circular orbit around Sun with semi-major axis a= + $1.5×10^6$ km.

In February 2003, the image of the infant cosmos only 380,000yrs old was received. The results from WMAP reveal that the CMB temperature variations follow a distinctive pattern predicted by cosmological theory: the hot and cold spots fall in characteristic sizes .The image of infant cosmos is shown in Figure G.2.
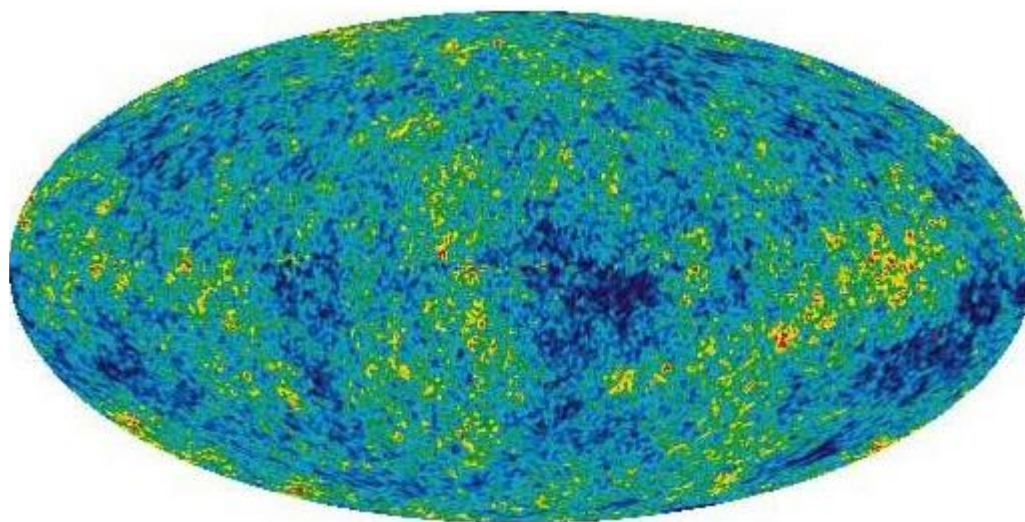

Figure G.2. Infant COSMOS when Universe was only 380,000 years old.

The hot spots or the red spots in CMB image are the images of compressed, dense plasma region and cold spots or the blue spots in CMB are the signature of rarefied plasma. The red spots will act as the seeds for super clusters. These super-clusters hierarchically gave rise to clusters, clusters gave rise to galaxies and galaxies rise to stars and solar systems.

In July 2003, Scientists superimposed SDSS data on the microwave intensity map developed by WMAP. They conclusively proved that there is what is known as integrated Sachs-Wolfe effect. Clustering of galaxies cause dimple in space- time fabric. Anti-gravity outward push tends to stretch out the dimples in an otherwise flat Universe and in the process tends to crush the Cosmic Microwave Background Radiation at and near the dimples meaning by anti-gravity push shifts the microwave radiation towards shorter wavelength. This precisely was observed in the superimposed map. This is a definitive proof of dark energy dominance in our present Universe.

The results from WMAP have been corroborated by SLOAN Digital Sky Survey(SDSS) and by Supernovae Cosmology Project[

Seife (2003), Goldhaber & Perlmutter(1998)] and they are the following:
i. There is 4% ordinary Baryonic matter, 23% dark matter composed of exotic particles and 73% dark energy;
ii. The Hubble Constant has been nailed at HO = Rate of expansion of our Universe= 71Km/(sec-Mpc);
iii. The age of our Universe is fixed at 13.7Gy;
iv. Supernovae Cosmology Project is consistent with Flat Universe with Cosmology Constant being non-zero and positive.
The result that there is 4% Baryonic Matter and 23% Dark Matter tells us that :
ordinary matter: dark matter == 1 : 5 on an average in the Universe.
G.1. Methodology of arriving at 4% Baryonic matter :23% Dark Matter:73% Dark Energy ratio.

Is this counter-intuitive model of our Universe made of dark matter and , blown apart by dark energy, correct ?
To determine the escape velocity from our Universe we must satisfy the equation:

$$\frac{1}{2}mv_{esc}^2 = \frac{GMm}{R} \; where \; R$$
$$= radius \; of \; our \; Universe \; and \; M(this \; includes \; baryonic \; matter + dark \; matter$$
$$+ \; dark \; energy) = mass \; of \; our \; Universe; \qquad\qquad G.1$$

Eq.G.1 gives the escape velocity as :

$$v_{esc} = \sqrt{\frac{2GM}{R}} \qquad\qquad G.2$$

Since we have Flat Universe by observation:

Recession Velocity of the Observable Horizon (vrec*) = vesc as given by Eq.G.2.

By Hubble's Law:

Recession Velocity of the Observable Horizon

$= v_{rec}^* = R \times H_0$ \qquad\qquad G.3

where H0 is the accepted value of Hubble Constant.
Equating Equation G.2 and Equation G.3 we get:

$$(R \times H_0)^2 = \frac{2GM}{R} \qquad\qquad G.4$$

Reshuffling the terms of Eq. G.4. we get the critical (matter+energy) density for our Flat Universe:

$$\Omega_{crit} = \frac{3H_0^2}{8\pi G} \qquad\qquad G.5$$

Substituting the numerical values of Hubble Constant and Gravitational Constant in Eq.G.5 we get the critical density as 9.38×10^{-27}Kg/m³. This works out as 5.6 Hydrogen atoms per m³. This by Einstein mass-energy equivalence works out to be 8.43×10^{-10}Joules/m³.
Let normalized actual (matter+energy) density $=\Omega_O$

Then: $\frac{\Omega_{act}}{\Omega_{crit}} = \Omega_0 = 1 \; for \; Flat \; Universe$ \qquad\qquad G.6

Let normalized matter density be:

$$\frac{matter \; density}{\Omega_{crit}} = \Omega_M \qquad\qquad G.7$$

Let normalized energy density be:

$$\frac{energy\ density}{\Omega_{crit}} = \Omega_\Lambda \qquad\qquad G.8$$

Einstein had introduced the term Ω_Λ as a cosmological constant in his Universe Equation to balance the gravitational collapse of the Universe and make it static.

Equating Eq.G.6 in terms of Eq.6 and Eq.G.7 we get:

$$\frac{\Omega_{act}}{\Omega_{crit}} = \ \Omega_0 = 1 = \Omega_M + \Omega_\Lambda \qquad\qquad G.9$$

Through the 42 type Ia Supernovae studies we get the following:

$$0.8\Omega_M - 0.6\Omega_\Lambda = \ -0.2 \mp 0.1 \qquad\qquad G.10$$

Using Eq.G.9 we solve Eq.G.10 we get:
$\Omega_M = 0.28$ hence $\Omega_\Lambda = 0.72$.
Since Light Emitting Matter = Ordinary Baryonic Matter which contributes 0.01 to the normalized matter density of 0.28 therefore we can say that:
 Baryonic Matter:Dark Matter:Dark Energy =
0.01:0.27:0.72 =
1% : 27% : 72%.
By further refining the measurements and making the corrections we get:
Baryonic Matter:Dark Matter:Dark Energy = 4% : 23% : 73%.
73% dark energy implies that eventually everything will become cold and hence dead therefore this is a very unlikely scenario and this one thing puts a big question mark on the Big Bang Theory.

G.2. What are the alternative to Big Bang ?
Paul Steinhardt of Princeton University and Neil Turok of Cambridge University have proposed a new hypothesis "Endless Universe-beyond the Big Bang" by Random Press.

They propose that we live in a 10-D space and 1-D time. In this 10-D space there are two 3-D Universes which are connected to each other by 7th dimension. The 7th extra dimension is the gap between two parallel objects called Branes. These two Branes collide and create the Big-Bang without any singularity and without any gravitational waves radiation. Everything else will remain the same. We would still get the CMB radiation map as we are getting. There will still be continuous expansion leading to a cold Universe. But before they are dead the two universes collide and reset the clock. The cycle again begins. This goes on ad-infinitum.